THREE-BODY ABRASIVE WEAR OF MATERIALS

By

Gavin Jewell

A thesis submitted to the faculty of Engineering and the Built Environment
of the University of Cape Town in fulfilment of the requirements
for the degree of MSc(Eng) in Materials Engineering

Centre for Materials Engineering
University of Cape Town
April 2000

ABSTRACT

This work is an investigation into the phenomenon of three-body abrasive wear. A specially designed three body abrasive wear apparatus has been built, modified and evaluated as part of this overall study. Further, a series of commercially available candidate materials has been evaluated for wear resistance using silica sand as the abrasive on this purpose made rig. The effect of normal load, abrasive particle size, abrasive feed rate and the type of abrasive on three body wear resistance has also been examined.

It has been shown that there is little increase in wear with an increase in particle size in the size range from 50μm to 180μm and that above an abrasive particle size of approximately 200μm there is a sharp decrease in the wear with increasing particle size, followed by a levelling off in the wear. The wear was found to increase linearly with increasing load. Varying the abrasive feed rate showed that at lower feed rates the abrasive particles were more efficient at removing materials, so the wear was higher than at higher abrasive feed rates.

It has also been shown that although the use of ash from coal-fired power stations as an abrasive produces wear of materials, the volume losses were much smaller than those obtained using silica sand and thus it is considered that the tests using silica gave results which were more reliable. The volume losses of alumina ceramics abraded against ash were insufficient to give reliable wear test data and it was concluded that ash could not be used to rank materials of high hardness.

A number of materials were ranked for wear resistance using silica sand abrasive particles. The alumina ceramics and tungsten carbide composite materials showed the best wear performance.

ACKNOWLEDGEMENTS

I would like to thank the following people, who were instrumental in making my masters project a success:

My supervisor Professor Colin Allen, for his invaluable advice and encouragement.

Mr Glen Newins, Mr Nicholas Dreze, and Mr Peter Jacobs for their ever smiling help and advice, in getting the rig up and running, and precise machining of parts. Mr David Dean for his assistance on technical matters, and Mrs Mira Topic for her advice on SEM.

Mr James Peterson and Mr Adriaan Loedolff for putting up with my demands for perfection with regards to photographic matters.

The staff and students of the Centre for Materials Engineering for all their help and encouragement.

My family and friends who have always believed in me.

Finally I would like to thank Eskom and the National Research Foundation (NRF) for their financial support.

TABLE OF CONTENTS

LIST OF FIGURES

LIST OF TABLES

LIST OF EQUATIONS

1 INTRODUCTION

The problem of three-body abrasive wear is experienced in many industrial situations where loose particles become trapped between moving surfaces. In spite of this, when characterising materials for abrasive wear applications in laboratories, much of the work has used two-body abrasion. This type of abrasion is easier to simulate in laboratory conditions, using simpler apparatuses, such as abrasive papers, or belts.

Two-body abrasive wear involves two surfaces rubbing together, whereas three-body abrasive wear involves a third unrestrained body in between the first two bodies. There is thus a need to simulate three-body abrasive wear since the behaviour of materials may differ substantially under two and three-body conditions.

The three-body abrasive wear situation has commonly been further classified into high stress and low stress three body abrasion depending on whether the abrasive particles are crushed (high stress) or not (low stress) during the abrasive process.

The present work had three principal objectives. Firstly, to build an apparatus that was capable of simulating three-body abrasive wear in a laboratory. Secondly, to perform wear tests using the apparatus, to evaluate process parameters that play a part in three-body abrasive wear. These parameters include the load applied on the specimen, the particle size of the abrasive, the type of abrasive, and the material being tested. The testing and ranking of commercially available wear-resistant materials constituted the third objective of the project.

It was also intended that three-body abrasion should be studied in the context of abrasive wear that has commonly been experienced in coal-fired power stations. Eskom (Electricity supply commission) supplies electricity to South Africa using various generation processes. Two thirds[1] of the power is generated in the country's ten coal-fired power stations.

The remainder of the 39 154 MW generating capacity is generated in hydroelectric, pumped storage, nuclear, and gas turbine (oil fired) power plants. Coal fired power stations generate electricity by burning crushed coal in boilers.

The by-products of the crushed coal, are coarse ash, fly ash, and flue gases. Coarse ash falls out of the bottom of the boilers, while fly ash is ducted out of the boiler carried by the flue gases. These ash particles are present in large quantities in South African power stations, and in many instances they become entrapped between moving parts of machinery which leads to operational downtime and financial losses. The results of this study were therefore expected to lead to a greater understanding of the operational factors and the use of candidate materials which would minimise the abrasive wear in such situations.

2 LITERATURE REVIEW PART 1

Three-Body Abrasive Wear and Pertinent Variables

2.1 Abrasive wear in general

Abrasive wear occurs when material is lost from surfaces in sliding contact though the presence of hard particles at the interface [2]. It is distinguished from another common form of wear called *sliding wear* by the presence of these hard particles.

Abrasive wear *can be* divided into *two-body abrasive wear and three-body abrasive wear*[3]. Figure 1 illustrates the difference between these two forms of wear involving hard particles. It shows that in two-body abrasive wear, abrasive particles are constrained by the one surface and unable to rotate. It is possible for the particles to rotate between the surfaces in three body abrasion.

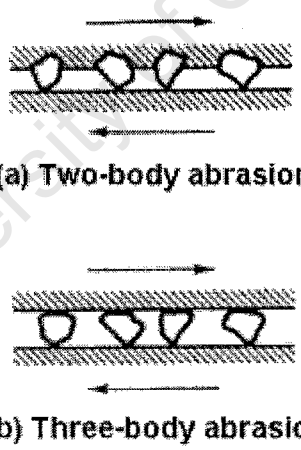

Figure 1 (a) two body abrasion and (b) three-body abrasion [after reference 3]

Two-body abrasive wear is often used advantageously in grinding or polishing applications. A belt sander, for example, removes material using the action of the hard grit particles attached to the belt. Grit particles trapped between two sliding surfaces are an example of three-body abrasive wear[3]. This situation is often encountered when a contaminant enters lubricating oil. Three-body abrasion is also a common cause of bearing damage.

Three-body abrasion may further be divided into closed and open three-body abrasion[4]. Closed three-body abrasion occurs when abrasive particles become trapped between two rolling or sliding surfaces. In open three-body abrasion, only one surface is involved in the abrasion, or the surfaces are far apart. The relationship between the different classifications of wear is summarised in Figure 2

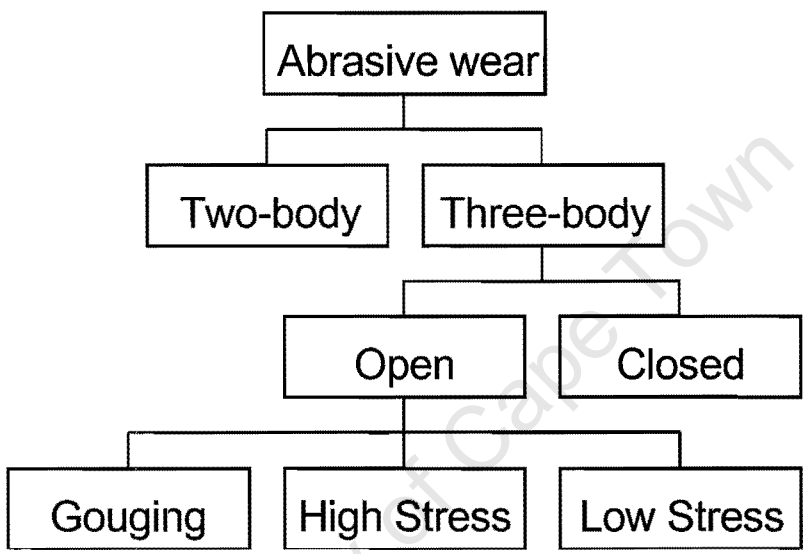

Figure 2 Classification of abrasive wear [after reference 3]

Open three-body abrasive wear is also divided into *high-stress* and *low-stress abrasion*. High stress abrasion is the term used when the crushing strength of the particles is exceeded, whereas in low stress abrasion, the particles remain uncrushed after the abrasive process.

Gates[5] has recently proposed an alternative classification of types of abrasive wear, based on the manifest severity of the wear. However in the present work, the well-established and understood abrasive wear types will be adhered to.

2.2 Variables in abrasion

Avery[6] divided the variables, which play a role in wear into two groups. Those for severity, and those for opportunity. Opportunity variables determine the possibility of wear occurring and severity variables determine how aggressive the environment is. Examples of each are tabulated in Table 1.

All of these variables can play individual and synergistic roles in ultimately determining the abrasive wear rate and it is extremely difficult therefore to establish their individual importance since the wear process is system dependent. Nevertheless, a number of these variables have received considerable investigation as detailed in the following sections 2.3 and 2.4.

Table 1 Examples of opportunity and severity variables (after Avery[6])

Opportunity variables	***Severity Variables***
Running time	Abrasive particle size
Travel distance	Abrasive angularity
Contact area	Abrasive hardness
Abrasive feed	Abrasive toughness
Fluid flow	Velocity
Specimen configuration	Impingement angles
	Proportion of cutting vs. deformation
	Gross loading on wearing surface
	Microstresses imposed on wearing surface
	Whether the presence of corrosion, temperature, fatigue, impact, and adhesive wear are significant

2.3 The influence of abrasive particle characteristics on abrasive wear

Particles which are harder than the interacting surfaces cause the damage associated with three-body abrasion and as a result, the characteristics of the particle play a most important role.

2.3.1 Abrasive hardness

Khruschov[7] stated that an essential condition for abrasive wear is that during the friction process, the surface of the abrasive material must be harder than that of the wearing material. Particles with lower hardness than that of the surface[3] cause much less wear than harder particles. If the hardness of the particles is significantly higher than the surface, then their precise hardness is not as significant. The ratio of hardness of abrasive to hardness of materials, is therefore important, and has been considered by a number of researchers.[3,7,8,9]

Hutchings[3] explained the effect by considering the contact mechanics of a single grit particle and a plane surface (Figure 3). If the surface material flows plastically once the yield point is reached, significant plastic flow will result if the mean contact pressure reaches approximately 3 times the yield stress Y. This contact pressure is the indentation hardness of the surface and the particle shape has little effect. Plastic deformation of the surface will only occur if, when the contact pressure is increased, the particle can withstand the pressure without deforming. If the particle fails by flow or fracture, before the pressure reaches approximately $3Y$, there will be no significant plastic deformation of the surface.

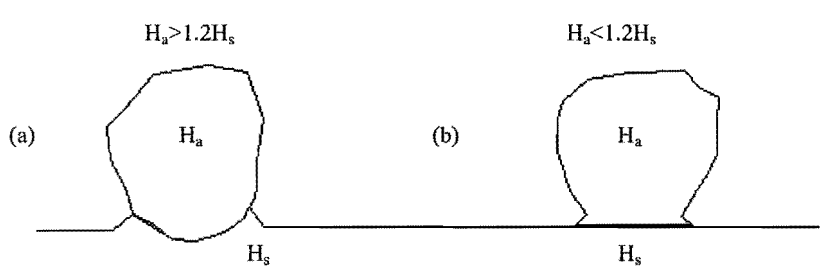

Figure 3 Contact between an abrasive particle and a surface: (a) particle indents surface; (b) plastic flow of particle occurs. [after reference 3]

The maximum contact pressure when a spherical particle is pressed against a flat surface is 0.8 times the indentation hardness of the particle material. Therefore a sphere of hardness H_a should cause plastic deformation to a surface with hardness H_s if H_s is less than 0.8 H_a (i.e. H_A/H_S>1.25). Experimentally, it has been shown that particles of any shape will cause scratching only if H_A/H_S >1.20. The case of H_A/H_S <1.20 is often termed *soft abrasion* and H_A/H_S >1.20 *hard abrasion.*

Khruschov[7] performed wear tests on 17 different metallic and non-metallic materials using 7 abrasives, varying in hardness from glass to boron carbide. The trends of the results are presented in Figure 4, which relates the ratio H_a/H_m (ratio of the abrasive hardness to the material hardness) to the relative wear resistance ε and relative wear $1/\varepsilon$ of the materials.

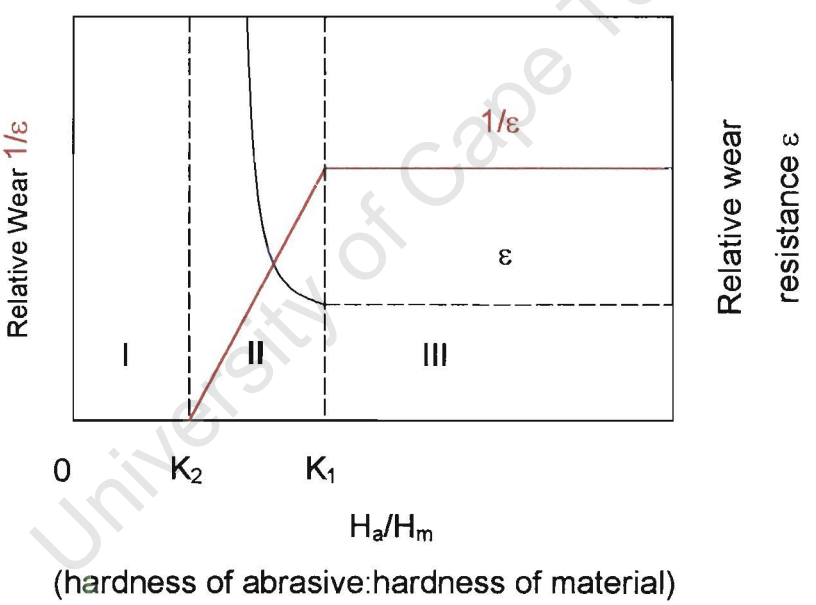

Figure 4 An illustration of the dependence on relative wear on the ratio of abrasive hardness to material hardness [after reference 7]

In Figure 4 the following should be noted:

For $H_a/H_m \leq K_2$ no wear takes place, and the wear resistance is infinite

For $H_a/H_m \geq K_1$ the relative wear has a maximum and a constant magnitude regardless of the magnitude of the ratio H_a/H_m

If the wear is between K_1 and K_2, then it is intermediate.

Based on a large number of tests, the following values of K_1 and K_2 were observed: K_1 = 1.3-1.7 K_2 = 0.7-1.1

Misra and Finnie[9] showed that hardness had the same effect for both two-body and three-body abrasive wear. Generally, the wear rate is constant for H_a/H_s>1.25 and is very low for H_a/H_s <0.83 where H_a is the hardness of the abrasive and H_s is the hardness of the surface.

Levy[10] studied the similarities between three-body abrasion and solid particle erosion. This research showed that, once the hardness or strength of the particles is great enough to prevent their fracture or shattering on contact with the surface, a further increase in hardness will have no effect on the abrasive or erosive wear.

2.3.2 Abrasive particle size

Many researchers[2,10,11,12] have observed that if the particle size is increased from low values, the wear rate initially increases until it reaches a critical value. Above this critical value, the wear rate is not affected by increasing particle size. The effect has been observed in tests using abrasive papers, where the particles are constrained, and three-body abrasion tests in which the particles are free to roll. A number of explanations for this phenomenon have been proposed. Rabinowicz and Mutis[12] proposed that this critical size corresponds to the size of adhesive wear fragments of the abraded material. The fragments separate the specimen and the wear wheel, resulting in a drop in the wear. Alternatively Mulhearn and Samuels[13] attributed the critical size effect to different mechanical properties of the large and small abrasive particles. They believe that the fine grit particles contained a large number of cracks, and thus broke during the abrasion process.

Miller[14] performed three-body abrasive tests using particle sizes of 60μm and less, using a lapping apparatus and abrasive slurry. He found that, for a given load, there was a critical size, above which an increase in particle size caused no further increase in wear rate, and even a decrease for smaller loads. It is interesting that Miller observed no increased presence of cracks in the smaller particles compared with the larger particles which conflict with the observations of Mulhearn and Samuels. Miller also failed to find adhesive wear particles to explain the results using Rabinowicz and Mutis' proposal. Importantly it has also been shown that the critical size effect becomes less pronounced with increasing load

Sasada, Oike and Emori[15] divided the effect of particle size, (using silicon carbide abrasives) into three regimes. A diagram of the regimes of wear can be seen in Figure 5. Firstly, if the grain-size is larger than critical value d_c, the wear rate is independent of particle size. In the second regime, the wear rate decreases with decreasing particle size below d_c up to a transition particle size of d_t (about 10μm). In the third regime, below d_t, the wear rate is high and independent of abrasive particle size. The researchers concluded that the

important dimension was, in fact, not the absolute particle size, but rather the size of the particles in relation to the size of the debris that forms during the wear process. In the region where particles sizes are smaller than d_t the wear mechanism is predominantly adhesive wear and the wear debris consists of flakes of metal mixed with abrasive particles. The action of the abrasive particles is to remove the metallic wear debris from the contact region.

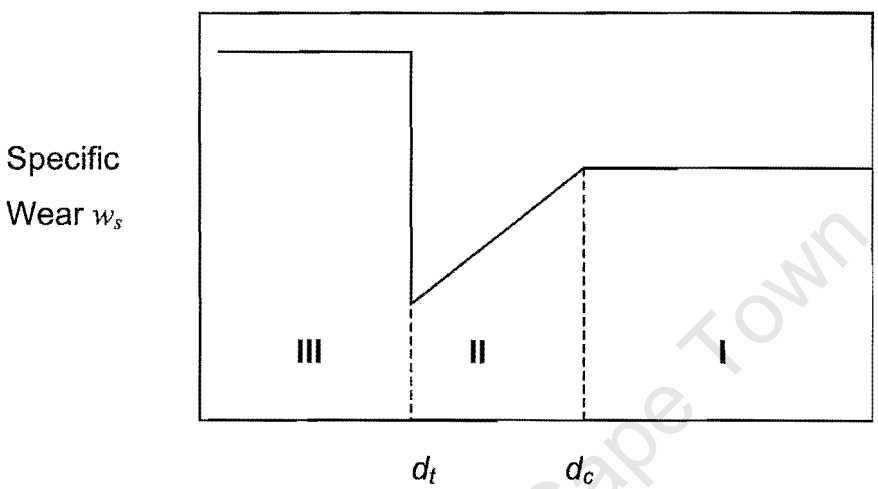

Figure 5 Diagram to show the three regimes of wear with respect to particle size [after reference15]

Levy[10] showed that the effect of abrasive particle size was common to both solid particle erosion and three-body abrasion. The wear rate increased with increasing particle size, and then, above a critical particle size, there was no further increase.

2.3.3 Abrasive particle shape

Wear rates depend strongly on *the* angularity of particles. Hutchings[3] states that differences between rounded and angular particles of the same type may result in wear rates, which may differ by a factor of ten or more. Although angularity is difficult to define, a *roundness factor* F can be used as a crude indication of the deviation of a particle shape from spherical. It is defined as

Equation 1 $$F = \frac{4\pi A}{p}$$

A is the area of the projection and p is the perimeter of the projection of the particle in two dimensions. The more a particle's outline deviates from circular, for which case F=1, the smaller the roundness factor. If many, randomly orientated particles are considered, an indication of the shape of particles can be obtained.

Prasad and Kosel[16] performed tests on high chromium white cast iron using a rubber wheel abrasion apparatus. They wished to study the effect of particle shape on carbide removal mechanisms. It was concluded that a small portion of the rounded Ottawa quartz abrasive particles fractured, resulting in a small number of particles with greater angularity which subsequently initiated fracture in the carbides.

Levy[10] claimed that, for wear using the particles sizes primarily found in fluidised bed combustors, of all the particle characteristics (particle shape, size and hardness) only the shape had a significant effect on the three-body abrasive and erosive wear rates.

2.4 The role of abrasive wear test parameters

2.4.1 Influence of sliding speed

Stevenson and Hutchings[17] found, when varying the sliding speed during a series of three-body wear experiments, using the rubber wheel test, that the wear rate increased with sliding speed to a maximum and then it decreased at higher speeds. During these tests, the sand feed rate was kept constant at 1.1g.s^{-1} and the load was a constant 98.1N. The effect was attributed to variations of the mechanical properties of the rubber wheel with strain rate and temperature. The temperature of the specimen and the rubber rose with an increase in sliding speed. The rubber softened as a result and a decrease in wear rate was observed. The effect of increasing wear rate with increasing rubber hardness was confirmed in another series of tests.

Misra and Finnie[2] investigated the change of wear rate as a function sliding speed for copper and aluminium. The apparatus used was a column of abrasive contained in a tube, pressed against a rotating disc. Conversely they found that the wear rate was observed to change only slightly in the speed range of 25-175mm.s^{-1}, which is much smaller than the speeds employed by Stevenson and Hutchings.

2.4.2 The thickness of the abrasive layer between specimen and surface

Stevenson and Hutchings[17] state that the layer of particles which is established between the specimen and the wheel is important in the wear process. The packing density is determined by two main factors. Namely, the rate at which the particles are fed onto the wheel, and the speed of the wheel. The researchers defined a packing fraction of abrasive particles, f, to describe the density of the layer of abrasive particles:

Equation 2 $f = 1 - e$

In Equation 2, e is the voidage and f the volume occupied by the particles divided by the total volume in the contact region. A close-packed single layer of spheres fills up 60.5% of the space (f=0.605).

The number of particles in the contact zone between the wear wheel and the specimen was denoted N_p. It was estimated by measuring the mass flow rate of particles past the specimen, W, and assuming the particles size distribution remained constant. For the assumption of all particles having equal size:

Equation3 $$N_p = \frac{wx}{vm_p}$$

x is the contact length between the wheel and the specimen, v is the relative sliding speed, and m_p is the mass of one particle.
The packing fraction f is :

Equation 4 $$f = \frac{W}{vdb\rho}$$

d is the particle diameter, b the wheel width, and ρ the material density.

Experimentally, it was shown that there is a limiting flow rate W_{lim}, which could be achieved. If the feed rate from the abrasive hopper, W_{feed}, is less than W_{lim} then all of the abrasive particles fed between the 2 surfaces will pass through. Therefore $W = W_{feed}$. If the feed rate from the hopper is greater than W_{lim}, then $W = W_{lim}$ and excess sand will fall off the edge of the wheel. W_{lim} will be the net abrasive flow rate at the slowest sliding speed. This situation was used for the majority of tests performed by Stevenson and Hutchings.

2.4.3 The effect of load

Simple models of abrasive wear[2] predict that the wear rate is proportional to load:

Equation 5 $$Q = \frac{KW}{H}$$

In Equation 5, commonly referred to as the Archard equation, Q is the volume of material removed per sliding distance, W is the applied normal load, and H is the indentation hardness of the material. When referring to wear, the wear resistance is often used. This is simply the inverse of the wear rate, i.e. $1/Q$.

Misra and Finnie[9] found that there was a differing influence of load for two-body and three-body abrasion. For three-body abrasion, the wear rate first increases non-linearly with load, and then linearly. The researchers proposed that, under low load, there is a lower degree of constraint of the abrasive particles. Two-body wear tests generally showed a linear dependence on load. Stevenson and Hutchings[17] performed three-body wear tests on 1020 steel, using a rubber wheel abrasive wear tester and they found that wear rate increased linearly with load.

Avery[18] referred to tests obtained using two rubber wheels with different hardnesses (Durometer hardnesses of A42 and A66 respectively) The test specimen was made from tool steel with a hardness of 65HRc. For the harder wheel, the relationship between wear rate and load was not linear, but the wear increased rapidly with increasing load. For the softer rubber wheel Avery noted that the wear rate decreased with increasing load, and this was attributed to the increasing contact area between the wheel and the specimen as the load increased.

Miller[14] performed three-body abrasive tests using particle sizes of 1μm to 60μm at a variety of loads. For particle sizes of 3μm and 6μm the wear rate increased with load until a critical load was reached, above which, it increased at a lower rate. For larger particle sizes the wear rate increased with

increasing load. The observation for the smaller particle sizes was attributed to Pritchard's[19] low pressure effect, by which, at low pressure, the particles had more mobility and the most effective cutting edges are used, resulting in a high wear rate.

2.4.4 The effect of material hardness

Although there are a number of ways to increase the hardness of a material, such as alloying, heat treatments and cold working, each of these will have different influences on the wear resistance of the resultant material.

2.4.4.1 Pure metals

It is generally known that the wear resistance of pure metals increases linearly with the hardness of the material.

Khruschov[7,20] showed in 1957 that, for two-body abrasive wear, there is a linear relationship between the hardness and the wear resistance of annealed pure metals and annealed steels.

Sundararajan[21] found that, for pure metals, the wear resistances for erosion and two-body abrasion increased linearly with increasing hardness. Rabinowicz *et al*[4] and Misra and Finnie[2] found similar results for low-stress open three-body abrasive wear.

2.4.4.2 Alloying effects

Alloying will increase the abrasion resistance only if the strengthening mechanism will lead to increased strength at high strains. Examples of such alloys are fine carbides in steels. Alloys with relatively soft precipitates, such as age-hardened aluminium-copper alloys will, however, not show increased strength. Although bulk hardness has been shown to be an important factor in two body abrasion of materials, microstructural changes in steels which have little effect on the bulk hardness can improve the wear resistance.

Yang and Garrison[22] studied two-body and three-body abrasive wear of steel and found that three microstructural features improved the two-body wear of steels. Namely: the precipitation of alloy carbides (secondary hardening), undissolved carbides, and large volume fractions of retained austenite.

Secondary hardening is a precipitation phenomenon that occurs in alloy steels, containing strong carbide forming elements[23]. When these steels are tempered between 450°C and 650°C, fine carbides, which are more stable than cementite form. This hardening phenomenon is related to the extent of replacement of primary carbides, cementite, by secondary carbides. Hardened steels strengthened by alloy carbides are more resistant to two-body wear than low alloy steels of similar hardnesses[23]. Undissolved carbides also improve two-body wear.[24]

A high percentage of retained austenite has also been shown to improve two-body wear resistance[25]. The abrasion resistance has been attributed to the transformation of the austenite to martensite during the process of wear. The researchers showed that the above results also applied to three-body abrasion, however three-body abrasion resistances are higher than those of two-body abrasion. Yang and Garrison[22] proposed that the improved abrasion resistance was caused by compressive stresses being induced in the surface, resulting in higher hardness and higher local ductility.

Tests performed by Khruschov[7] on various structural steels, hardened and tempered at various temperatures showed that the wear resistance increased along a linear path in relation to the hardness. The higher the percentage of carbon and carbide forming elements, the higher the wear resistance was, and the steeper the gradient of the rise in wear resistance with hardness. An equation was proposed by Khruschov as follows for steel:

Equation 6 $\varepsilon = \varepsilon_0 + b^1 (H-H_0)$

In Equation 6, ε is the relative wear resistance, ε_0 and H_0 are the relative wear resistance and hardness respectively of annealed steel and b_1 is a coefficient of proportionality for different grades of steels.

Gore and Gates[26] compared the hardness effect on wear using three different apparatuses. A dry sand rubber wheel apparatus (DSRbrW), a dry sand steel wheel (DSStlW) and an impact abrasion tester were used.

The results for the DSRbrW were as expected and the wear resistance generally increased with increasing hardness. The wear resistances of white cast irons and tool steels were however higher than the other materials, which were homogeneous in microstructure. The cast irons and the tool steels all contained hard alloy carbides in their microstructures, which appeared to improve their wear resistances.

For the steel wheel tests, however, the materials with hard second phase particles showed wear resistances that were lower than the homogeneous materials. The trend exhibited for these materials was a decreased wear resistance with increasing hardness. These results were explained by considering that the friction of the hard carbide particles was lower and therefore there was minimal rolling. Another possibility proposed was a microfracture mechanism, but there was no conclusive evidence of such a mechanism.

For the DSStlW, the wear results for homogeneous materials were similar to those obtained on the DSRbrW apparatus. For a given material, the rates obtained on the different apparatuses were within an order of magnitude

Micrographs of specimens of varying hardnesses, which had been tested on the DSStlW apparatus, showed a transition from indentation for the softer materials to grooving as the hardness increased. This was interpreted to show that, for the softer of the materials tested (aluminium), particles are rolling as opposed to sliding across the specimen surface. Gore and Gates explained that the relative hardness of the wheel was important. If the wheel had a hardness of 600HV and the specimen 80HV, the sand particles indented the aluminium, thereby increasing the coefficient of friction of friction of the specimen-sand interface in comparison to the sand wheel interface

2.4.4.3 Work hardening

For a group of pure metals, which had been mechanically work-hardened to give different hardnesses, it was found that the wear resistance, in general, remained unchanged if the hardnesses were increased[7]. Khruschov concluded that the maximum hardness of a metal is obtained during abrasive testing. This hardness is higher than any pre-test hardening because the abrasion causes very high strains at the surface of a material. It was assumed that this was the maximum hardness before destruction. Furthermore, when comparing hardness to wear resistance, the surface hardness provides better correlation than the bulk hardness of the material resistance.

Misra and Finnie[2] observed that increasing the hardness of copper and tantalum by work hardening did not increase the wear resistance of the materials.

2.4.4.4 Heat treatment

Das, Prasad et al[27] performed abrasion tests on 0.98% carbon steel specimens, which had been heat treated to obtain hardnesses varying from 180HV to 900 HV. The results of the wear test showed that the wear resistance increased linearly with an increase in bulk hardness.

Misra and Finnie[2] tested an AISI 4340 stainless steel, of which the hardness had increased after heat treatment. The wear resistance increased at a slower rate.

Sundararajan[21] tested both pure metals and alloys. The abrasion resistance of the pure metals and alloys increased linearly with hardness. For alloyed metals such as steels, which had been quenched and tempered, although the abrasion resistance did increase with increasing hardness, this increase was not as significant as the case of pure metals of increasing hardnesses. This was in contrast to the erosive wear results obtained. For erosion there was no effect on the wear resistances with increasing hardness of steels resulting from quenching and tempering. It was concluded that the erosion and abrasion had different dependencies on hardness.

Prasad and Kulkani[28] performed tests on carbon steels with 0.1-1.2%C and they obtained a V-shaped curve between weight loss and hardness. They stated that an understanding of the hardness and toughness was necessary to explain the relationship.

However, Zum Gahr and Doane[29] obtained an S-shaped curve of volume loss versus hardness for high chromium cast iron, which had been heat treated to different hardnesses. They also tested the fracture toughness of the materials, but could not make a clear correlation between the wear and the fracture toughness.

Fang, Zhou and Li[30] found similar results to Zum Gahr and Doane[29] An S-shaped curve of weight loss versus hardness was obtained. To explain these results the researchers performed short-travel three-body abrasion tests. The graphs of weight loss versus travel showed that there was an inflection point early in the test. First the curve rose steeply, quickly dropping and then rising at a shallower gradient. The researchers attributed this to the curve representing the effects of both cutting wear, and plastic deformation, superimposed. For pure plastic deformation, the curve would start off at a shallow gradient and then rise until a steady-state had been reached Once this steady-state had been reached mass loss would be linear with travel distance and the gradient higher than the initial gradient. For the case of cutting, for which a curve of weight loss versus travel was obtained using a short-travel two-body abrasion test, the curve rises steeply at first, and then it drops to a steady state with a lower gradient.

Using the results of the weight loss versus travel tests, the researchers proposed an explanation for the s-shaped curve of weight-loss versus hardness. Assuming the coexistence of cutting wear and plastic deformation, the weight loss due to three-body abrasion can be expressed by Equation 7.

Equation 7 $W=pW_c+(1-p)W_d$

W is the total weight loss, W_c is the weight loss caused by cutting, and W_d is the weight-loss caused by plastic deformation, while p is the probability of cutting wear.

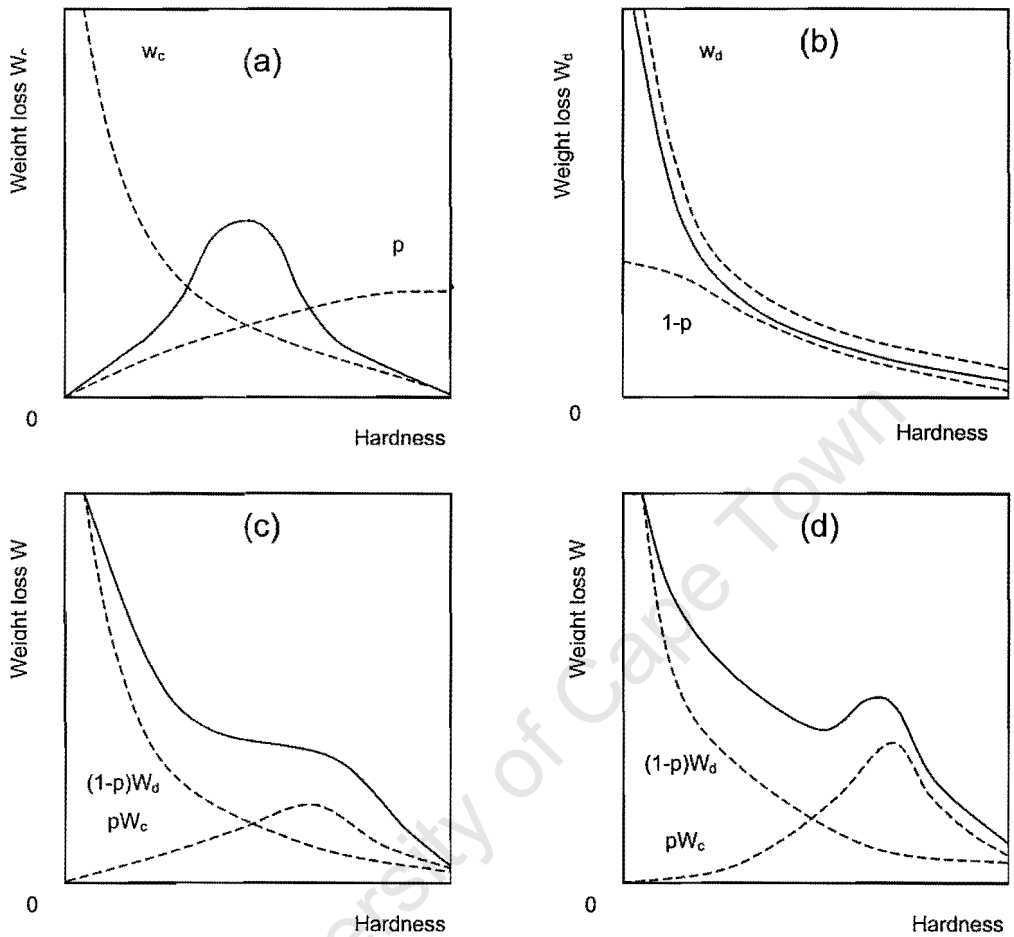

Figure 6 The influence of cutting wear and plastic deformation on the total weight loss of materials in relation to their hardnesses [after reference 30]

The researchers found that the number of scratches increased with the hardness of the materials, and thus they made the assumption that the probability of scratching p increases with hardness. However the weight loss as a result of cutting W_c decreases with increasing hardness. These factors are included in the first term of Equation 7 and are shown by the dotted lines in Figure 6(a). The combined effect of these factors is shown by the solid line in Figure 6(a).

Kraghelsky[31] proposed a mathematical model of plastic deformation, showing that the weight loss W_d caused by plastic deformation was inversely proportional to the material hardness. Thus, the second term in Equation 7 can be expressed by the solid line in Figure 6(b). By superimposing Figure 6 (a) on Figure 6(b), the weight loss caused by three-body abrasion may be obtained (Figure 6(c) and (d)). Figure 6(c) shows the case of low intensity of cutting wear, as seen by line pW_c. The general trend is one of decreasing weight-loss with an increase in hardness. Figure 6(d) shows the case of high intensity of cutting wear. The curve of weight-loss versus hardness is S-shaped, in agreement with results obtained by Zum Gahr and Doane[29] and by the authors who proposed the explanation[30].

2.4.4.5 Thermochemical treatments

Kim and Kweon[32] investigated thermochemical treatments of plain carbon steels to improve their three-body abrasion resistance. Gas carburizing, gas carbonitriding, gas nitrocarburizing, ion nitrocarburizing, and ion nitriding were tested as methods. Gas carburized and ion nitrocarburized specimens showed the best wear resistance.

2.4.5 The effect of humidity

Larsen-Basse[33] performed three-body abrasion tests using SiC abrasives in which the level of humidity was closely controlled. He found that the wear rate increased sharply with humidity above ambient conditions. There was little effect below ambient conditions. He attributed the effect to the moisture assisted fracture of abrasive grains, which causes more sharp particles to come into contact with the abrading surface.

2.5 Mechanisms of abrasive wear

Abrasive wear can involve both plastic flow and brittle fracture[3]. The two mechanisms often occur together. Models, however, generally examine the two groups of wear mechanisms in isolation.

2.5.1 Abrasive wear by plastic deformation

A simple model of plastic deformations is outlined by Hutchings[3]. An abrasive particle, idealised as a cone, of semi-angle α, is dragged across a surface of ductile material that will flow under an indentation pressure *P*

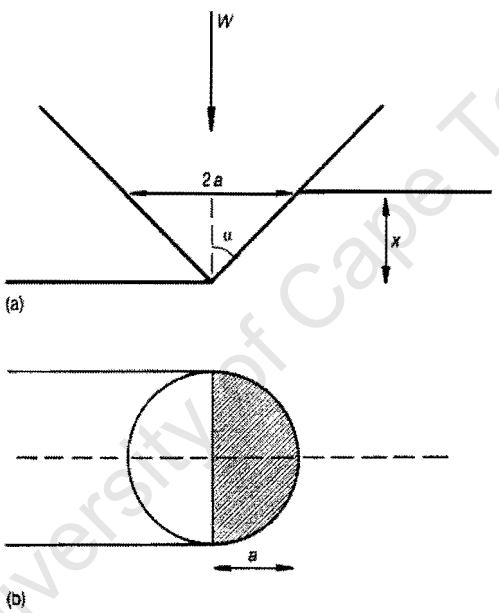

Figure 7 Geometry of contact between an idealised conical abrasive particle and a surface: (a) in elevation (b) in plan view [after reference 3]

A groove is formed in the material and the wear occurs by the displacement of material from the groove by the abrasive particle. The normal load w, (Figure 7) carried by the particle, is supported by the plastic flow beneath the particle, which causes pressure *P* to act over an area of contact between the particle and the surface. Only the front of the cone is in contact because the cone is moving forward, so:

Equation 8 $$w = \frac{P\pi a^2}{2} = \frac{1}{2} P\pi x^2 \tan^2 \alpha$$

If the quantities *a* and *x* are defined as in Figure 7, then the material displaced from the groove by the cone in sliding a distance *l* across the surface is $l\ a\ x$, or $l\ x^2\ tan\ \alpha$. If the fraction η of the material displaced from the groove is actually removed, then the volume of material removed per unit sliding distance, q, is:

Equation 9 $$q = \eta x^2 \tan \alpha$$

Combining Equation 8 and Equation 9:

Equation 10 $$q = \frac{2\eta w}{\pi P \tan \alpha}$$

This can be summed over many particles, and assuming P≈H, the indentation hardness of the material, the total volume removed per unit sliding distance Q is:

Equation 11 $$Q = \frac{KW}{H}$$

W is the total normal applied load and *K* is a constant, which depends on the geometry of the particles (α) and the fraction of displaced material η.
Equation 11 is the same as the Archard wear equation, for sliding wear (Equation 5). The equation derived in Equation 11 indicates that the wear should be directly proportional to the distance of sliding and to the normal load. This behaviour has usually been observed in practice for two-body abrasive wear.

Equation 11 also suggests that the wear rate should be inversely proportional to the hardness of the material, H. This is the case for many pure metals[2], but alloys[7] do not often behave this way. The effect of material hardness has been previously discussed in section 2.4.4

2.5.1.1 K- the wear coefficient

The wear coefficient, K, found in the Archard equation (Equation 5) can be used as a measure of the severity of wear. It is dimensionless. As stated in the previous section, K depends on the geometry of the abrasive particles[3], namely the value of α, as defined in Figure 7, and the fraction of displaced

material η. Values of K for two-body abrasion range from approximately $5x10^{-3}$ to $50x10^{-3}$. The values for three-body abrasion are generally lower: between $0.5x10^{-3}$ to $5x10^{-3}$, indicating that it is a less severe form of wear.

2.5.1.2 Wear modes

Challen and Oxley[34] presented three modes by which material can be removed from a rigid-plastic surface. Figure 8(a) shows a *cutting* mode in which the material is deflected through a shear zone and up the front face of the particle, to form a chip. All of the material displaced by the particle is removed in the chip, in the same manner as an orthogonal machining process. Figure 8(c) shows the *ploughing* mode by which the material is pushed along ahead of the particle. During ploughing, material flows beneath the particle and no material is removed from the surface. In the *cutting* mode, material flows up the front face of the particle, whereas in *ploughing* it flows down.

A third wear mode of deformation, *wedge formation*, represents intermediate behaviour. It can be seen in Figure 8(b). Limited slip or possible adhesion occurs between the front face of the particle and a raised "prow" of material. The deformation consists of growth and eventual detachment of the prow. This process occurs repeatedly. As with cutting, the process leads to removal of material.

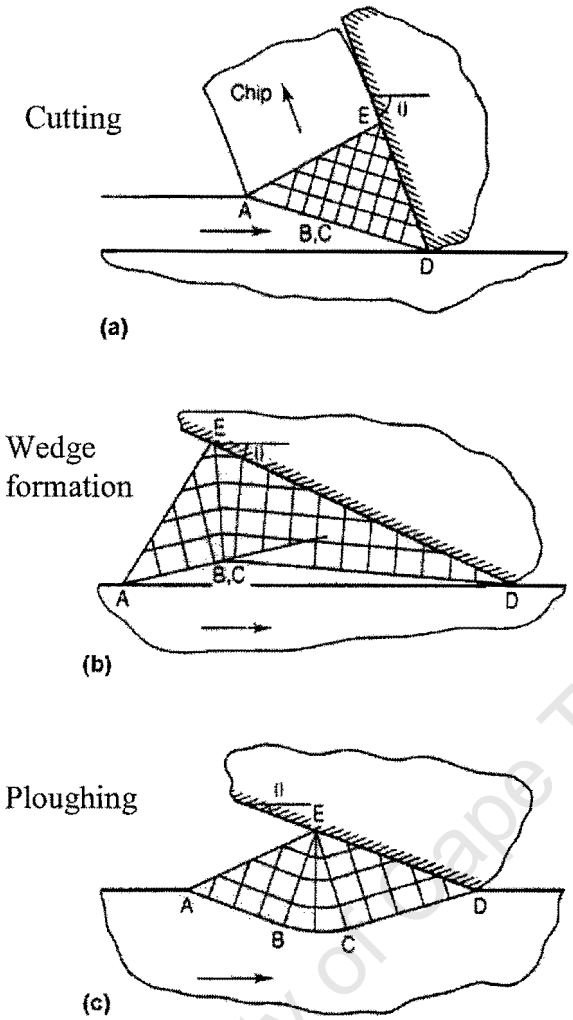

Figure 8 Slip-line fields for the deformation of a perfectly plastic material caused by the sliding of a 2-dimensional wedge from left to right: (a) cutting (b) wedge formation (c) ploughing [after reference 34]

If the forces involved in the deformation modes shown in Figure 8 are considered, then the operative mode, that which requires the lowest tangential force, can be determined, for a certain set of sliding conditions. The attack angle, θ, as seen in Figure 8 is one important variable. The second is the shear strength of the interface between the particle and the material. This quantity may be expressed as f, the ratio between the shear stress at the interface and the shear stress of the material. For the case when $f = 0$, this implies perfect lubrication. For $f < 0.5$ only two modes, cutting and ploughing, are possible. For low values of the θ, ploughing is favoured, but above the critical attack angle θ_c, cutting is the preferred mode. Above $f = 0.5$ all three

wear modes may occur. The critical attack angle of a rigid-ideal plastic material depends only on f, whereas in a real material, the work hardening rate and the elastic properties also need to be considered, in other words E/H, the elastic modulus over the hardness. The critical angle increases with an increase in E/H. As cutting will generally cause more material removal than ploughing, if the wear situation favours cutting, a higher wear rate can be expected.

Mulhearn and Samuels[13] plotted a frequency distribution of attack angles of contacting abrasive particles in silicon carbide abrasive papers. The proportion of the particles, which have an attack angle above the critical attack angle, determines the proportion of particles, which will damage the surface by cutting. This therefore effects the value of K.

Liang Fang, Xianglong Kong and Qingde Zhou[35] designed a wear tester that was capable of observing the movement pattern of abrasive particles, during three body abrasive wear. The movement could be monitored and recorded using a camera. They were able to observe whether the attack angles of the particles were greater than the critical attack angle, and the resulting cutting. For the particles with lower attack angles it was observed that the particles rolled. The apparatus was used to calculate the ratio of rolling to sliding statistically and hence the probability of cutting wear.

It is possible for transitions between the wear modes to occur. A summary of the results obtained by Hokkirigawa and Kato[36] is shown in Figure 9.

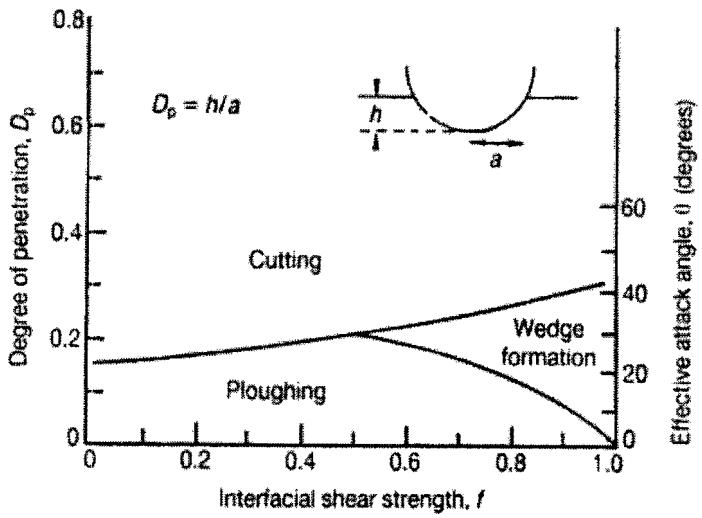

Figure 9 The influence of degree of penetration, interfacial shear strength and attack angle on the modes of wear [after reference 36 and reproduced in 3]

Hokkirigawa and Kato[36] performed an experimental and theoretical investigation into the modes of cutting, ploughing and wedge formation of metals. They used a steel pin with a tip radius of 27μm to scratch polished metal surfaces. The wear apparatus was mounted inside a scanning electron microscope so that the wear could be observed and recorded during the wear process. The tests showed that the wear modes are very sensitive to load, the metal abraded, and the pin radius. Thus they defined a degree of penetration D_p as a severity index of sliding, where:

Equation 12 $D_p = h/a$

a *is* the radius of contact, and h, the depth of the groove. D_p can also be expressed as a function of load, using geometrical considerations. Experimental work showed that the wear mode changed from ploughing, to wedge forming, to cutting with increased D_p.

Hokkirigawa and Li[37] also performed in-situ experiments in the scanning electron microscope to investigate the wear mechanisms of steels on a microscopic level. It was found that the critical degree of penetration for the transition between wedge forming and cutting modes decreases with increasing hardness.

For the wear of lubricated brass, Kayaba et al[38] observed a fourth wear mode which they termed *flaking–type wear.* It had similar characteristics to cutting wear, except that thin flakes of debris pile up at the end of the groove, as opposed to ribbon-like wear debris which characterises cutting wear. They also stated that the transition between wear modes was strongly dependent on the lubrication conditions.

2.5.1.3 Plastic indentation

Wang and Wang[39] disagreed with the view that the majority of material loss from a material surface is as a result of cutting. Rabinowicz[4] made this assumption when developing his model. The researchers explained that all wear debris from three-body abrasion did not appear to be chips, which would be the case if cutting were the predominant mechanism. Metal surfaces showed much evidence of rolling. Examination of the particles revealed that on the whole, the edges were round, and even though some of the particles had irregular shapes, they lacked sharp cutting edges. They postulated that there were two orientations of particles that caused large volume losses. For the abrasives used, none of the particles had sharp edges on all sides. Therefore it was assumed that the abrasive is often in contact with the metal on its smooth surfaces and is experiencing rolling. Rolling particles produce many overlapping grooves in the metal surface, and material experiences so called "lump failure" by plastic fatigue. The second situation was caused by the sharp edges, which resulted in a surface such as that caused by two-body abrasion. The sharp edges act as a wedge indentor, deforming the metal.

2.5.2 Abrasive wear by brittle fracture

The second simple model[3] of abrasive wear assumes that material removal takes place primarily by brittle fracture.

If a brittle material is indented by a blunt object, such as a sphere, a hertzian cone crack will form if the contacts stresses are elastic. If this indentor slides over the surface a series of incomplete conical cracks will form. The cracks will intersect the surface in a row of circular arcs. Whereas, this situation will not readily lead to material removal, an angular particle in contact with the surface may will cause wear of a brittle surface by localised plastic deformation.

Lawn and Swain[40] examined the mechanism of cracking in a brittle material subjected to a point indentation (Figure 10).

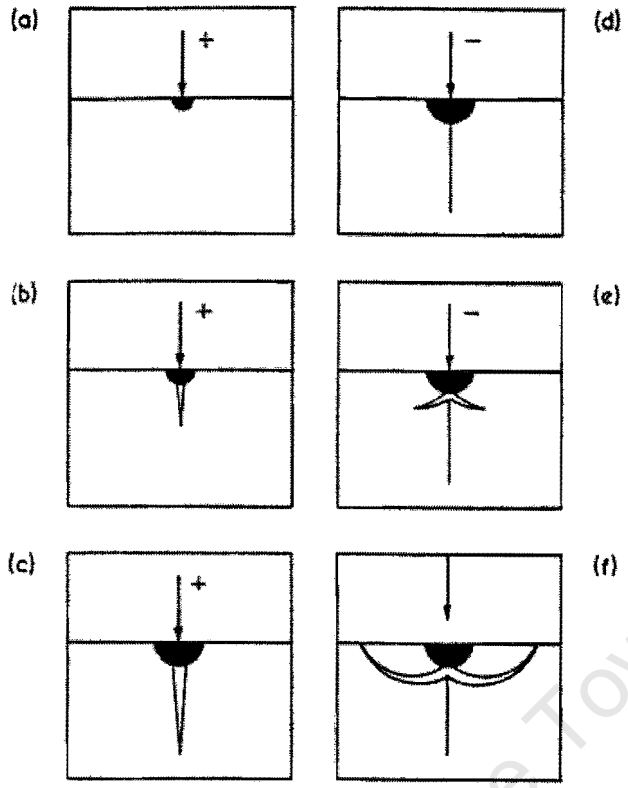

Figure 10 Illustrations of vent crack formation in a brittle material under point indentation. (+) represents loading, (-) unloading. The black area represents the deformation zone [after reference 40]

In (a),(b) and (c) of Figure 10, a point load is applied to a surface of a brittle material and, as the load is increased, a median vent crack grows into the material. When the load is removed (d) the crack closes. Relaxation of the deformed materials in the contact zone prior to the removal of the indentor superimposes large residual tensile stresses on the applied field. As a result of these stresses lateral cracks known as *lateral vents* form. In the final stage, (f), lateral vents grow and may cause chipping. The median cracks do not result in material removal, unlike the lateral cracks.

Lateral cracks will only form when the indentor load reaches a critical value[3] w^*. This critical value depends on the fracture toughness of the material K_c, and the hardness, H. According to one theory:

Equation 13 $$w^* \alpha \left(\frac{K_c}{H}\right) K_c$$

H/K_c is used as a brittleness index, with a low value of H/K_c corresponding to a high value of w^*. In other words a material with low value of brittleness index, resists fracture on indentation.

A simple model of abrasive wear of brittle materials is shown in Figure 11.

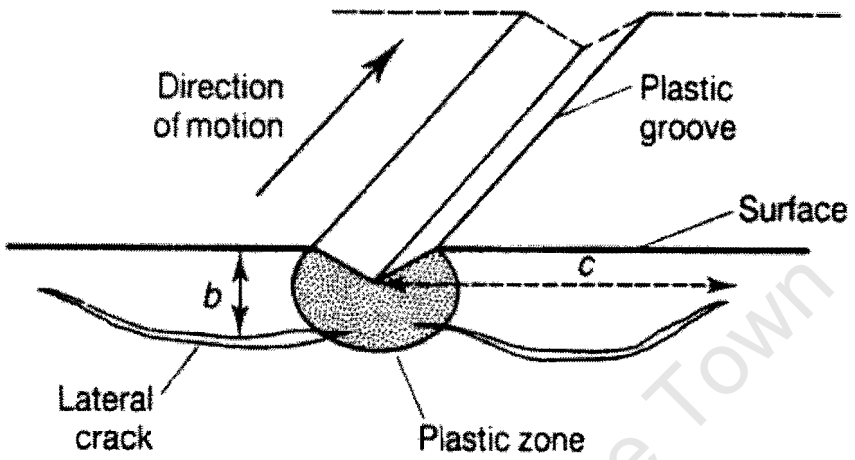

Figure 11 A model of material removal in brittle material by the extension of lateral cracks [after reference [41]]

As a sharp particle scrapes over the surface, lateral cracks grow from *the* plastic zone to the surface of the material. Material is removed as chips bounded by cracks and the free surface.

2.6 Abrasive wear of ceramics

Yamamoto, Olsson & Hogmark[42] performed three-body abrasion tests on eight different ceramic materials, including alumina, silicon carbide and sialon. Angular quartz and silicon carbide were used as abrasive particles. It was determined that particle types had a significant effect on the wear rate and the wear mechanisms. The harder abrasive, SiC resulted in higher wear rates than the quartz for all the materials. For quartz, the dominant wear mechanism was brittle fracture, whereas for SiC there was a combination of brittle fracture and plastic deformation. The researchers proposed that high hardness combined with high fracture toughness are necessary for high abrasion resistance in ceramic materials. Olsson, Kahlman & Nyberg[43]

performed tests on four different grades of silicon carbide and alumina. SiC abrasive particles resulted in wear rates 5-10 times higher than alumina abrasive. Both groups of researchers concluded that microstructural features of the surface are important in controlling wear. The features mentioned by Olsson, Kahlman & Nyberg are surface porosity, homogeneity, secondary phases and defect-rich regions.

2.7 Coatings

A commonly used method of improving wear behaviour of materials is to apply a coating of more wear-resistant material to the surface. There are a number of methods by which this may be achieved and they are discussed in the following sections.

2.7.1 Plating and anodizing

Electroplating has been used to coat steels with chromium and nickel, to serve as a hard coating[3]. Metal and alloy coatings are applied by means of electrodepositing the metals from an aqueous solution, and ceramic materials can be deposited from a molten salt bath. Chromium coatings have hardnesses between 850 and 1250HV, and nickel up to 400HV. For aluminium, *hard anodizing* is used to coat the metal in a protective layer with a layer of alumina (hardness of 350-600HV). The layer is formed by the oxidation of the metal and is different to *electrodeposition* in that the material being coated is the anode in the process instead of being the cathode.

2.7.2 Fusion processes

Coating processes in which the coating is applied in a molten state are known as fusion processes. Examples are welding and thermal spraying. Welding, often known as *hardfacing,* is a process suited to applying thick coatings (1mm to 50mm). The surface of the substrate is heated to the melting point of the coating, similar to conventional welding processes.

2.7.3 Vapour phase processes

Coatings may also be applied in the vapour phase. They may be divided into two groups[3]: namely *chemical vapour deposition* and *physical vapour deposition.*

In the process of *chemical vapour deposition* (CVD), reagents of a thermally induced chemical reaction are supplied in vapour form to the heated surface

of a material. A disadvantage of CVD processes is that they generally require high temperatures in the range of 600°C to 1100°C.

Physical vapour deposition (PVD) is a group of processes in which the coating material is introduced to the surface in atomic, molecular or ionic form. The coating material is derived from a gas, liquid or vapour via a physical method, rather than a chemical means. The advantage of these methods lies in the relatively low temperatures at which they are applied (50°C to 500°).

3 LITERATURE REVIEW PART 2

Simulating Wear in a Laboratory

Tucker and Miller[44] listed several requisites for tests of materials to be used in wear applications:

1. The test should duplicate the actual conditions as closely as possible.
2. The geometries of the specimens should be simple so that they can be easily manufactured.
3. The test should be of reasonably short duration.
4. The test should be able to reliably rank materials and the results should correlate well to their observed performance in service, as well as being able to be reproduced in different laboratories.

Tylczak et al[45] state that laboratory wear tests provide a good measure of relative wear behaviour of a materials if the laboratory and the field wear tests exhibit similar mechanisms. Tucker and Miller share the opinion that it is only possible to predict in-service performance quantitatively using laboratory obtained results, in cases where the apparatus is essentially identical to that in service. Therefore, in general, the test variables need to be closely monitored and controlled to provide meaningful wear data. A number of standards have been introduced for testing methods for abrasive wear[46,47]. The standards however, cover only specific types of wear testers, and their guidelines may need to be altered for other non-standard wear apparatuses.

A common problem in considering the wear performance of materials is that there is no established way in which wear losses are reported. Some researchers use the total loss of material from the start of the test to the end of the test divided by the total distance of sliding. Others use the instantaneous rate, namely the loss over an increment of a test, divided by the incremental distance. The first is useful for showing trends in the wear-in period of a material. The second instance is useful if materials are being ranked.

The duration of a test is an important factor to consider when choosing a test procedure. Certain materials may produce different results when measuring the mass loss after different increments of time, or number of wheel revolutions. For example, if small increments are used to test mild steel[44], the mass losses are higher than if larger increments of wheel rotation are used, as seen in Figure 12.

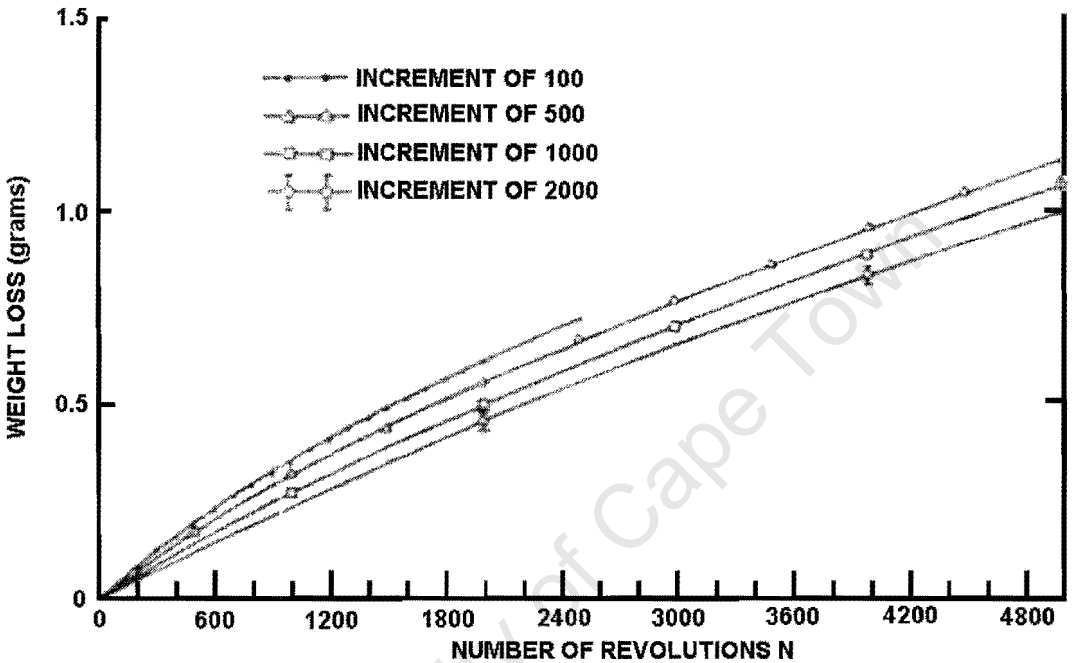

Figure 12 The influence of abrasion test increment size on weight loss of mild steel [after reference 44]

In comparing wear tests to service conditions, care should be taken which abrasive particles are used[3]. Although abrasives such as silicon carbide or alumina are commonly used for industrial applications, the abrasive particles which are naturally found are usually much softer. The particle hardness, shape and size characteristics will control the relative importance of the various wear mechanisms and the wear resistance of materials tested using different abrasive particles may appear to change dramatically.

The compliance of the abrasive support in various abrasive tests will contribute to differences in wear between different types of abrasion[3]. In a rubber wheel abrasion test (discussed in the detail later in this chapter),

particles in contact with harder phases in a two-phase or composite material will penetrate deeper into the rubber, as in Figure 13(a) below. They will thus carry less load than if the support is rigid, as in Figure 13(b), commonly the case in two-body abrasion. Hard brittle phases are thus, more likely to fracture with a rigid abrasive support.

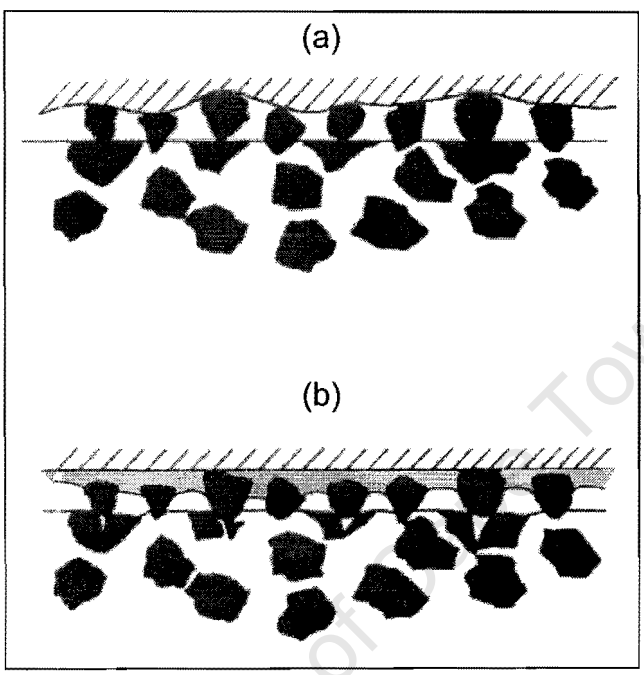

Figure 13 The effect of the compliance of the abrasive support in abrasive wear (a) a rubber backing allows particles in contact with hard second phases to deflect the support, thus carrying less load in contrast with a rigid support shown in (b) [after Hutchings[3]].

Spero, Hargreaves, et al[48] reviewed the test methods for examining the wear associated with the grinding of coal for coal-fired power stations. A number of types of testers are outlined in the following section.

3.1 Tests for gouging wear

One of the few apparatuses to simulate gouging wear is the jaw crusher gouging wear test, which was reviewed by Blickensderfer, Madsen and Tylczak[49]. The test is more severe than most other abrasive wear tests, and as a result the values of the wear coefficient are higher, and the volume losses are larger. A flat plate is moved relative to a stationary plate in an elliptical motion. The mass loss of the plate after a fixed amount of abrasive has been crushed, determines the wear rate of the material. The test was conceived to test the abrasiveness of rocks.

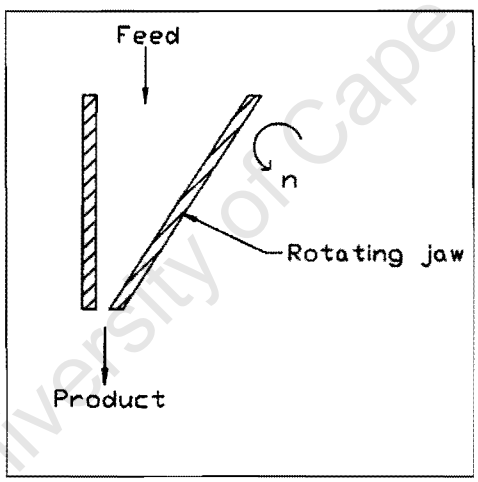

Figure 14 Jaw crusher gouging wear test [after reference 50]

3.2 Low stress wear tests

Low-stress tests are tests in which the majority of abrasive particles remain uncrushed after the wear test. Most of these tests were developed to simulate the low stress abrasion associated with the handling of ores, such as coal.

The first such apparatus is the *Yancey, Geer and Price* (YGP) tester (reviewed by Spero et al[48]), seen below. The YGP test is used by the ASTM as a test for the abrasivity of coal.

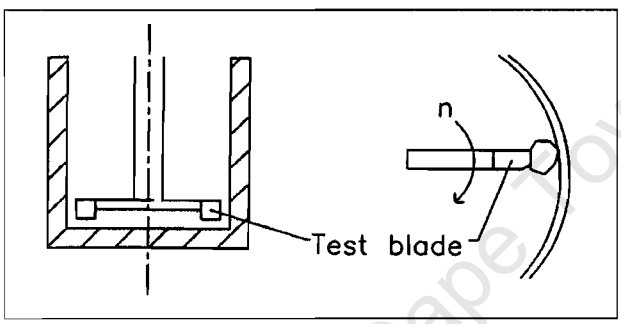

Figure 15 Yancey, Geer and Price (YGP) abrasion test [from Hagström[50]]

The test consists of four carbon steel blades fixed to a rotating arm. This arm rotates in 2kg of dry coal. The abrasion index of the coal is calculated by the ratio of mass loss of metal to the mass of the coal used in the test.

A second, similar type of test, reviewed by Spero et al[48] is the *CE-hammer mill* abrasion test. (Figure 16) This tester has two blades, and it uses a constant flow of abrasive particles through the machine, enabling particles to be used only once. This allows a better control on particle characteristics.

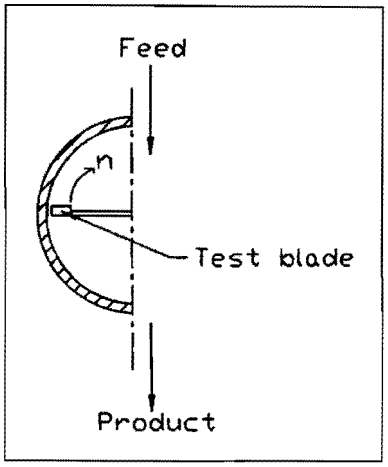

Figure 16 CE-hammer mill abrasion test

The *Tribo-tester or Scieszka*[51] *mill* (Figure 17) is similar to the YGP apparatus, however, it uses only one blade, rotating in a cylindrical container, containing the abrasive. The load is applied by pressing the blade and the holder plate down onto the abrasive.

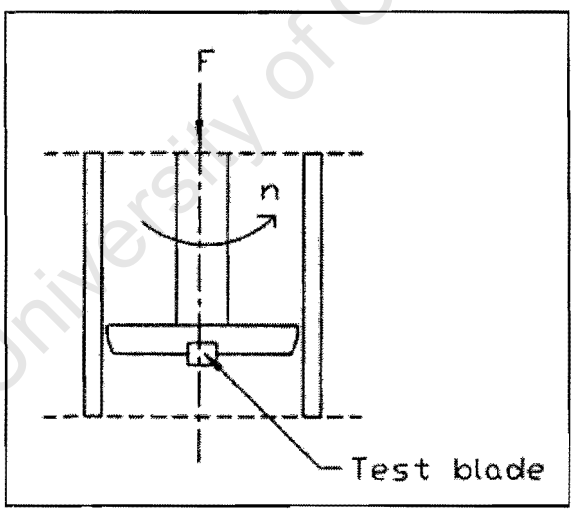

Figure 17 The tribo-tester or Scieszka mill

The *BCURA –roll mill*[48] test differs from the YGP, CE, and the Tribo-testers, in that it causes abrasion by the action of two rollers. The abrasive particles are introduced between the pressurised interface between the rollers.

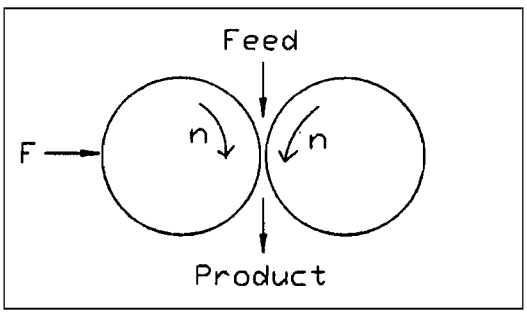

Figure 18 BCURA-roll mill abrasion test

The final low stress three-body abrasion tester that Spero et al considered, is the 10E10 ring and ball mill tester. It is a full scale abrasion test used to test fuel ores. The dimensions of the apparatus, as well as the loads are much higher than other testers. Abrasive particles are fed into the cavity between ring and a ball. The test simulates a ring and ball milling operation.

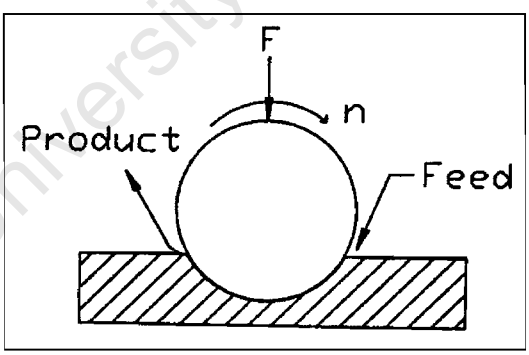

Figure 19 10E10 ring-and-ball mill

3.3 High stress wear tests

These wear tests exert pressure on the abrasive particles so that some of the particles get crushed. The division between low and high stress three-body abrasion is not absolute, owing to the fact that particles may be crushed in any abrasion test to a greater or lesser extent. Nevertheless, a high-stress tester will cause a high degree of crushing of abrasive particles.

The *marked ball wear test*[48], shown below, works in a similar way to an automatic washing machine. 126 balls, fourteen of which are marked, are rotated in a drum, containing abrasive particles. There is a large amount of particle crushing, owing to the small contact area between the abrasive and balls. This results in high stresses. The volume loss of the marked balls is measured, to determine the wear.

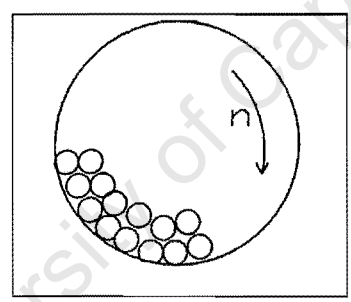

Figure 20 Marked-ball wear test

Another test that uses balls is the *rotating electrode ball wear test*[48]. It consists of three steel balls and a porcelain ball. The steel balls are rotated on top of the porcelain ball. It is used to test mineral ores, oils and greases, to test their abrasiveness. The wear is determined by measuring mass loss of the steel balls.

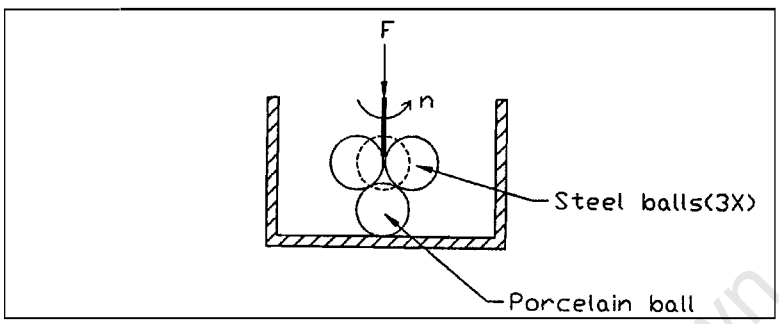

Figure 21 Rotating electrode ball wear test

A final high-stress test is the *loaded abrasive column* wear test[48]. This test is similar to the pin on disc wear test, used in two-body wear testing, but the pin is replaced by a column, containing abrasive particles. The column is pressed against the rotating disc and volume loss measurements of the disc are taken.

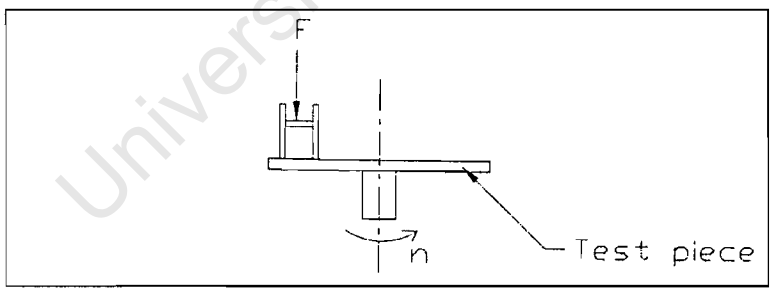

Figure 22 Loaded abrasive column wear test

3.4 Rubber wheel abrasion tests

Rubber wheel three-body abrasion tests were originally used in 1949 by Haworth to test dry three-body wear. Haworth's tester, described in Stevenson and Hutchings' work[17] consisted of a rubber wheel which had shallow grooves in it to pick up abrasive particles from an abrasive tray as the wheel turned. The specimen was in contact with the vertical edge of the wheel. A rubber wheel was used, to maintain the contact pressure on the surface as the specimen wore.

A disadvantage of this apparatus was that the particles were reused, and therefore during the test, it was possible for the particle characteristics to change. The mass of abrasive passing between the surfaces could not be measured. As the specimen wore, the contact between the wheel and the specimen deviated from the 90° tangential contact.

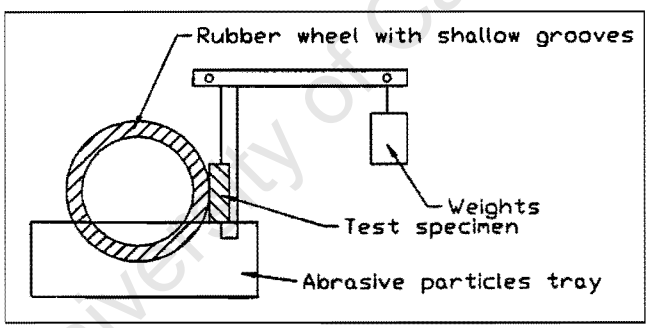

Figure 23 Haworth's rubber wheel abrasion test [drawing from Hagström]

The Abex research centre developed a similar apparatus to Haworth's in the 1950's. Between 1950 and 1978 many materials were tested and characterised using the tester. The design uses a gravity feed to introduce the abrasive between the two surfaces. Thus the particles are used only once and can be collected. It also uses the same lever arm design as the Haworth apparatus, although in a horizontal plane.

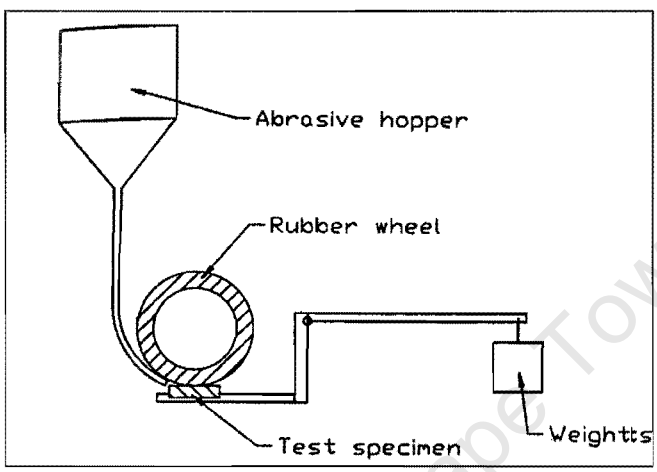

Figure 24 Abex research centre test [drawing from Hagström]

Tucker and Miller[44] used modified Abex apparatus during the 1970's and they used conditions similar to those that became the standard for rubber wheel abrasion testing. A standard was introduced in 1980 (ASTM G65)[46]. The specimen is applied vertically to the wheel. The standard test still has disadvantages, however, including the problem of the changing direction of the normal force, as the material wears. Further disadvantages are the large specimen size (25mm x 76mm x 10mm), which makes testing expensive. The test duration is relatively long (5000 wheel revolutions for very wear resistant materials). Large amounts of abrasive are used for a test (3-4kg). The mass of abrasive used in the test is not controlled during a test. Particles flow by gravity through the interface and are collected below.

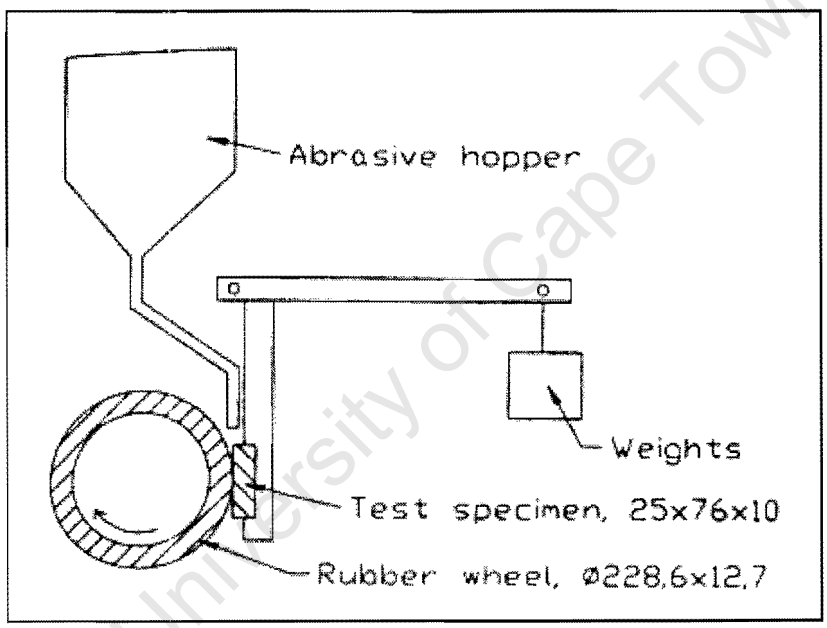

Figure 25 Dry-sand rubber wheel standard test ASTMG65-91

A *standard test*[47] was also developed for wet three-body abrasion testing using a rubber wheel. The standard apparatus has a constant normal force, made possible by using a smaller wheel. Disadvantages are large specimens, long test duration and complicated testing procedure. The slurry circulates, so the particle characteristics cannot be controlled. There is not a constant flow of slurry, and there is no flow measurement.

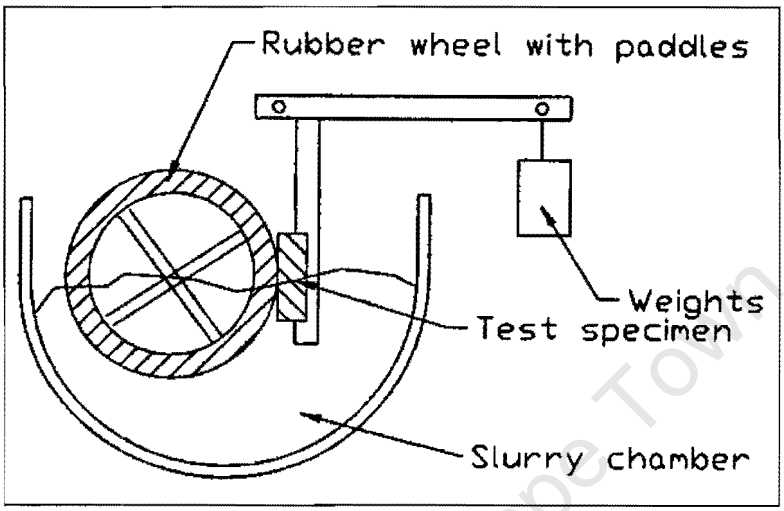

Figure 26 Wet-sand rubber wheel standard test, ASTM G105-89

Hutchings and Stevenson[17] looked at the design of the standard rubber wheel test and they built an apparatus to solve some of the problems associated with the standard test (Figure 27). Their apparatus is one of the most recent three-body abrasive wear test machines. The specimen is horizontally situated, and a load-cell can measure the friction force. The specimen is always perpendicular to the interface of the wheel and specimen. Abrasive particles are fed through a funnel onto a chute, via a rotating drum. The base of the chute is aimed at the interface between the wheel and the specimen.

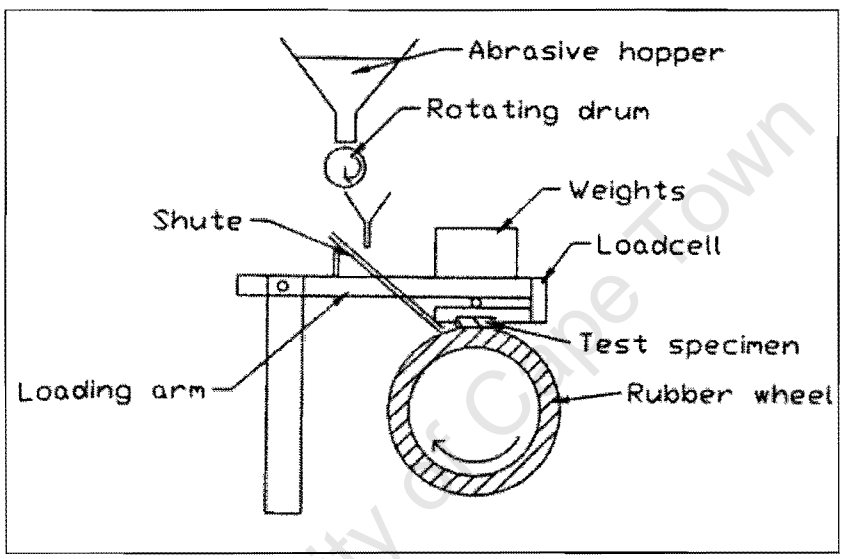

Figure 27 Hutchings/Stevenson design for a dry-sand test standard

Abrasive particles are also collected, and the design allows the particles that fall off the wheel edge, as well as those that move through the interface to be separated.

The disadvantage of this apparatus, and all rubber wheel apparatuses, is that the particles are constrained by the rubber wheel, and are not free to slide or roll. This situation may be seen as two-body abrasion. In general the particles are not crushed during the wear process.

3.5 A wear tester to observe particle movement

Liang Fang, Xianglong Kong and Qingde Zhou[35] designed a wear tester that was capable of observing the movement pattern of abrasive particles, during three body abrasive wear. The tester allowed the movement to be monitored and recorded using a camera. The apparatus was used to calculate the ratio of rolling to sliding statistically and hence the probability of cutting wear.

4 BUILDING THE APPARATUS

Various methods have been developed for testing materials under three-body abrasive wear conditions. In the preceding chapter, they were briefly discussed. To decide on a design for a new tester, it was necessary to critically assess existing testers to determine whether they could be adapted to rank materials for the power generation industry. Table 2 is a summary.

Table 2 Summary of features of various abrasive wear testers

Wear tester	***Features and advantages***	***Disadvantages***
Gouging test		
Jaw crusher	Used to simulate rock crushing, specimens weighed after fixed mass of rock is crushed	Not appropriate for smaller abrasive particles or smaller specimens
Low stress tests		
Yancey Gear and Price YGP	Used to test abrasiveness of coal	Not designed to test materials
CE- hammer mill	Used to test abrasiveness of coal	Not designed to test materials
Scieszka mill	Simulates ball-race coal pulverisor	Only useful for specific application
BCURA roll mill	Abrasive is fed between rollers	Not a simple test specimen
10E10 roll mill	Full scale tester to test ores	Not appropriate, too large
High stress tests		
Marked ball	126 balls, 14 are marked, rotate in a drum containing abrasive	Specimens are balls, difficult to manufacture from new materials
Rotating electrode ball	3 steel ball rotate on a ceramic ball – used to test ores, oils and greases for abrasiveness	Specimens are balls
Loaded column	Column of abrasives pressed against rotating disc specimen	Specimen relatively large & needs machining to disc shape
Rubber wheel tests		
Haworth's rubber wheel	Vertical specimen and recycled abrasive	Contact angle changes, particles may degrade, abrasive adheres to wheel
Abex Research Centre	Horizontal specimen, fresh abrasive	Contact angle changes
ASTM standard dry sand rubber wheel	Widely used test. Mass of abrasive is not measured during the test. Specimen is vertical, simple specimen	Contact angle changes, large amount of abrasive needed, large specimen, long test duration, abrasive adheres to wheel
ASTM standard wet sand rubber wheel	A test to simulate wet three-body abrasion	Contact angle changes, specifically for slurries, slurry recycled.
Hutchings/Stevenson rubber wheel	Abrasive fed from funnel onto rotating drum into 2nd funnel & down a chute, specimen is horizontal	Contact angle changes, abrasive adheres to wheel
Other types of testers		
Fang, Kong, and Zhou	Apparatus is fitted with a camera to observe particles	Too complicated, test designed to observe particle movement

In the present work, the apparatus was required to grade material for possible use in the power generation industry, where both high and low stress abrasion are important. An apparatus was needed which could quickly test many different types of materials, using specimens which are easy to fabricate.

Hagström[50] initially designed an apparatus at the University of Cape Town Department of Materials Engineering, to simulate wear. The present work was a continuation of his work, and it included modifications to his theoretical design, and practical assembly of the apparatus. A large proportion of the project duration was involved with developing the apparatus.

The principal motivation behind a new three-body apparatus was to build an apparatus, which was truly "three-body". The majority of testers used to test materials under three-body conditions use a rubber-wheel type tester. It was felt that a rubber wheel does not accurately simulate three-body abrasive wear, in which the abrasive particles are able to move freely during the test. In a rubber wheel, the abrasive particles embed themselves in the rubber wheel, and the abrasion is caused by particles, many of which are constrained by the wheel. The principal concept of the new apparatus was to test materials using a rigid steel wheel. In industry, many of the situations in which three-body abrasion manifests itself are a result of hard particles or contaminants finding their way between two metal surfaces.

This chapter discusses Hagström's design, and its shortcomings and the process of developing the existing design.

4.1 The original design for the three-body abrasive wear apparatus

Hagström's apparatus, shown schematically in Figure 28, consists of a rotating metal wheel, with a load plate, resting on the wheel. The specimen holder is attached to the load plate. This allows a specimen to be in contact with the rotating wheel and experience abrasive wear. The specimen is held perpendicular to the wheel, which is an improvement on other similar apparatuses. Abrasive particles are fed between the two mating surfaces by means of a chute and three-body abrasive wear of the specimen results.

The load plate is located on four smooth vertical rods, and four Teflon® bushes would provide low friction between the rods and the plate. This plate can move freely in a vertical direction, sliding on the rods. One of the aims of the work was to use ash and sand abrasive particles to test materials, and therefore the apparatus was designed with this in mind.

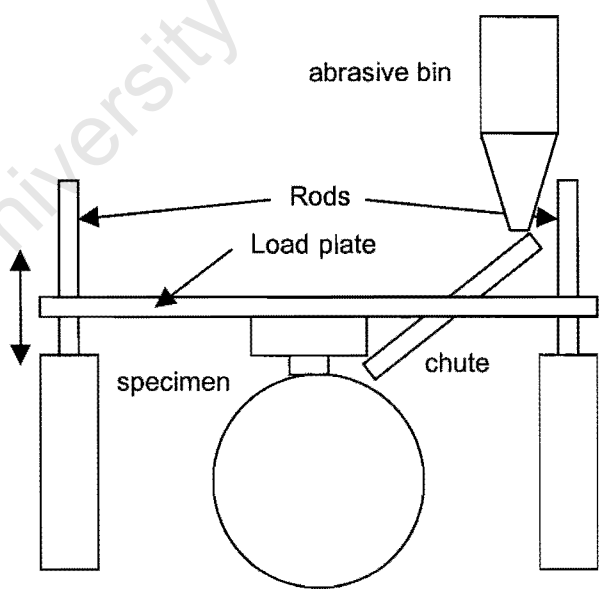

Figure 28 The general layout of Hagström's three-body abrasive wear apparatus

4.1.1 Problems with the original design

The original design was in the process of being built when it became apparent that major modifications were necessary. The most significant problem was that of the load plate and the bushes. It was found that the plate could not slide freely on the rods, owing to the fact that any misalignment of the rods causes jamming against the bushes. The result was that the specimen did not come into contact with the wear wheel at all. This is discussed further in section 4.1.1.2.

4.1.1.1 Feed system

Originally, the design of the rig allowed the abrasive particles to be fed between the wheel and the specimen using a chute. The design of the chute was similar to that of Stevenson and Hutchings' apparatus[17] When the particles reach the bottom of the chute, the movement of the wheel pulls the particles between the two moving surfaces, shown below in Figure 29. The angle at which the chute feeds abrasives to the wheel could be adjusted. In practise, it was found that the chute needed to be machined to precisely fit the profile of the wheel. Although sand particles did flow down the chute, even with a low friction Teflon® chute, the ash particles adhered to the chute, and the effect of gravity was not sufficient to allow the ash particles to slide down the chute.

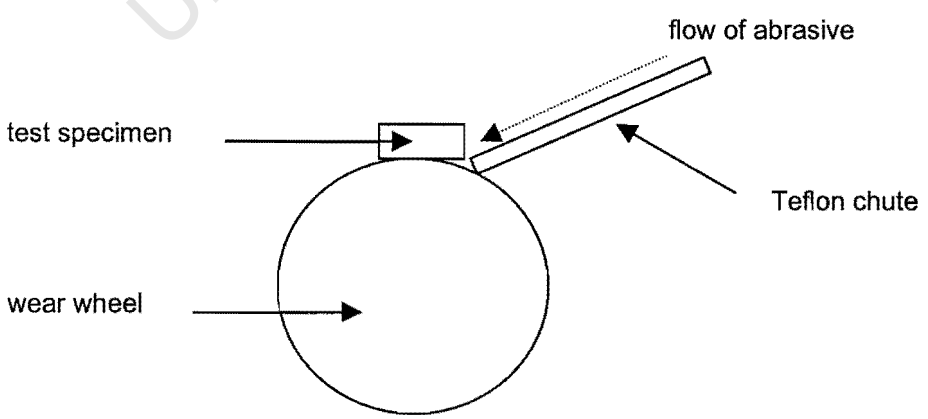

Figure 29 Schematic diagram of the abrasive feed system of the original apparatus

4.1.1.2 Application of load to the specimen

The load is applied by means of an aluminium load plate which "floats" with the aid of four low-friction Teflon® bushes on four vertical rods, shown schematically below.

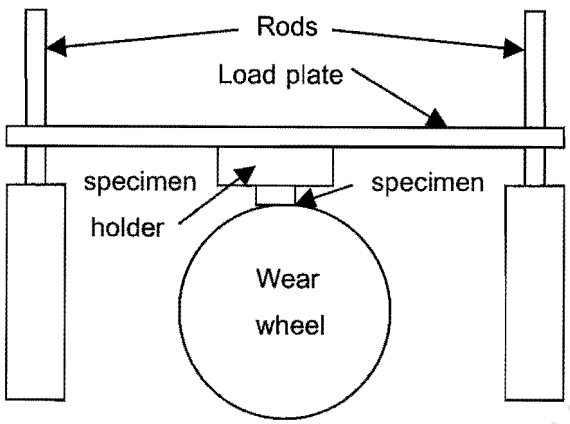

Figure 30 Schematic drawing of the original three-body wear apparatus showing the aluminium load plate of the original design, supported by four vertical rods.

The specimen holder is situated in the centre of this aluminium load plate above the wheel, and thus rests on the wheel. The load plate did, however not work in practise. For the plate to slide freely up and down the four rods, it is necessary that the rods are perfectly smooth and perfectly vertical at all times.

Although the rods were machined to a very smooth surface finish, the plate did simply not slide on the rods. The reason for this is that it is very easy for the rods to be misaligned from the vertical in any axis. Even a slight misalignment of the rods at their base, causes a displacement at the rod end which is considerable (between 0mm and 5mm). This was discovered when assembling the original three-body apparatus. It is assumed that, even if the rods were perfectly aligned, it is likely that the load plate would have become jammed when the wheel was rotated. The rotation of the wheel in contact with the specimen causes a friction force, which is parallel to the plate, and orthogonal to the direction of movement of the plate on the rods, causing the rods to jam against the bushes owing to these lateral forces.

4.2 The current design for the three-body abrasive wear apparatus

4.2.1 Overcoming problems with the original design

4.2.1.1 The new feed system

Hagström's design used a chute to introduce the abrasive to the specimen-wheel interface. The angle of the chute could be adjusted to change the mass flow rate of the abrasive down the chute. The chute had the disadvantage that sometimes the abrasive particles bulked in the chute, resulting in an erratic delivery of abrasive particles to the specimen-wheel interface. There was no way to control this.

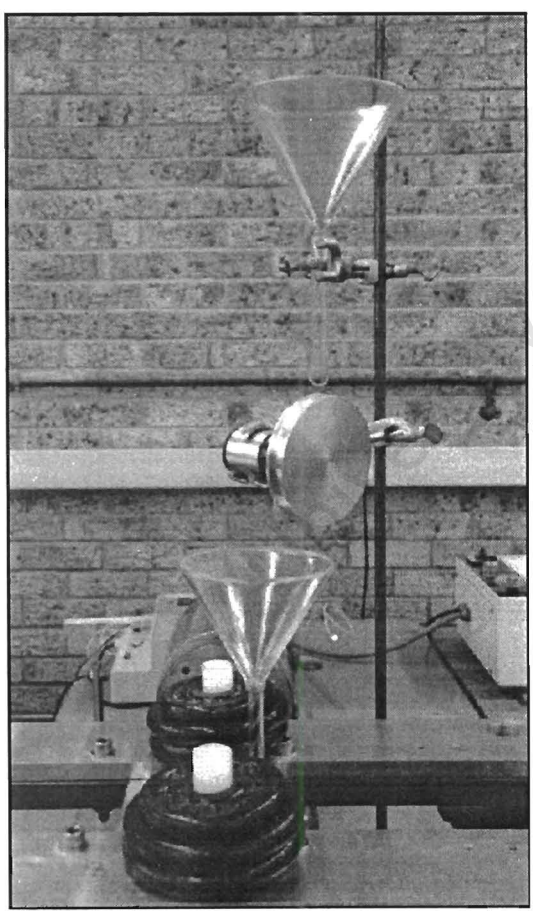

Figure 31 The two-funnel abrasive feed system

The new feed system uses two funnels to introduce the abrasive (as seen in Figure 31). The top funnel feeds abrasive onto a rotating wheel, which is connected to an electric motor. The motor's speed can be controlled. The aluminium wheel has a groove machined in its circumference and the surface of the groove has a smooth surface finish so that the abrasive flows freely off the wheel as it turns. The wheel is positioned so that the abrasive falls off the wheel and into a bottom funnel.

The bottom funnel passes through the specimen holder, delivering the abrasive to the interface between the wear wheel and the test specimen (Figure 32).

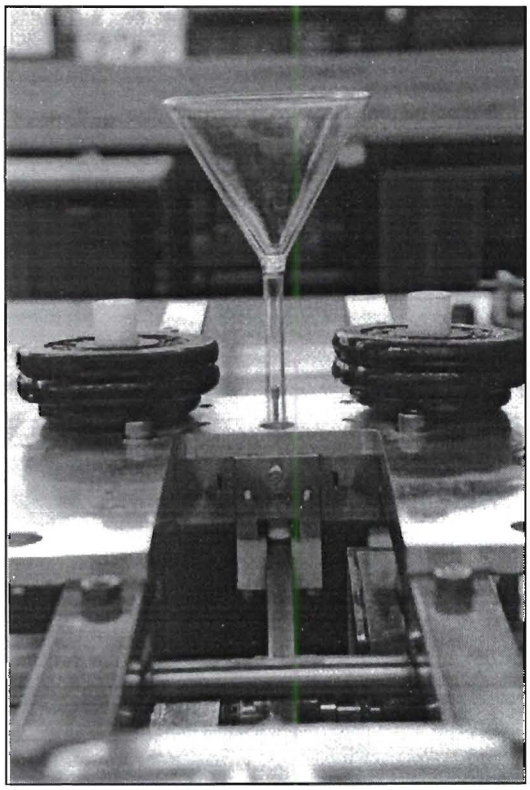

Figure 32 A view of the bottom funnel of the feed system showing the funnel feeding abrasive through the specimen holder onto the wheel

A further modification to the specimen holder was the use of acetal polymer blocks attached to the sides of the specimen holder (seen below, in Figure 33).

These blocks extend down the side of the wear wheel, and provide a cavity for the abrasive particles to fill as they exit from the base of the funnel. A detailed drawing of the specimen location and the feed system can be seen in Appendix A, page ii.

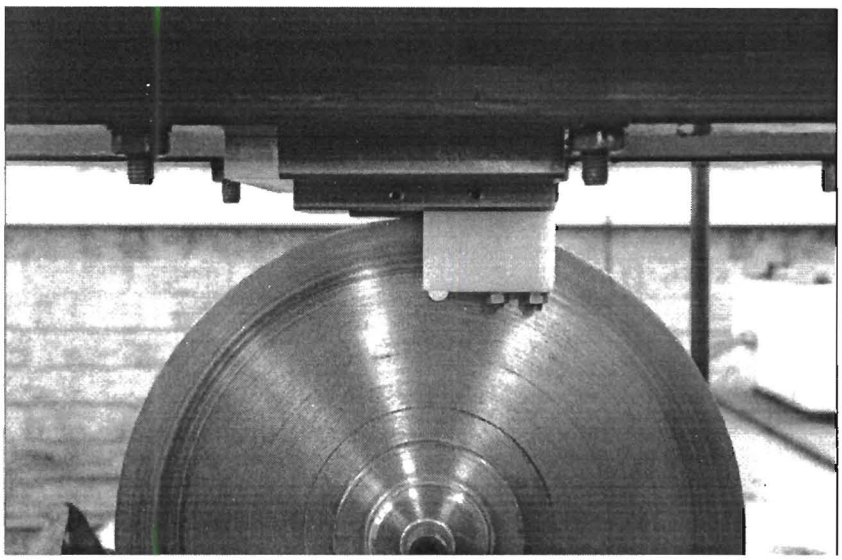

Figure 33 The wear wheel showing the polymer blocks to shield sand from falling down the side of the wheel.

4.2.1.2 Applying the load to the specimen

As it was clear that the 'floating' load plate would not work, it was necessary to modify the load plate. The simplest way to do this was to use a traditional pivoting arm to apply a force to the wheel. The original reason why this was not done was because Hagström[50] wished to have the specimen constantly perpendicular to the wheel, even when the wheel wore. This was accounted for by introducing a height adjustment system, by which the plate could be lowered frequently so that it always lay exactly horizontally on the top of the wheel and hence the specimen was always perpendicular to the top edge of the wheel. Testing with the mild steel wheel and frequent measurement of the wheel diameter showed that the rate of wear on the wheel was not so significant that the diameter changed during a test.

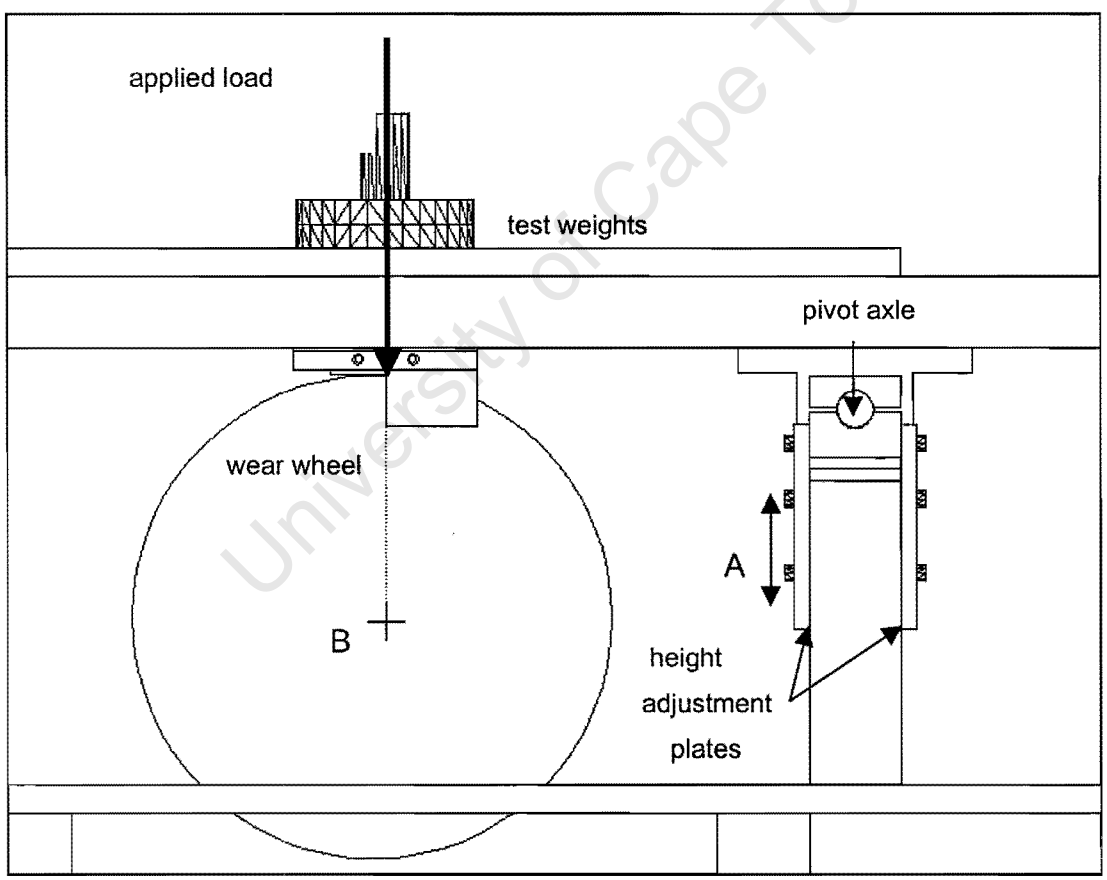

Figure 34 Side view of the modified three-body apparatus showing height adjustment system and the application of load through the wheel centre. As the wheel wears, the adjustment plates can be lowered (A) so that the load-line is always through the wheel centre (B).

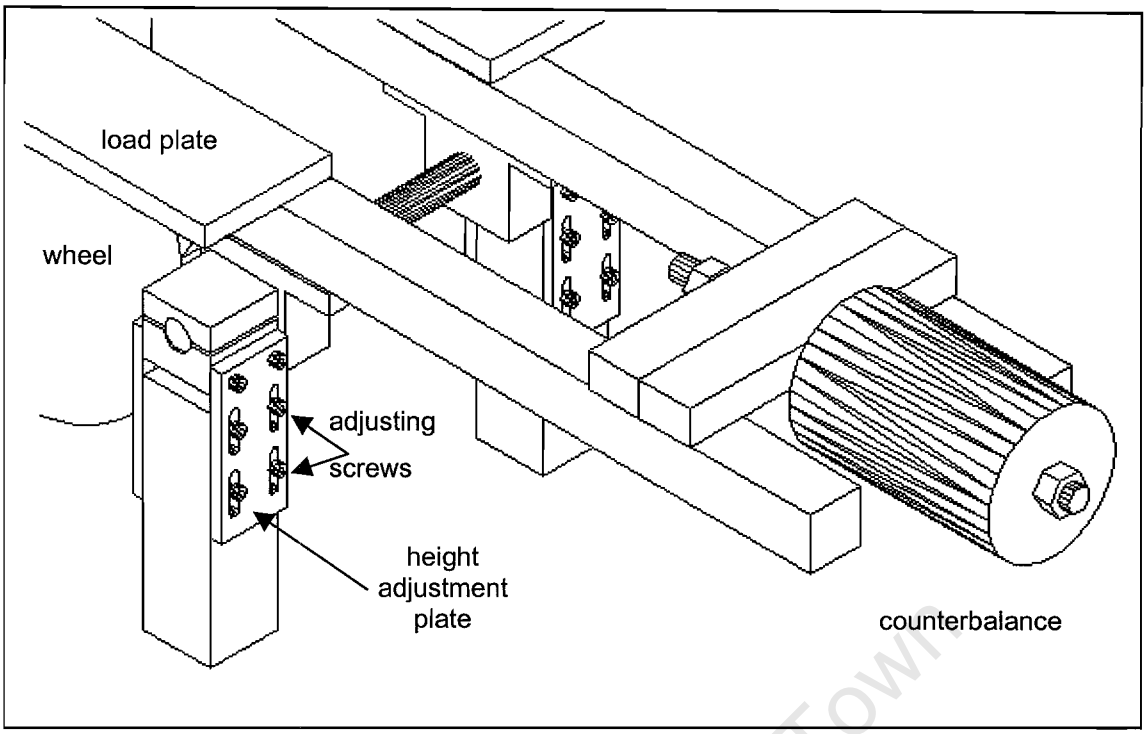

Figure 35 Detailed view of the apparatus, including the height adjustment system and the counterbalance, which is adjusted to zero the load on the specimen by turning a nut.

The current design has the load plate attached to a pivoting frame. The specimen holder is attached to the under side of the load plate, allowing the specimen to come into contact with the wheel. There is a counterbalance on the other end of the frame, which is adjustable to effectively zero the load that is applied to the specimen holder. This is achieved by turning a nut, which moves a steel cylinder along a threaded bar. Fine adjustments can be made until there is no load being applied to the specimen.

4.2.2 Replacement of the gearbox

The original gearbox that Hagström used, provided a maximum tangential wheel velocity of 0.314 $m.s^{-1}$. To provide a greater range of velocities, the gearbox was replaced with a gearbox of a high transmission ratio. The new gearbox enabled the wheel velocity to be varied in the range $0.05m.s^{-1}$ to $1.5m.s^{-1}$ enabling both low velocity and high velocity abrasion tests to be performed on the apparatus.

4.2.3 Summary of the features of the current apparatus

The current design incorporates the features of a number of different designs for three-body abrasion testers. It also incorporates innovative ideas. The combination of *two funnels and a feeder wheel*, uses an idea that Stevenson and Hutchings developed[17]. However, its usefulness is enhanced by feeding the abrasive particles through the specimen holder with the aid of a nozzle attached to the funnel base. Furthermore, the polymer *abrasive guide blocks* help to deliver an even flow of abrasive to the specimen-wheel interface. This is considered a vast improvement over the feed systems of both Stevenson and Hutchings, who fed the abrasive through two funnels and then into a chute, and Hagström[50], who used a gravity feed from an abrasive bin into a chute. The elimination of a chute enabled abrasives which do not flow easily, such as ash, to be used. Ash flows through the glass funnels and over the aluminium feeder wheel which are low friction, into the cavity behind the test specimen.

The problem of maintaining the tangential contact between the wheel and the specimen as the wheel wore, was overcome by developing a *height adjustment system*, by which the load plate could be adjusted periodically to compensate for the change in diameter of the wheel as the wear wore.

A *counterbalance* located on the frame of the apparatus allowed the load on the specimen to be essentially zeroed by the simple adjustment of a nut. Once this was achieved, the load applied to the centre of the load plate represented the load that was applied to the interface.

The selection of a *steel wear wheel* was one of the most significant differences between the current design and Stevenson and Hutchings' apparatus, which used a rubber wheel. Whereas a rubber wheel adheres to the abrasive particles as they move between the wheel and the test specimen, indicating two-body abrasion in which the abrasive particles are constrained, particles are able to move more freely between a steel wheel and

a specimen, providing a more accurate simulation of three body abrasive wear.

Versatility of specimen size is ensured by using *dummy specimens*, which locate an undersize specimen within a standard sized specimen.

Table 3 summarises the features and specifications of the current apparatus.

Table 3 Key features of the new apparatus

Feature	***Description***
Wheel type	Mild steel of diameter 250mm
Orientation of test specimen	Horizontally located above the wear wheel
Loading system	Pivoting load arm with counterbalance to zero the load
Abrasive feed system	Top funnel feeds abrasive onto a grooved feeder wheel with adjustable speed, and then into bottom funnel Base of funnel feed protrudes through specimen holder
Specimen dimensions	15mm thick 50mm long 25mm wide dummy specimens can accommodate specimens of smaller dimensions
Velocity range	0.36rpm to 115rpm equivalent to 0.05m.s^{-1} to 1.5m.s^{-1}
Compensation for wheel wear	Height adjustment system for the pivot axle, ensures specimen is horizontal
Abrasive type	Silica sand and ash have been tested, any abrasive possible Particles are not recycled during test
Abrasive size range	25µm to 1000µm (at least)
Load range	1N to 1000N

5 EXPERIMENTAL PROCEDURE

A number of different types of tests were performed to investigate the effect of changing parameters pertaining to three-body abrasive wear. The parameters which were varied, were applied load, abrasive particle size, abrasive type, abrasive feed rate and test material type.

5.1 Specimen Preparation

Mild steel specimens were used for all of the general three body abrasive wear testing. Mild steel was chosen because it is normally employed as the standard in wear testing and its properties are well known. The specimens were machined on a milling machine and then ground to a surface roughness of 1.2μm R_a. The mild steel specimens had dimensions of 25mm by 50mm with a thickness of 15mm. This size allowed each specimen to be used for four different tests with each wear test being performed on a different position on the specimen.

Other wear-resistant materials which were tested, were used for only one test per specimen. The materials were supplied in different plate thicknesses and sizes. A full list of these materials, together with their nominal compositions is shown in Appendix B. For the materials supplied in sizes thinner than the standard specimen sizes of 25mm by 50mm by 15mm, a "dummy" specimen was machined (Figure 36). These dummy specimens were machined from stainless steel and they had the dimensions of the standard specimen. A recess was machined in the dummy specimen into which the smaller specimen could fit. Thus the small specimen was housed in the dummy specimen of standard size. This was inserted into the specimen holder and the test was performed in the usual manner. During the wear test, the dummy specimen is not in contact with the wheel and thus does not experience wear. The metal specimens were machined on a milling machine and then ground to a surface roughness of 1.2μm R_a parallel to the wear direction. The ceramic specimens, and the tungsten carbide composites were tested in the as received state, with no surface grinding. Where necessary they were cut to the correct dimensions using a diamond wheel.

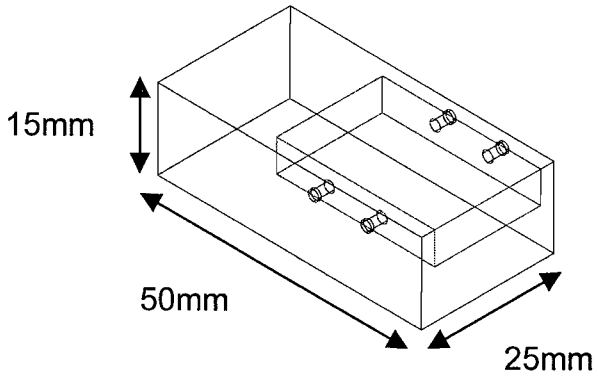

Figure 36 A dummy specimen showing the position of the smaller test specimen. The smaller specimen is held in place by grub screws

5.2 Abrasive particles

Silica sand and ash particles were used for abrasive testing. Sand was selected because it is widely available, and it is commonly the cause of abrasive damage in situ. Ash was used in order to compare its abrasivity with that of silica since the abrasion experienced in the power generation industry is mainly due to contact with ash.

5.2.1 Sand

Silica (SiO_2) sand was obtained from *Consol Industrial Materials.* The sand used for testing was Consol number 2 silica sand. The sand was sieved using *Kingtest* sieves that had mesh ranging from 38μm to 1000μm. The sieves were vibrated using a *Fritsch* vibratory sieving apparatus. After each 30 minute batch of sieving, the sieves were cleaned using a laboratory air hose, and a soft brush.

5.2.2 Ash

Ash was obtained from *Eskom TSI.* It was sourced from various coal-fired power stations throughout the Mpumalanga province of South Africa, so that a representative ash was used for test purposes. This ash was kept consistent throughout the testing procedure.

5.3 General three-body abrasive wear tests

The specimen was first cleaned ultrasonically in alcohol and then weighed on a *Sartorius* digital balance with an accuracy of 0.1mg. Before weighing, the specimen was dried using a hairdryer and left to stand for sufficient time for the specimen to reach room temperature (usually ten minutes). After the mass of the specimen had been recorded, it was clamped in the specimen holder and placed in position above the wheel in the apparatus. The funnel was inserted through the specimen holder and then the abrasive particles were inserted into the top funnel. For the majority of tests, a measured mass of 50g of sand was used for each run. The motor was switched on, at a velocity of 24 revolutions per minute, which translates to a tangential velocity of 0.314 $m.s^{-1}$. This was the slowest velocity that was possible using the original gearbox and motor. Testing was performed using two different procedures which are discussed in the following two sections.

5.3.1 Tests in which the flow rate of the abrasive particles was the controlling factor

The time required for 50g of abrasive to pass through the rig with a wheel velocity of 0.314 $m.s^{-1}$, was 43 seconds. This was monitored for each test to ensure that the feed rate between the wheel and the specimen was a constant 70g per minute. After the gearbox had been replaced with one of a higher transmission ratio, it was possible to obtain velocities which varied from 0.05 $m.s^{-1}$ to 1.5$m.s^{-1}$.The velocity of the test was kept standard at 0.314 $m.s^{-1}$ to allow comparison with other results.

This process was repeated 4 times for each specimen, with the mass loss being measured each time. This allowed a graph of cumulative mass loss of specimen versus cumulative abrasive to be plotted. As the wear rate reached a steady state, the slope of the graph was an indication of the specific wear rate. The specific wear rate for this type of test was defined as the cumulative mass loss of the test specimen per cumulative mass of abrasive particles. To account for density differences when comparing different materials, the wear rate was converted to a specific volume wear rate by dividing the mass loss

by the density of the material. The resulting specific volume wear rate may be defined as the cumulative volume loss of a specimen per cumulative mass of abrasive particles.

5.3.2 Tests in which the number of wheel revolutions were the controlling factor

The second type of tests used to characterise materials were tests in which a mass loss (converted to a volume loss) was measured after a single test run of a set number of wheel revolutions. This is equivalent to the specimen sliding in contact with the wheel over a set distance. For these tests the wheel velocity was also set at $0.314 m.s^{-1}$ and the test duration was 2 minutes. This translates to a distance of 38 metres. The abrasive feed rate used for these tests was the limiting feed rate w_{lim} defined by Stevenson and Hutchings[17] in which the abrasive was allowed to flow freely into the cavity behind the specimen-wheel interface. There was thus a "saturated" flow of abrasive particles which could be pulled between the wheel and the specimen as the wheel turned.

5.4 Tests to determine the effect of load applied to the specimen

Abrasion tests were conducted on the apparatus using a range of different weights. For this set of tests, the feed rate was kept at 70g.min^{-1} and the wheel velocity at 0.314m.s^{-1}, and the test was performed as described in 5.3.1. The weights were placed on the weight holder directly above the point of contact between the specimen and the wheel. The weights corresponded to different loads being applied during the test, and hence different stresses on the specimen. The loads that were used are tabulated in Table 4. Before the loads were added to the apparatus, the load on the specimen was zeroed, by adjusting the nut of counterbalance, until there was negligible load on the test specimen. This was measured by placing a button load-cell, which was mounted inset in a test specimen, in the specimen holder.

Table 4: Loads used for three-body abrasion testing

Applied load (N)
3
20
40
60
90
100

5.5 Tests to determine the effect of particle size

The different ranges of particle size, which were obtained from sieving, were used to perform abrasion tests. The particle size was taken as the average of the largest and smallest particles in the size range. The tests were performed using the methods outlined in 5.3.2. with a test duration of two minutes. Silica sand particles were used as the abrasive for the tests.

5.6 The effect of the position of the wear scar on the wear resistance

Tests were performed on two identical test specimens. The first test specimen was tested using the standard test procedure of section 5.3.1. The second specimen was also tested at a wheel velocity of 0.314m.s^{-1} and a feed rate of 70-g.min^{-1}. Each run of the test exposed an unworn part of the specimen to wear. The purpose of this test was to determine whether there was a difference in the wear rate if each run of the wear test was done on virgin material and as opposed to tests which were continued in a position that had already been worn. The mass losses of the two identical specimens were compared.

5.7 Tests to determine the effect of introducing abrasive between two moving surfaces

A wear test was performed on a mild steel specimen using a mass feed rate of 70g.min^{-1}and the standard test procedure of 5.3.1. The rate was plotted as a relationship between mass loss and time. A second specimen was tested in a similar manner. However, for the second specimen, no sand was fed between the wheel and the specimen. the test was run for a total time which was the same as the test performed using abrasive. These tests showed the relative severity of the abrasive wear when metal-on-metal with sand between was compared with metal-on-metal without sand between the two surfaces.

5.8 Hardness tests

5.8.1 Macrohardness tests

Hardness tests were performed on each of the materials, on a *Vickers* hardness tester using a Vickers diamond pyramid, and a load of 30kg. An average was obtained after 10 tests.

5.8.2 Microhardness tests

A *Matsuzawa MXT α7* digital microhardness tester was used to measure the hardness of the abrasive particles. The particles were mounted in an epoxy

resin, and then polished so that the particles were exposed at the surface of the resin. The hardness tester microscope was used to position the indentor diamond in the centre of the exposed surface of the particle. Ten measurements were taken and an average hardness was calculated.

5.9 Surface roughness measurement

The roughnesses (R_a) of the specimens were determined using a *Surtronic 3P* surface profilometer, with a stylus traverse of 25mm. An average of 10 readings was taken. On machined specimens the roughness was taken perpendicular to the machining direction.

5.10 Microscopy

5.10.1 Scanning Electron Microscopy

5.10.1.1 Abrasive particles

Abrasive particles were viewed using scanning electron microscopy (SEM). A *Cambridge S200 microscope* was used and a 20kV acceleration voltage. The particles were first sputter coated with a layer of conductive gold-palladium so that an improved image of the ceramic particles could be obtained. The images were produced using secondary electrons.

5.10.1.2 Abraded surfaces

Metal specimens were ground and then polished to a mirror finish. They were then tested using a very small number of abrasive particles. They were sputter coated with gold-palladium for three minutes, so that there was no excessive charging of the specimen in the SEM. They were examined using the secondary electron detector on the SEM. Energy dispersive spectroscopy (EDS) was used to identify surface features elementally.

5.10.2 Optical Microscopy

Optical microscopy was performed using a *Reichert MeFsA* metallurgical microscope to characterise the microstructures of test materials.

6 RESULTS AND DISCUSSION

6.1 Abrasive parameters

As abrasive particles play an important role in abrasive wear, it is necessary to determine the particle characteristics such as shape and hardness when using abrasives for three-body abrasive wear. The particles were characterised using scanning electron microscopy and using a microhardness tester.

6.1.1 Characterisation of the abrasive particles

The abrasive particles were sieved and the sizes obtained are tabulated below. The mean was calculated for each of the ranges and was used as the particle size when plotting the results of wear tests.

Table 5 The particle sizes obtained from sieving silica sand abrasive

Particle size range	*Calculated mean particle size*
38µm to 63µm	51µm
63µm to 106µm	85µm
106µm to 125µm	116µm
125µm to180µm	153µm
180µm to 250µm	215µm
250µm to 425µm	338µm
500µm to 600µm	550µm
600µm to 710µm	655µm
710µm to 1000µm	855µm

6.1.1.1 SEM of Sand particles

Scanning electron microscopy (SEM) images of silica of different size ranges showed that the particle shapes did not vary significantly between the smaller and larger sizes (Figure 37 and Figure 38). The particles were found to be of a variable shape, with rounded edges. Some of the particles are elongated, but the large majority were approximately equi-axed.

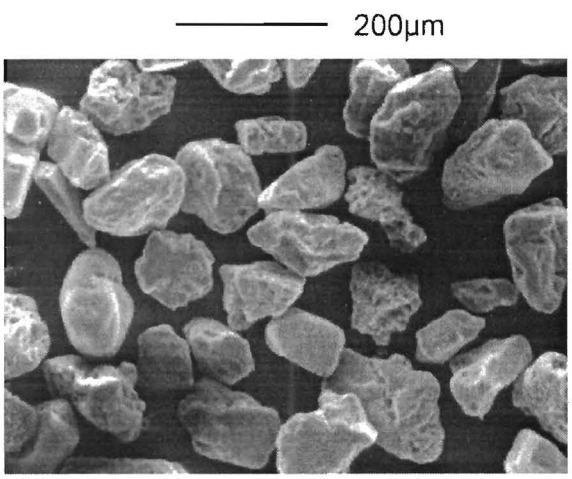

Figure 37 Silica sand particles of size 63µm-106µm. The edges of the particles are rounded.

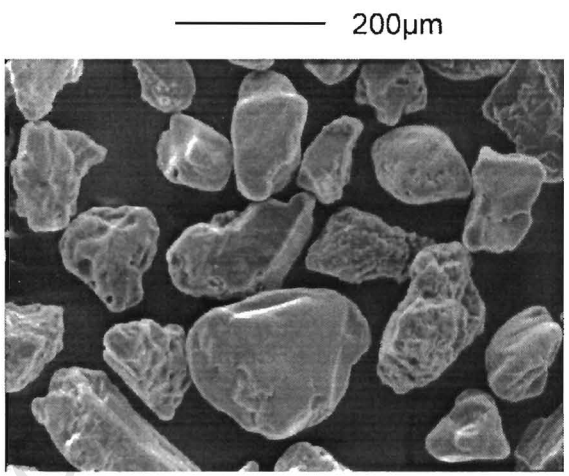

Figure 38 Silica sand particles of the size range 180µm-250µm. The particles appear similar to those of the smaller size range shown in **Figure 37.**

6.1.1.2 SEM of ash particles

The ash abrasive used in testing had a particle size less than 180µm and consists of a number of particle types as seen in Figure 39 and Figure 40. The majority of the ash is made up of conglomerates of smaller particles, which contain porosity and unburned coal. Some are spherical in shape, although they are not solid. Such ash is very friable and tends to fracture readily during testing. This size range was selected for ash, since Suckling[52] has shown that 80 to 90% of fly ash has a particle size of between 2µm and 500µm and approximately 95% of this fly ash is smaller in size than 125µm. This fly ash causes the majority of abrasive wear problems in the power generation industry in South Africa. Therefore, the size range selected for the testing was considered representative of the fly ash found in power stations in South Africa.

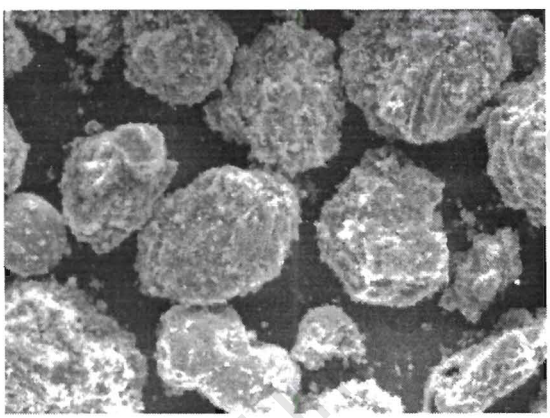

Figure 39 Ash particles of a rounded, non-spherical shape. Smaller ash particles adhere to the surface of the particles.

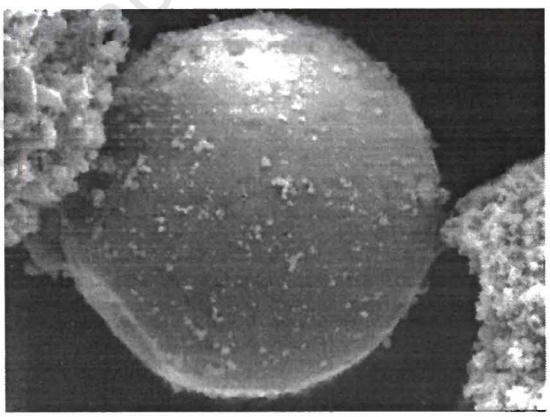

Figure 40 A spherical ash particle

The results of testing with fly ash, were compared to the results found in similar circumstances with silica sand in the same size range.

6.1.1.3. Microhardness tests

The average hardnesses obtained using the microhardness tester for the two types of abrasives used in this study are tabulated below. There was a large variation in the values for ash. Owing to the irregular nature of fly ash particles, it was difficult to measure the surface hardness. For both particle sizes, the hardness of 125µm to 180µm size range was measured which was also considered to be representative of all the ash and silica employed.

Table 6 The hardnesses of the abrasive particles used

Silica hardness	1308 HV 100gf
Ash hardness	927 HV 100gf

6.1.2 Testing the effect of particle size

The results of a set of tests, which were performed using fixed test duration, with silica sand are plotted in Figure 41. It shows that the volume loss does not vary greatly in the range 50μm to 180μm although it could be considered that there is a gentle increase of volume loss with particle size in this range. Above a particle size of approximately 200μm the volume loss follows a steady and significant decrease with an increase in abrasive particle size. There is also evidence that above a particle size of 600μm the volume loss with increasing particle size levels off to a constant value.

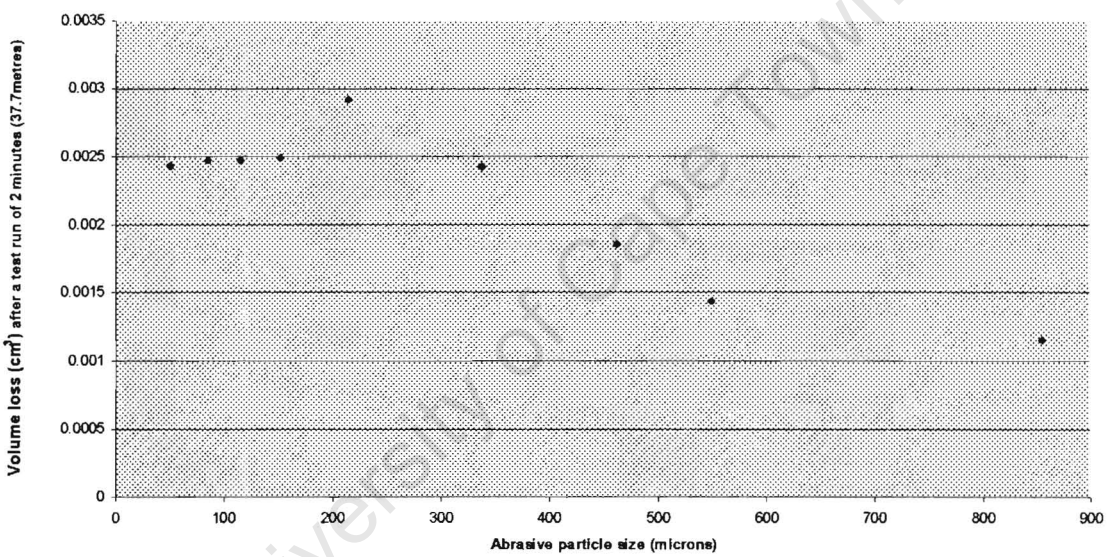

Figure 41 Average volume losses of mild steel using 50N load and varying the sand particle size

If the surfaces of the worn specimens are examined, as seen in the macro photographs shown in Figure 42, it is interesting to note that the wear scar becomes larger for the larger particle sizes, even though the volume losses with large silica sand particles are lower. The damage caused by the particles of sizes smaller than approximately 180μm is confined to a smaller area on the surface of the specimen. If the area of damage is smaller, it is apparent that the depth of the wear scar must be higher for the smaller particle sizes,

because the volume losses are higher. This suggests that smaller particles are more efficient at removing material than large sizes of silica.

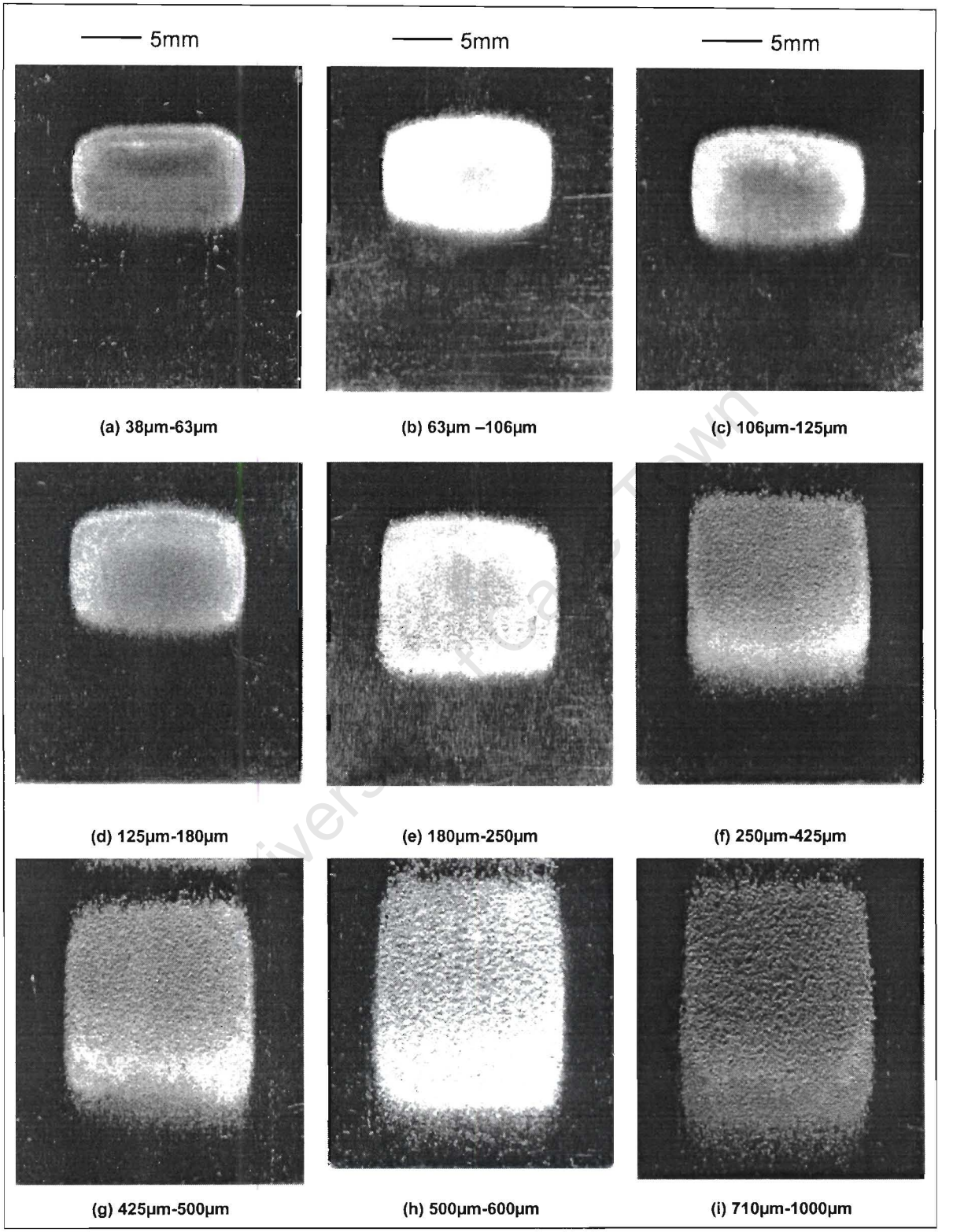

Figure 42 The wear scars on mild steel specimens abraded using various particle sizes at a load of 50N. (Wear occurred from the bottom to the top)

One simple possible explanation of the decreasing volume losses with increasing particle size can be offered if consideration is given to the stress on the particles at the point of contact. The nominal stress at the point of contact, using the assumption of an even distribution of load over the area, is lower for the larger particle sizes because the wear scar is larger and thus the wear is lower (Figure 43). However, this does not take into consideration that in reality the stress on the portion of large particles in contact with the surface of the counterface will be larger than those of smaller particles. Further it does not explain the approximately constant value of wear observed for the size range below 180µm.

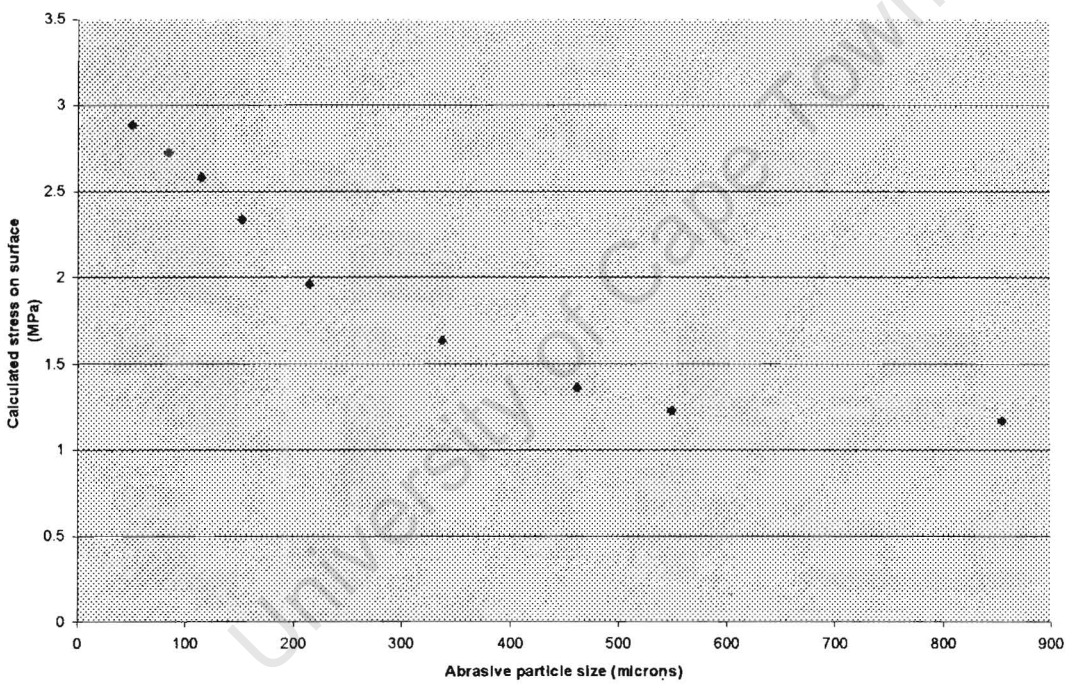

Figure 43 The calculated stress on the surface of mild steel specimens tested using 50N load and various particle sizes

Explanations for these changing wear rates with changing particle sizes have occupied a number of workers. Mulhearn and Samuels[13] attributed a critical size effect (i.e. no further increase in wear with increasing particle size above a certain particle size) to differences in mechanical properties between large and small abrasives. Miller[14] observed a critical size above which, there was no further increase in wear, with particle size. For low loads, the wear decreased above the critical particle size. The critical size effect observed by

Rabinowicz and Mutis[12] was explained by large adhesive wear particles separating the test specimen and the surface.

It is proposed that the present trend of decreasing volume loss with increasing particle size, can be attributed to a similar phenomenon to that observed by Rabinowicz and Mutis[12]. Although no adhesive wear fragments were observed during the present testing, observation of the wear tests in progress showed that the two wear surfaces (the wheel and the specimen) were forced apart by the abrasive. The larger particles within a particular size range separate the wear surfaces, allowing the small particles within the size range to move freely between the two surfaces without contact, causing relatively low volume losses. As the nominal particle size increases, the larger particles separate the surfaces to a greater extent than the larger particles in a smaller size range so that even fewer particles are able to the remove material from the surface of the specimen. Quantification of the degree of the to which the surfaces separated was however, difficult.

In the smallest size ranges virtually all of the particles come into contact with the steel wheel making the removal efficiency high. With larger particles in this range, the stress per particle is larger, yet the number of particles in contact with the surface is lower and so the wear rates do not change significantly. At a critical size, this changes, and the larger particles move the surfaces apart sufficiently that some particles start to pass through without affecting the steel surface, and so the wear decreases with increasing particle size.

implying that more material is removed by a larger particle than by a smaller particle. At first this may seem to contradict the results in Figure 41 but the results in Figure 41 represent volume losses on a specimen using a fixed volume of abrasive, which will consist of considerably more particles for small particle sizes than for large particle size. These results show in general that smaller particles remove more material per unit mass of abrasive than larger particles. However, if the material losses are viewed in terms of losses per particle it is clear then that a single larger particle will remove more material than a smaller particle.

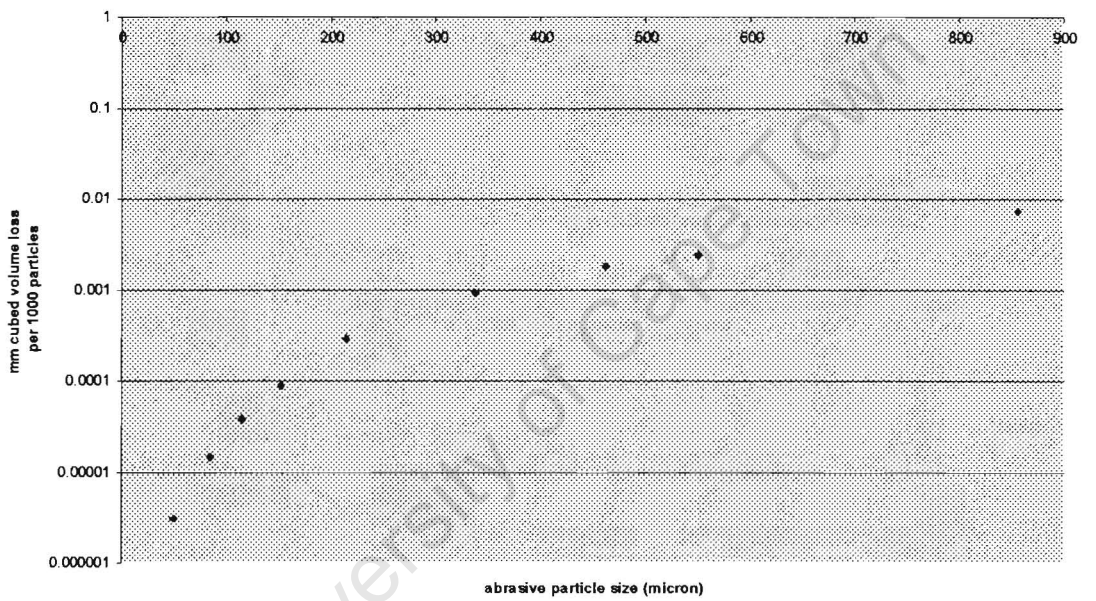

Figure 44 The volume loss per particle for mild steel specimens tested using different sized particles. The load used was 50**N.**

6.2 Changing test parameters

6.2.1 The effect of load

A series of tests was performed using mild steel specimens abraded against 125μm to 180μm silica sand using loads of 3N to 100N. The trend that was observed was essentially linear, with most of the data points lying very close to a best-fit line as seen in the chart below.

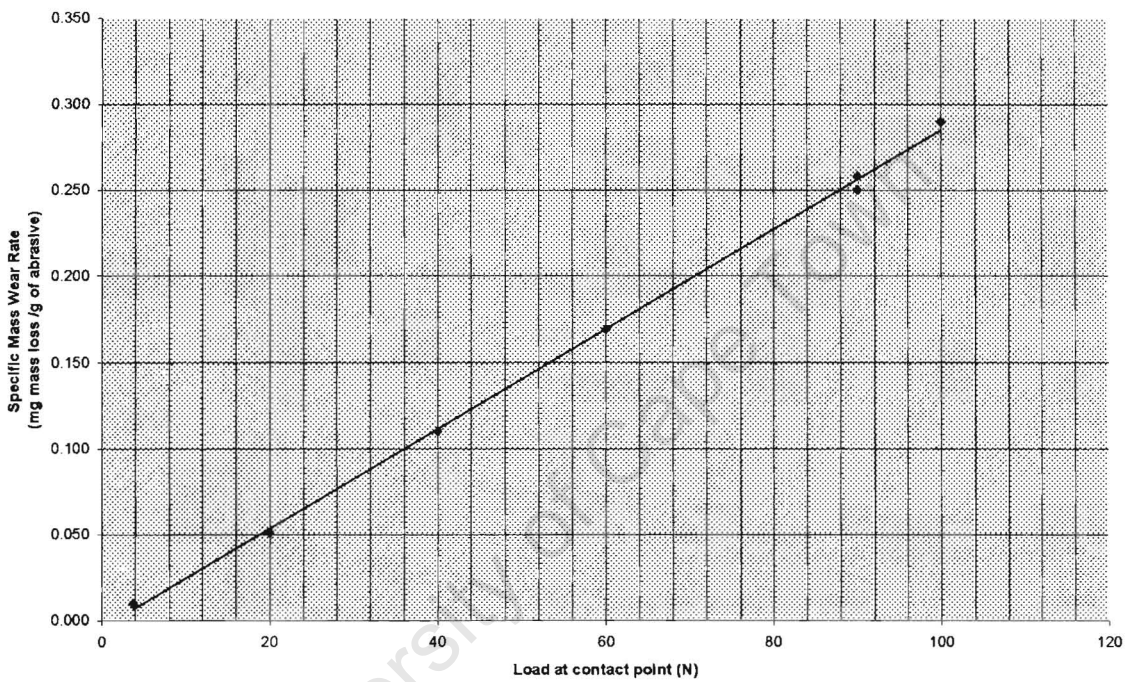

Figure 45 The effect of load on wear rate of mild steel using 125μm to 180μm silica sand

The results agree with those that Misra and Finnie[2] obtained for two-body abrasive wear. For three-body abrasive wear Misra and Finnie found that there was a different effect to two-body abrasion. At low loads the wear rate was non-linear, but as the load increased the wear became linear with increasing load. This was attributed to the lower degree of constraint of the abrasive particles at low loads. In the present work this was not observed, and there was a simple linear trend shown over the entire range of loads, as in the case of Stevenson and Hutchings'[17], work using a rubber wheel abrasion

tester. Misra and Finnie used an apparatus that consisted of a column of abrasive particles contained in a tube, and pressed on a rotating metal disc. This type of wear tester is classified a low stress tester, meaning that the majority of the abrasive particles remain uncrushed. It is therefore appears that the new three-body abrasive wear apparatus is a more severe form of wear. However it was found that for the low loads used in this study, the silica particles did not fracture whilst at high loads they did. Thus there appears to be no difference in the wear rate depending on whether the test is low or high stress abrasion in this present testing which agrees with the previous work of Hutchings.

6.2.2 The effect of wheel velocity

The initial set of tests performed on the apparatus to determine the effect of wheel velocity on the wear rate showed an increasing wear rate with an increase in wheel velocity. On further analysis of the results, it was concluded that they were erroneous since the duration of each test run was kept constant for each velocity, which indicates that different amounts of abrasive were used for each test. For a true indication of the effect of velocity on the wear rate, it is necessary to run each test for the same number of wheel revolutions which ensures that the specimens experience the same linear distance of abrasive wear. Further, such testing requires that the feed rate of abrasive particles is kept constant,

Consequently, the number of wheel revolutions was kept constant at 20. For a wheel velocity of 0.131m.s^{-1} (10rpm), the required test duration was 120 seconds. If a mass feed rate of 60g.min^{-1} were selected, the required mass of sand would be 120g. If the velocity were increased to 0.524m.s^{-1} (40rpm), the test duration would be 30 seconds. However, a lower mass of 30g would be required to ensure that the feed rate was kept constant. However, it was difficult to feed the particles between the specimen and the wheel at the same rate for different velocities, because the feed rate is partially controlled by the velocity of the wheel. Stevenson and Hutchings[17] showed that there was a limiting feed rate past the specimen, which could be achieved. Above this limiting feed rate, no more abrasive could be fed between the wheel and the specimen. The testing process to determine the effect of velocity therefore requires that, for each velocity selected, a calibration of the feed rate be performed. Although the feed system of the rig allows a certain variation and control of the feed rate, for velocity tests to be accurately performed, different funnel diameters (or diameters of nozzles fitted to funnels) are necessary. The calibration of velocity has to take into consideration both the influence of the velocity of the wheel in "pulling" abrasive particles through, and also the rate at which particles can be fed using the funnels. The relationship between abrasive feed rate and the wheel velocity proved to be an insurmountable

obstacle in testing the effect of wheel velocity on abrasive wear rates in isolation.

6.2.3 The effect of abrasive feed rate

The feed rate was adjusted by varying the feeder wheel speed to give four different mass feed rates of abrasive. Each of the tests lasted 2 minutes, after which time the volume loss was measured. The results are shown in Figure 46.

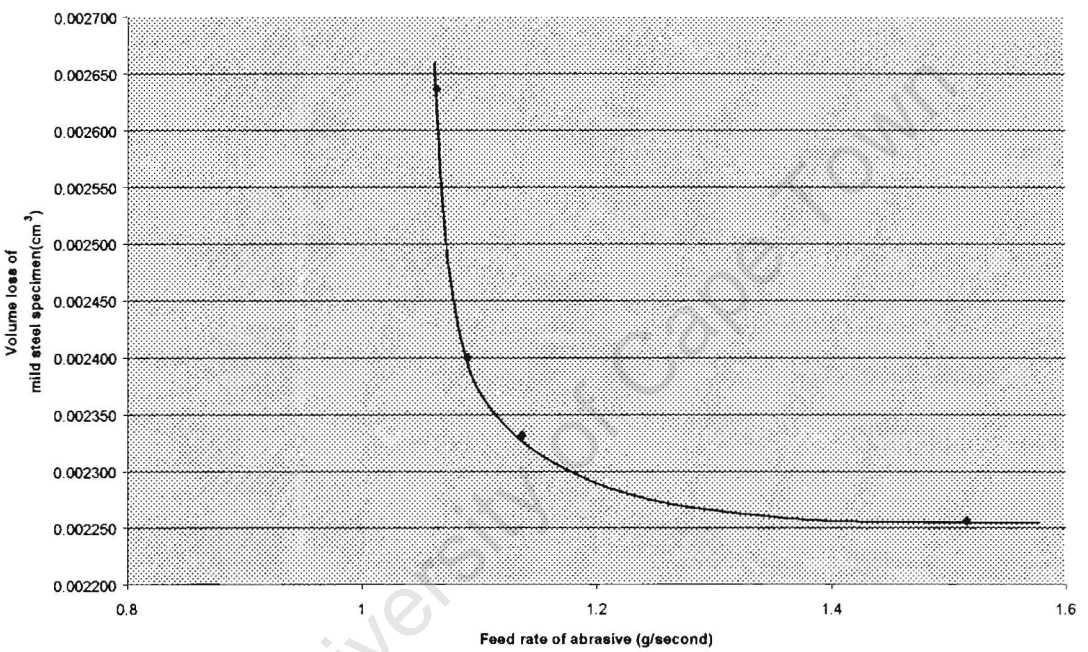

Figure 46 The effect of abrasive feed rate on volume loss (50N load and 125-180μm silica abrasive)

A trend line has been inserted in the figure. The relationship shows that at low feed rates the volume losses are higher, and volume losses decrease with an increase in feed rate. This result is similar to that obtained with increasing particle size on wear rates. In this test, as the volume of particles increases, there are more particles moving through the specimen–wheel interface and a corresponding decrease in the number of particles which can or are causing damage to the steel surface. The larger number of particles between the two surfaces, forces the surfaces apart and fewer particles come into direct

contact with the counterface. For the highest feed rate, the condition discussed by Stevenson and Hutchings[17] is apparent. More abrasive particles are fed onto the wheel, than can be pulled through by the motion of the wheel. The higher number of particles moving through the interface leads to a lowering of efficiency of the wear process.

6.2.4 Metal-on-metal versus 3-body abrasion

A wear test was performed on a mild steel specimen using a mass feed rate of 70g.min^{-1}. The rate was plotted as a relationship between mass loss and time. A second specimen was tested in a similar manner. However, for the second specimen, no sand was fed between the wheel and the specimen. the test was run for a total time which was the same as the test performed using abrasive. These tests showed the relative severity of the abrasive wear when metal-on-metal with sand between the surfaces, was compared with metal-on-metal without sand between the two surfaces. The wear rate of the former was approximately 6 times higher as shown in Figure 47.

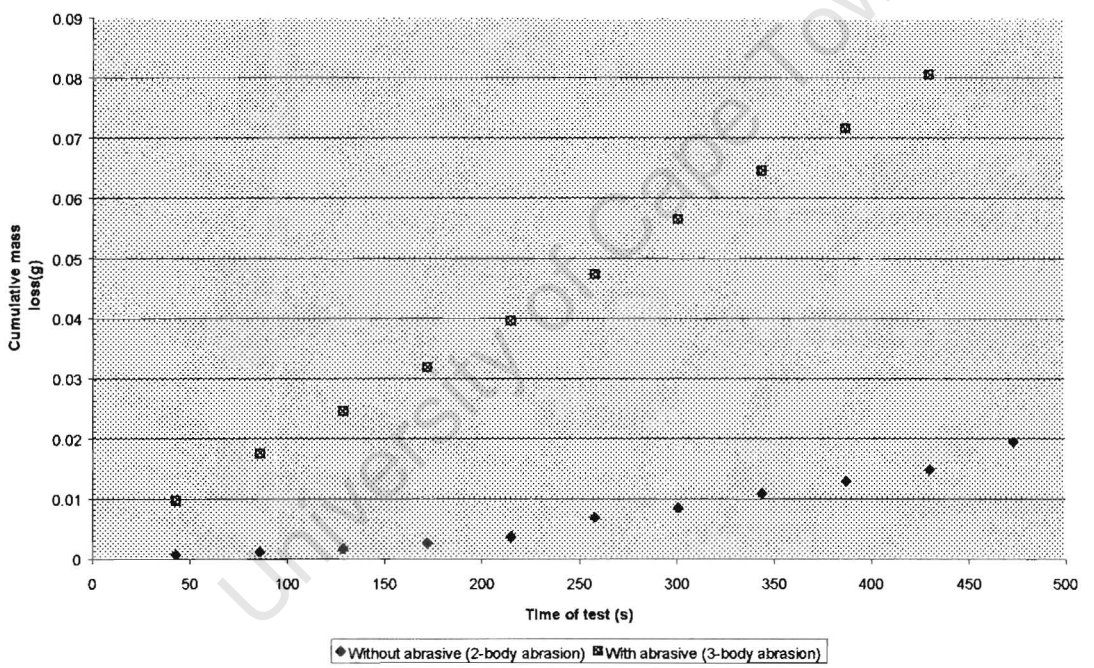

Figure 47 The influence of abrasive particles on abrasive wear.

This test was performed to show the effect of possible wheel contact during testing and it's effect on the wear rate measured. Although this set of tests shows that the mass losses are larger if abrasive particles are fed between two metal surfaces than if no abrasive is used, the tests discussed in 6.2.3, it is important to consider the results of the previous section. They showed that lower abrasive feed rates were more efficient at removing material from metal

surfaces than higher feed rates. So although eliminating the abrasive from between two moving surfaces plays a large role in reducing wear, small amounts of abrasive fed between the surfaces may be destructive.

6.3 Summary of results obtained by varying test parameters

6.3.1 Particle size

When tests were performed using different abrasive particle sizes, the wear rate showed only a slight increase with an increase in particle size in the size range from 50μm to 180μm. Above 200μm particle size there is a steady decrease in the wear with increasing particle size. The observed effects of particle size were attributed to larger particles within each size range separating the wheel and the specimen so that the efficiency of the material removal process was lowered, as fewer particles were in contact with the specimen to remove material. For smaller particle sizes most of the particles were able to remove material, and thus the material removal was more efficient.

6.3.2 Load

Tests using various loads showed a trend of increasing wear with increasing load. This was attributed to a lower degree of constraint of the abrasive particles for lower loads.

6.3.3 Wheel Velocity

No relationship between the wheel velocity and the wear rate was established, as the connection between abrasive feed rate and the wheel velocity proved an insurmountable obstacle in testing the effect of wheel velocity on wear in isolation.

6.3.4 Abrasive Feed Rate

Tests using four different abrasive feed rates showed that lower feed rates resulted in higher wear. This was attributed to the separation of the wheel and the specimen surfaces at higher feed rates, resulting in fewer particles being in contact with the specimen, and a lowering of the efficiency of the material removal process.

6.3.5 Comparing metal-on-metal wear versus three-body abrasion

Tests showed that by introducing abrasive particles between two moving surfaces the wear rate increased by approximately six times. The first test was run without abrasive particles. The second test was run for the same duration with abrasive particles.

6.4 Material effects

One of the objectives of the project was to obtain a wear resistance ranking of some commonly used materials. Therefore, approximately 20 materials were tested under three-body abrasion conditions using silica sand as the abrasive.

6.4.1 Wear resistance of different materials

There are many ways to define the wear resistance. Firstly, it is the inverse of the wear rate. A wear rate may be defined as the volume loss per unit time or sliding distance. This is commonly the case for sliding wear. In tests in which loose abrasive particles are involved, it is more useful to incorporate the mass of abrasive into the wear rate (such as in erosion testing). Thus, for testing of three-body abrasion, in which the abrasive particles are fed between the two surfaces at a fixed feed rate, the wear rate may be defined as a volume loss per unit mass of abrasive.

If this wear rate is converted to wear resistance, a definition of wear resistance can be derived. Namely, the mass of abrasive required to remove a unit volume of material. In the present work, the wear resistance is thus defined as the mass of abrasive required to remove $1cm^3$ of material. The abrasives were fed at the same feed rate for each test. The load applied to the specimens during the tests was 50N.

The results of the wear tests are shown in Figure 48. The general groups of metals tested were the stainless steels, various hardened steels, alumina ceramics, hard coatings on metals, and composite materials containing tungsten carbide chips in matrices of copper, nickel and iron.

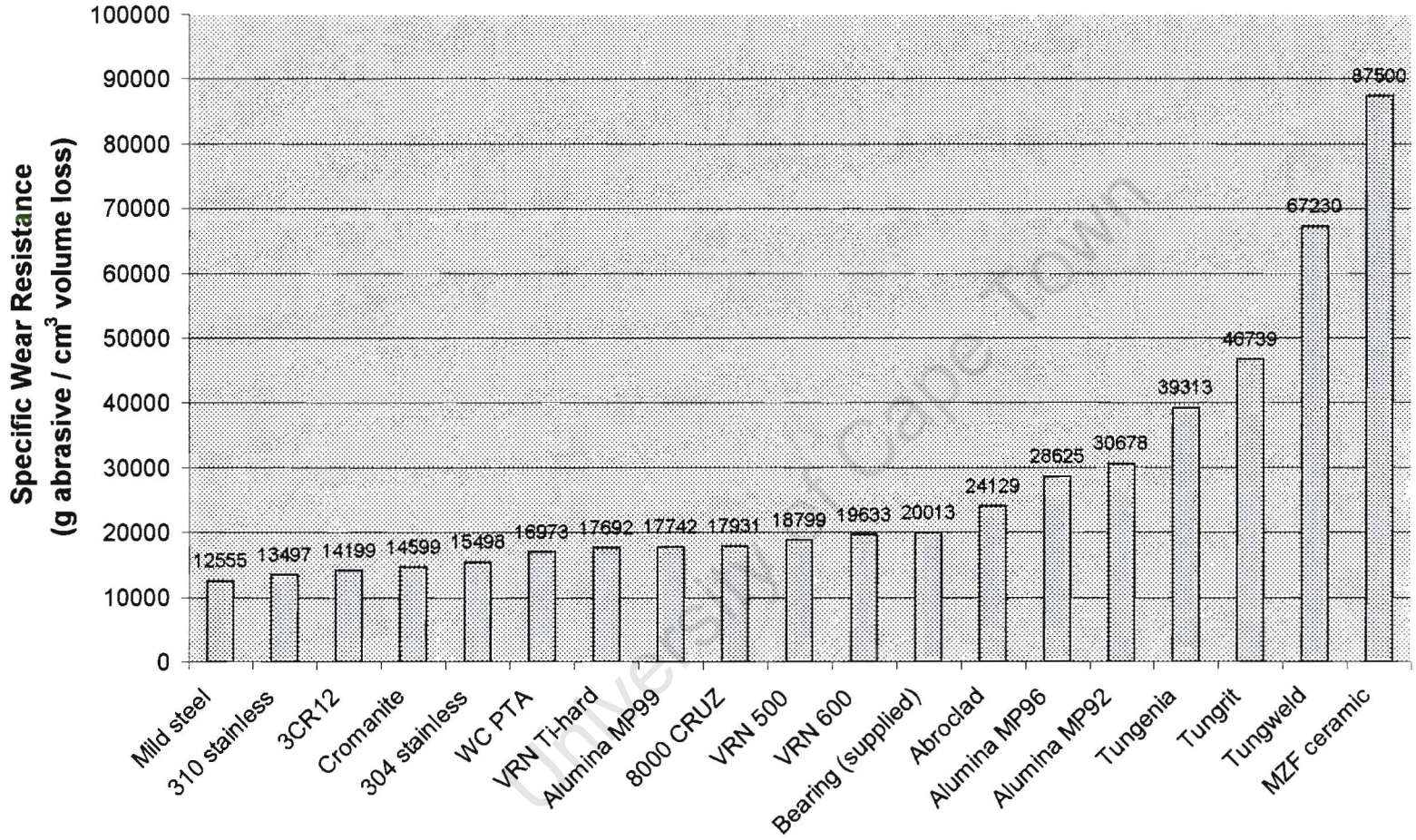

Figure 48 The wear resistances of all of the tested materials (feed rate of 70g.min^{-1} at 50N load)

6.4.2 Hardness tests

Material bulk hardness is an important variable in wear of materials, as to some extent it contributes to the wear resistance of a material. The pre-test hardnesses of the materials tested are plotted in Figure 49 below. The materials are shown in order of wear resistance ranking determined by the series of wear tests discussed in the previous section.

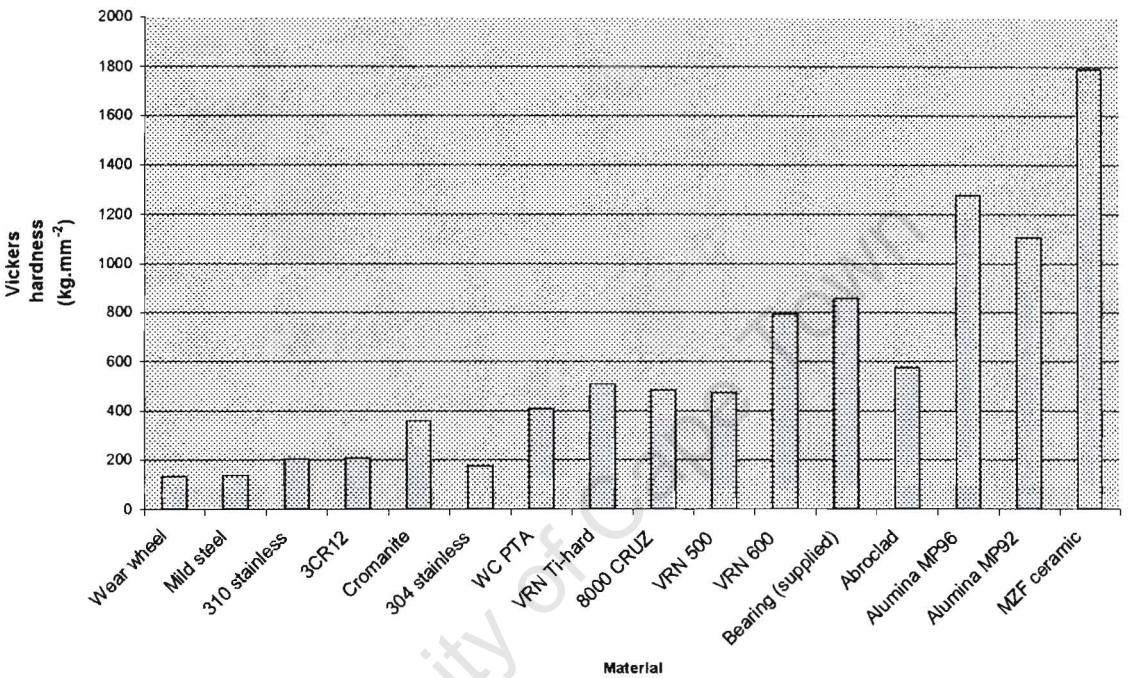

Figure 49 The Vickers macrohardness of materials which were tested (average of ten measurements). Materials are ranked from left to right in order of increasing specific wear resistance

The wear resistance and hardness values of Figure 48 and Figure 49 are summarised in Table 7.

The general trend is of increasing wear resistance with an increase in hardness. There is, however not complete correlation. Khruschov[7] showed that for pure metals of different hardnesses, there is a linear relationship between hardness and wear resistance. The dependence of the wear resistance on hardness depends on the material type.

Table 7 Hardnesses and specific wear resistance values of tested materials

Material	***Specific wear resistance*** g of abrasive per cm^3 volume loss	***Vickers hardness*** HV	
Wear wheel (mild steel)	-	138	
Mild steel	12555	138	
310 stainless	13497	203	
3CR12	14199	207	
Cromanite	14599	358	
304 stainless	15498	231	
WC PTA	16973	404	
VRN Ti-hard	17692	509	
8000 CRUZ	17931	481	
Alumina MP99	17742	1442	
VRN 500	18799	432	
VRN 600	19633	792	
Bearing (supplied)	20013	857	
Abroclad	24129	620	
Alumina MP96	28625	1277	
Alumina MP92	30678	1105	
Tungenia	39313	327_{min}[1]	1077_{max}[2]
Tungrit	46739	68_{matrix}[3]	1925_{grit}[4]
Tungweld	67230	717_{matrix}	1600_{grit}
MZF ceramic	87500	1792	

[1] $_{min}$ is the minimum hardness measured over the entire surface

[2] $_{max}$ is the maximum hardness measured over the entire surface

[3] $_{matrix}$ is the hardness of the binder matrix, diamond indentor on only the matrix

[4] $_{grit}$ is the hardness of the particles held by the matrix, diamond indentor on only the particle

6.4.3 Performance of specific materials

6.4.3.1 Mild steel

Mild steel was selected as a reference material, as it is easily machinable, and its properties are well known, and it is commonly used as a reference material in wear tests. Of the materials tested, it had both the lowest hardness and the lowest wear resistance.

Scanning electron microscopy of the wear tracks created by single particles moving over the surface of mild steel specimens show evidence of two types of material removal mechanisms. Figure 50, shows micro-ploughing, whereas Figure 51, shows more severe micro-cutting The width of the latter is of a similar size to the sand particles, showing that the particle penetrated deeper into the metal. The micro-ploughing displaces material laterally.

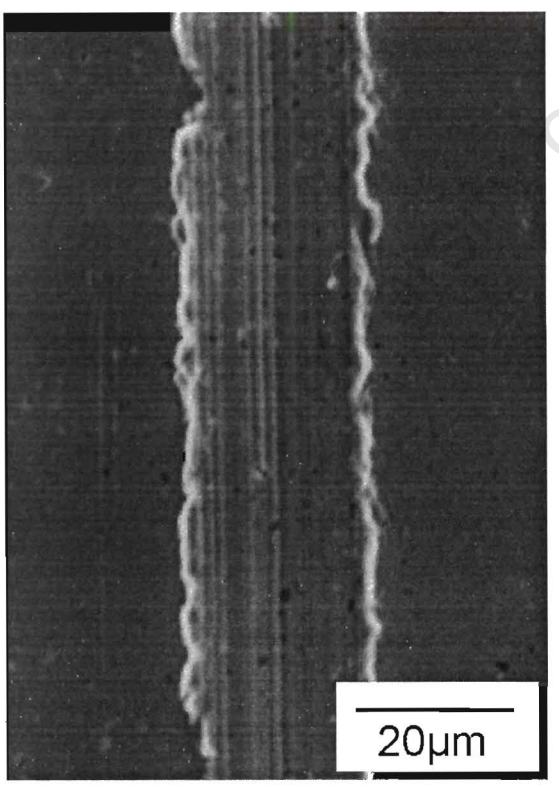

Figure 50 A wear track in mild steel showing micro-ploughing

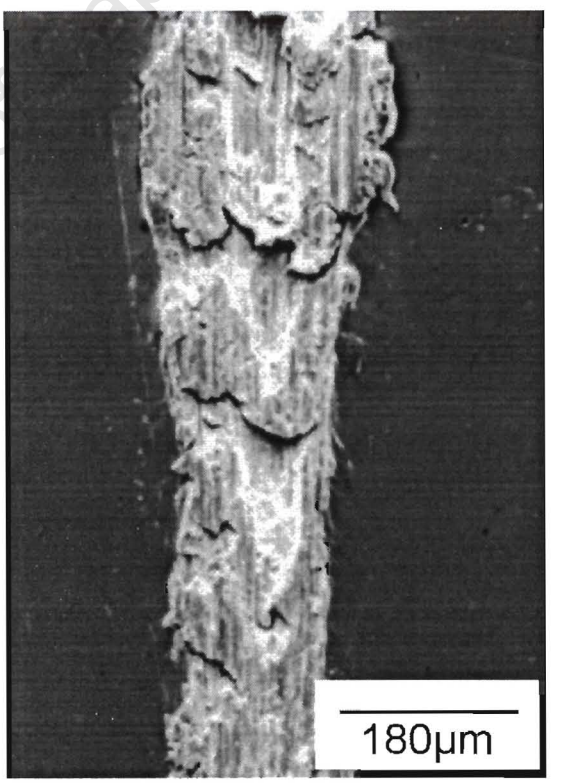

Figure 51 A wear track in mild steel showing micro-cutting caused by the passage of a sand particle

6.4.3.2 Stainless steels

The 304 austenitic stainless steel showed the highest wear resistance of the stainless steels tested. The material experiences work hardening during the abrasion test, as seen by the change in hardness during testing, as shown in Table 8. Although the pre-test hardness of the 304 stainless steel is 231HV, 127 HV lower than the Cromanite (a high nitrogen stainless steel), its wear resistance is 6% higher. The Cromanite however, also showed an increase in hardness during the test. In contrast, the 310 stainless steel, a corrosion resistant steel used for high temperature applications, showed wear resistance 5% lower than 3CR12, even though its hardness was only 4HV lower. The 3CR12 and the 310 stainless steel did not show work-hardening behaviour. The results of post test hardness testing show that hardness values cannot be used to give an accurate ranking of expected wear performance.

Table 8 Comparison of pre-test and post test hardnesses of stainless steels

Material	Pre-test hardness (HV)	Post-test hardness (HV)	Specific wear resistance (g of abrasive per cm^3 volume loss)
3CR12	207	206	14199
310	203	204	13497
304	358	366	15498
Cromanite	231	241	14599

6.4.3.3 Hardened steels and hard coatings

A number of hardened steels were tested, including the material that is currently used for bearings inside electrostatic precipitators in power stations. The bearing material was the most resistant material within the hardened steels. VRN600 had very similar performance. VRN 600 is a material made up of a layer of steel containing chromium carbide, over-laid on a mild steel

backing. The material is applied to surfaces as a weld overlay, and is used in cases where extreme wear is experienced, such as excavator buckets and bulldozer blades. The supplied condition of the material is extremely rough, and there are many cracks present in the material. The bearing steel that was supplied had been surface hardened on the contact surfaces, and performed favourably.

Abroclad was the most wear resistant of the metals tested. The material consists of a carbon steel base, and a cladding made of high chromium molybdenum steel. The microstructure consists of very hard primary carbides and fine precipitates of secondary carbides in a martensite base. After the wear test, the hardness was measured and showed an average value of 620HV. Secondary hardening, a result of the chromium and molybdenum forming carbides, imparted high wear resistance to the steel.

The wear resistance of the Abroclad was mid-way between the bearing steel and the MP96 alumina. The pre-test hardness of the Abroclad, is however substantially lower than both of these materials, showing again that examination of hardnesses cannot always be used to predict wear resistance.

6.4.3.4 Ceramics

Alumina ceramics are lightweight and have high hardness. MP96 and MP92 alumina were amongst the most wear resistant materials The grain sizes of all of the ceramics tested were all approximately 3µm (see Appendix B). The third grade MP99, however, did not perform as well. This is surprising, as the measured hardness of the alumina was in excess of 1400HV. The ceramics are produced by sintering spherical ceramic particles. Scanning electron microscopy showed that the MP99 alumina contained pores between the alumina particles. The edges of these pores seem to act as initiation points for fracture, as seen in Figure 52 and Figure 53. Another ceramic, MZF, containing stabilised zirconia, had extremely high wear resistance.

The microscopic evidence suggests that a material which has high hardness may not necessarily indicate a material with high wear resistance. This is in agreement with work by Olsson, Kahlman and Nyberg[43], who concluded that microstructural features of a ceramic surface are important in determining the wear resistance of ceramics. Surface porosity, secondary phases and defect-rich regions may have a deleterious effect on the wear resistance.

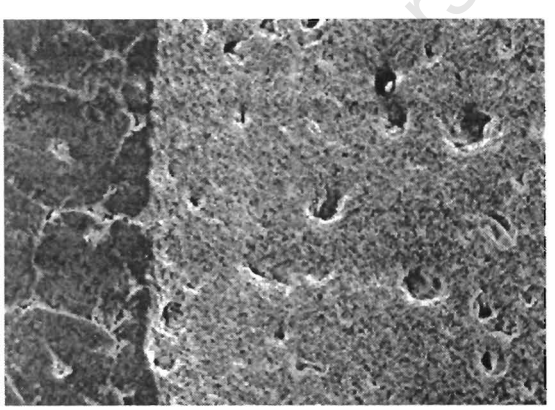

Figure 52 Abraded MP99 alumina. The right-hand side is abraded and the left-hand side shows unabraded sintered particles. Porosity is visible between grains and the pores act as initiation points for material loss.

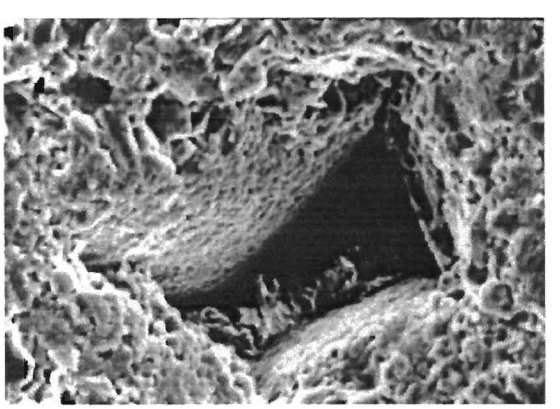

Figure 53 MP99 sintered alumina, showing the edges of the sintered alumina particles. Brittle fracture is evident

6.4.3.5 Tungsten carbide composites

Three materials containing tungsten carbide particles were tested. They contained macro scale tungsten carbide particles, which varied in average size from 1217μm to 4717μm. They also had matrices of differing hardnesses.

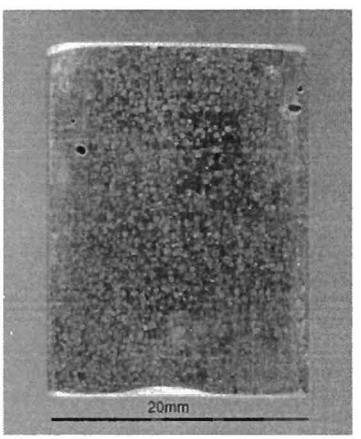

Figure 54 Tungenia

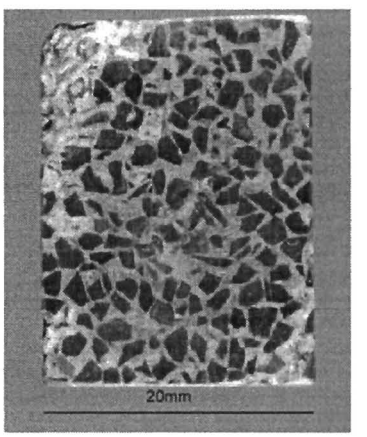

Figure 55 Tungrit

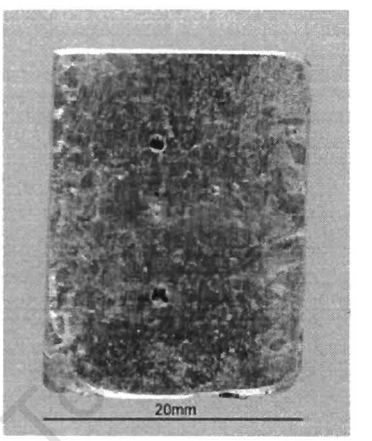

Figure 56 Tungweld

The first material had a trade name of *Tungenia.* The matrix was a weld material which was a nickel based alloy with a hardness of approximately 330HV. The material contained spherical tungsten carbide particles with an average diameter of 1217μm. The maximum hardness of the material's surface was measured as1077HV. The wear resistance was the lowest of the three composites.

The second material was named *Tungrit*, and it contained larger tungsten carbide particles, which were angular. The matrix was an extremely soft copper-zinc brazing alloy, with a hardness of 68HV. In contrast the particles were extremely hard (1925HV). During the wear tests, the soft matrix was very quickly worn away, near the surface. After this initial wear, the particles protruded from the surface, held by the matrix. The resulting wear resistance of the material was high in relation to the plain metals, and the material was also more wear resistant than the alumina ceramics. Wear of this type of material is likely to occur by particle "pull-out" once a sufficient volume of

matrix has been removed so that the hard second phase particles can not be supported

The final material was *Tungweld*, which had a matrix of high chromium, molybdenum steel. The material had tungsten carbide particles of intermediate size (2917μm). The hardnesses of both the matrix (717HV), and the particles (1600HV) were high, resulting in a material of very good wear resistance. It is likely that the material removal from the matrix will be low, and therefore, particle "pull-out" may only occur after extended periods of wear. Of all of the three tungsten carbide composites, this material showed the most promising performance.

6.4.4 Testing materials using sand and ash abrasive particles

In order to determine the difference in wear behaviour using both ash and sand abrasives, a number of different materials were selected, the results of which are seen in Figure 57. It is immediately apparent that the relative wear resistances between materials are different for sand and for ash. This is most noticeable for the MP92 alumina.

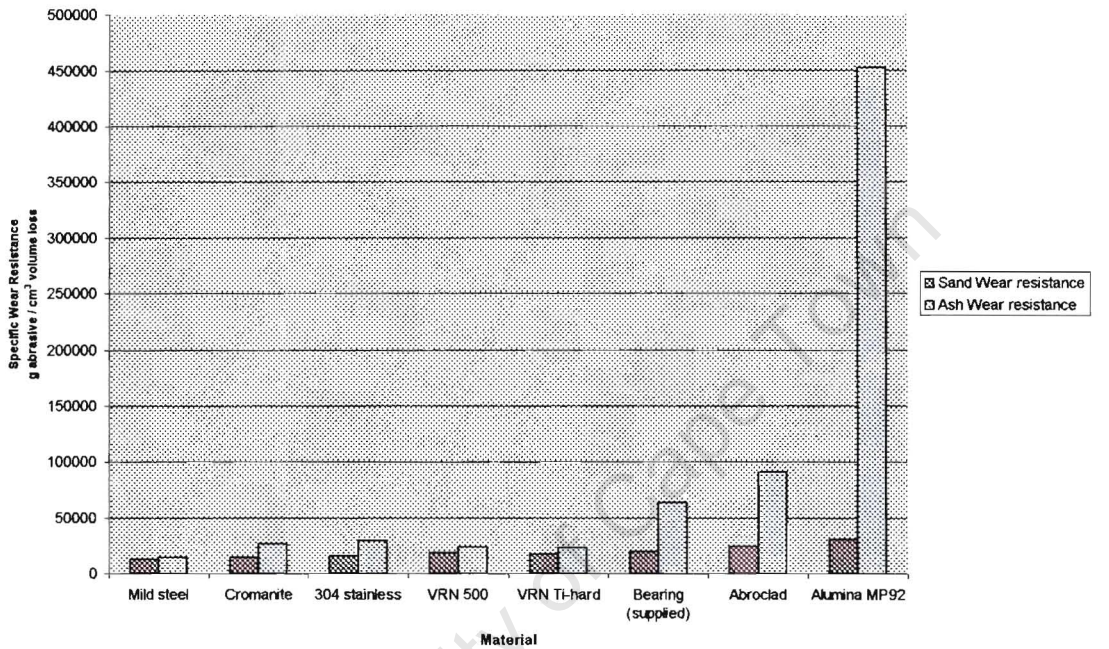

Figure 57 Specific wear resistances (mass of abrasive required to remove 1cm^3 of material) of a group of materials tested using silica and fly ash abrasive particles

The ability of an abrasive particle to cause damage on the surface of a material has been studied by numerous researchers (Hutchings, Khruschov, Moore, Misra and Finnie amongst others). All are in agreement that the hardness of the abrasive needs to be at least 1.2 times the hardness of the surface that it contacts.

Khruschov performed tests on 17 different materials using 7 different abrasives and verified this theoretically derived relationship. It was thus considered essential to calculate these ratios for the combinations of materials

and abrasives used in the present work. The values for ash and sand are shown in Figure 58.

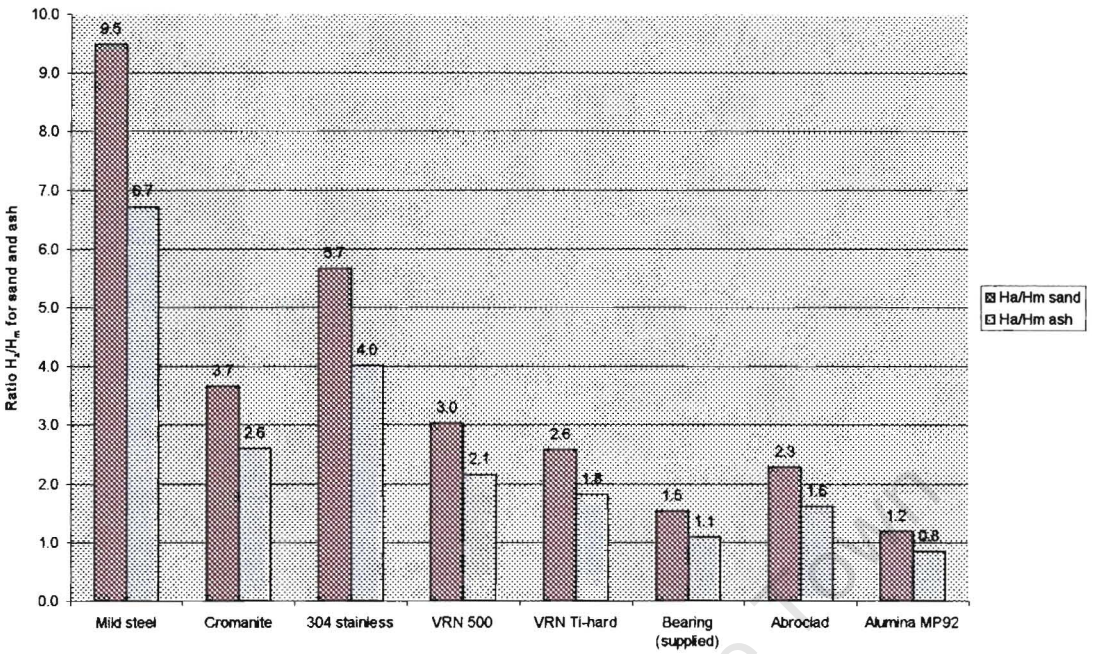

Figure 58 Ratios of the abrasive hardness to the material surface hardness for the materials tested.

The results of the tests with ash are not surprising if the hardness ratios are considered. If the limiting value of 1.2 of previous researchers is used, then it is clear that ash abrasive particles are not hard enough to cause substantial damage to alumina. The hardness ratios of the bearing material, Abroclad and alumina are all close to 1.2, and this is evident by their relative wear resistances in ash tests. If the results of the sand wear tests of the same three materials are considered the wear resistances do not show such extremes. The sand hardness ratios of the bearing material and Abroclad are both above 1.2.

The purpose of performing ash tests was to rank a selected group of materials and correlate the results to the ranking obtained by sand testing. For the materials whose hardnesses are approximately 1.3 times less hard than the abrasives, which they are tested with, it is felt the results should show similar

rankings. However, the ranking of hard materials is likely to be unreliable. Volume losses in the wear tests will be very small.

6.5 Summary of results of materials testing

6.5.1 The comparison of hardness values and wear resistance values

All of the materials were tested under three-body abrasive wear conditions and their wear resistances were ranked. The hardnesses of all of the materials were measured and the materials were placed in the same order as the ranking obtained for wear resistance. Although there was a general trend of increasing wear resistance with increasing hardness there were exceptions.

6.5.2 Materials with high wear resistances

The most wear resistant materials were the tungsten carbide composites and the ceramics. Abroclad performed best of all of the metals tested. Of the stainless steels, 304 stainless steel was the most wear resistant.

6.5.3 Wear mechanisms observed for mild steel

SEM showed evidence of micro-cutting and micro-ploughing on mild steel wear specimens. The micro-cutting appeared to be a more severe form of wear.

6.5.4 Wear of ceramics

Examination of MP99 alumina using SEM showed that the ceramic experienced material loss as a result of brittle fracture at the edges of the pores between the sintered particles.

6.5.5 Tungsten carbide composites

Tests of these dual-phase composites showed that materials with particles of high hardness contained in a matrix of a hard metal showed the best wear performance of the three composites tested.

6.5.6 Testing materials using ash abrasive

When ash abrasive was used to test very hard materials, the materials with ratios of abrasive hardness to material surface hardness less than 1.2, showed very low mass losses. Therefore it was concluded that ash could not be used to rank materials of these high hardnesses.

7 CONCLUSIONS

An apparatus was built which is capable of ranking materials for three-body abrasive wear resistance under a wide range of test conditions.

The three-body abrasive wear apparatus permits a variation in load between 1N and 1000N, wheel speed between 0.05m.s^{-1} to 1.5m.s^{-1}, abrasive type and size, abrasive feed rate. All tests use a steel wheel, rotating in contact with a test specimen while abrasive particles are fed between the wheel and the specimen.

A number of materials were ranked in order of increasing wear resistance, using sand abrasive. The reference material was mild steel and it was found that the most wear resistant materials were the alumina ceramics and tungsten carbide composites.

Although ash tests did cause volume losses on the steels, the ash particles were too soft to remove significant material from ceramic specimens, owing to low ratios of abrasive hardness to material hardness. It was thus concluded that ash wear rankings for very hard material cannot be reliably used.

SEM showed that porosity in alumina ceramics was deleterious to the wear properties, as the edges of the pores acted as initiation points for material removal. In mild steel, both micro-ploughing and micro-cutting mechanisms of material removal were observed.

An increase in wear with an increase in load on the specimen was observed with a set of tests of varying loads.

Hardness tests of materials used in wear tests showed that although there was a general trend of increasing wear resistance with hardness, there were deviations from the trend, and these were attributed to microstructural influences.

For tests performed using silica sand particles between 50μm and 180μm in diameter, there was little change in wear with an increase in particle size. However, above approximately 200μm there was a steady decrease in wear with increasing particle size followed by a levelling off of the wear. This was attributed to lowering of efficiency due to the separation of the wear surfaces by larger particles.

At lower abrasive feed rates the particles are more efficient at removing material than at higher feed rates, and thus the wear is higher at the lower feed rates than at higher feed rates. This is because at high feed rates the abrasive particles separate the wheel and the test specimen and fewer particles are in contact with the test specimen.

REFERENCES

[1] Eskom website: http://www.eskom.co.za/

[2] A. Misra and I. Finnie, *An experimental study of three-body abrasive wear*, **Wear,** 85, (1983) 57-68.

[3] Hutchings, I. M. (1992) Tribology: Friction and Wear of Engineering Materials. London, Edward Arnold, 134.

[4] E. Rabinowicz, L. A. Dunn and P.G. Russel, *A study of abrasive wear under three-body conditions*, **Wear**, 4, (1961) 345-355.

[5] J. D. Gates, *Two-body and three-body abrasion: a critical discussion,* **Wear**, 214, (1998) 139-146

[6] Howard S. Avery, *Classification and precision of abrasion tests,* **Proc. Int. Conf. On Wear of Materials**, ASME, New York, 1977, p. 148-157.

[7] M.M. Khruschov, *Principles of abrasive wear*, **Wear**, 28 (1974), 69-88.

[8] Moore, M. A., Materials in Engineering Applications **1**, 97-111, 1978.

[9] A. Misra and I. Finnie, *Correlations between two-body and three-body abrasion and erosion of materials,* **Wear**, 68 (1981), 33-39.

[10] A. V. Levy *The abrasion/erosion and erosion-corrosion characteristics of steels*, **Wear**, 138 (1990) 111-123.

[11] J. Larsen-Basse, *Influence of grit diameter and specimen size on wear during sliding abrasion,* **Wear**, 12 (1968) 35-53.

[12] E. Rabinowicz and A. Mutis, *Effect of abrasive particle size on wear*, **Wear**, 8 (1965) 381-390.

[13] T. O. Mulhearn and L. F. Samuels, *The abrasion of metals; a model of the process,* **Wear**, 5 (1962), 478-498.

[14] N. E. Miller, *Three-body abrasive wear with small size diamond abrasives*, **Wear**, 58 (1980) 249-259

[15] T. Sasada, M. Oike and N, Emori, *The effect of abrasive grain size on the transition between abrasive and adhesive wear*, **Wear**, 97 (1984), 291-302.

[16] K. V. Prasad and T. H. Kosel, *A study of carbide removal mechanisms during quartz abrasion II: Effect of abrasive particle shape*, **Wear**, 95 (1984) 87-102.

[17] A. N. J. Stevenson and I. M. Hutchings, D*evelopment of the dry sand/rubber wheel abrasion test*, **Wear**, 195 (1996), 232-240.

[18] H.S. Avery, *An analysis of the rubber wheel abrasion test* in S. K. Rhee, A.W. Ruff and K.C. Ludema (eds.), **Proc. Int. Conf. on Wear of Materials**, ASME, San Francisco, 1981, pp. 367-378.

[19] C. Pritchard, *Abrasion under low bearing pressures,* **Wear**, 17 (1971), 185-194.

[20] M.M. Khrushov, *Resistance of metals to wear by abrasion as related to hardness*, **Proc. Conf. on Lubrication and Wear**, 1957, Institute of Mechanical Engineers, London, 1957, pp. 655-659.

[21] G. Sundararajan, *The differential effect of the hardness of metallic materials on their erosion and abrasion resistance*, **Wear**, 162-164 (1993) 773-781.

[22] G. H. Yang and M. Garrison, *A comparison of microstructural effects on two-body and three-body abrasive wear*, **Wear**, 129 (1989), 93-103.

[23] N. J. Kar, *investigation of the role of microstructures on the two-body abrasive wear resistance of steels*, Proc. Int. Conf. on Wear of Materials, ASME, New York, 1987, pp. 415-425

[24] H.S. Avery, *Proc. Symp. on Materials for the Mining Industry*, Climax Molybdenum Company Vail, CO, July 1974,pp.43-77.

[25] K.H. Zum Gahr, ***Z. Metallkd.*** *,68 (1977)* 783.*-792.*

[26] G.J. Gore and J.D. Gates, *Effect of hardness on three very different forms of wear*, **Wear**, 203-204 (1997) 544-563.

[27] S. Das, B. Prasad et al., *Three body abrasive wear of 0.98% carbon steel*, **Wear**, 162-164 (1993) 802-810.

[28] N. Prasad and S.D. Kulkani, *Relation between microstructure and abrasive wear of plain carbon steels.*, **Wear**, 62 *(1980)* 613-620.

[29] K.H. Zum Gahr and D.V. Doane, *Metall. Trans. 11A* (1980) 613.

[30] L. Fang, Q. D. Zhou and Y. L. Li, *An explanation of the relation between material hardness in three-body abrasive wear*, **Wear**, 151 (1991) 313-321.

[31] I.V. Kraghelsky, *Calculation of wear rate*, Trans. ASME, J. Basic Eng., 87 (1965) 785-790.

[32] H. -J. Kim and Y. -G. Kweon, *The improvement of three-body abrasive wear of plain carbon steel by thermomechanical treatments,* **Wear**, 171 (1994), 201-208.

[33] J. Larsen-Basse, *Influence of atmospheric humidity on abrasive – I. 3-body abrasion*, **Wear**, 13 (1975) 373-379.

[34] J.M. Challen and P.L.B. Oxley, *An explanation of the different regimes of friction and wear using asperity deformation models,* **Wear**, 53 (1979) 229-243.

[35] Liang Fang, Xianglong Kong and Qingde Zhou, *A wear tester capable of monitoring and evaluating the movement pattern of abrasive particles in three-body abrasion,* **Wear**, 159 (1992), 150-120.

[36] K. Hokkirigawa and K. Kato, *An experimental and theoretical investigation of ploughing, cutting, and wedge formation during abrasive wear,* **Tribology international,** Vol 21 No 1 (1988) 51-57.

[37] K. Hokkirigawa and Z.Z. Li, *The effect of hardness on the transition of abrasive wear mechanisms of steels,* **Proc. Int. Conf. on Wear of Materials**, ASME, New York, 1987, Volume 1, 585-593.

[38] T. Kayaba, K Hokkirigawa and K. Kato, *Analysis of the abrasive wear mechanism by successive observations of wear processes in scanning electron microscope,* **Wear**, 110 (1986), 419-430.

[39] Y. Wang and Z. Wang, *An analysis of the influence of plastic indentation on three-body abrasive wear of metals*, **Wear,** 122 (1988) 123-133.

[40] B. R. Lawn and M. V. Swain, *Microfracture beneath point indenters in brittle solids*, **Journal of Materials Science**, 10 (1975), 113-122.

[41] Evans, G.A. *The Science of Ceramic Machining and Surface Finishing II,* Hockey, B.J. and Rice, R.W. (Eds), National Bureau of Standards Sp. Pub. 562, US Govt. Printing Office, 1979, pp.1-14.

[42] T. Yamamoto, M. Olsson and S. Hogmark, *Three-body abrasive wear of ceramic materials*, **Wear**, 174 (1994) 21-23.

[43] M. Olsson, L. Kahlman and B. Nyberg, *Abrasive wear of structural ceramics*, **American Ceramic Society Bulletin**, Volume 74, No. 2, pp 48-52, 1995.

[44] C.J. Tucker and A.E. Miller, *Low stress abrasive and adhesive wear testing,* Selection and Use of Wear Tests for Metals, ASTM, STP 615, ASTM, Philadelphia, 1976, 68-90.

[45] J.H. Tylczak, J.A. Hawk, R.D. Wilson, *A comparison of laboratory abrasion and field wear results,* **Wear**, 225-229 (1999) 1059-1069.

[46] ASTM G 65-91, *Standard test for measuring abrasion using a dry-sand/rubber wheel apparatus, ASTM,* Philadelphia, 247-259.

[47] ASTM G 105-89, *Standard test for conducting wet sand/rubber wheel abrasion tests, ASTM,* Philadelphia, 431-439.

[48] C. Spero, D. J. Hargreaves, R. K. Kirkcaldie, and H.J. Flitt, *Review of test methods for abrasive wear in ore grinding* , **Wear**, 146 (1991),389-408.

[49] R. Blickensderfer, B.W. Madsen, and J. H. Tylzak, *Comparison of several types of abrasive wear tests*, Proc. Int. Conf. on Wear of Materials. ASME, New York, 1985, 313-323.

[50] D. Hagström, Undergraduate Thesis, *Three body abrasive wear tester,* department of Materials Engineering, University of Cape Town, 1997.

[51] S. F. Scieszka, *Modelling durability of coal grinding systems*, **Wear** 114 (1987) 29-39.

[52] M. Suckling, *High temperature erosive wear of a boiler tube steel*, PhD Thesis, University of Cape Town, 1996.

APPENDIX A

DRAWINGS OF THE THREE-BODY ABRASION APPARATUS

THREE–BODY ABRASION TESTER

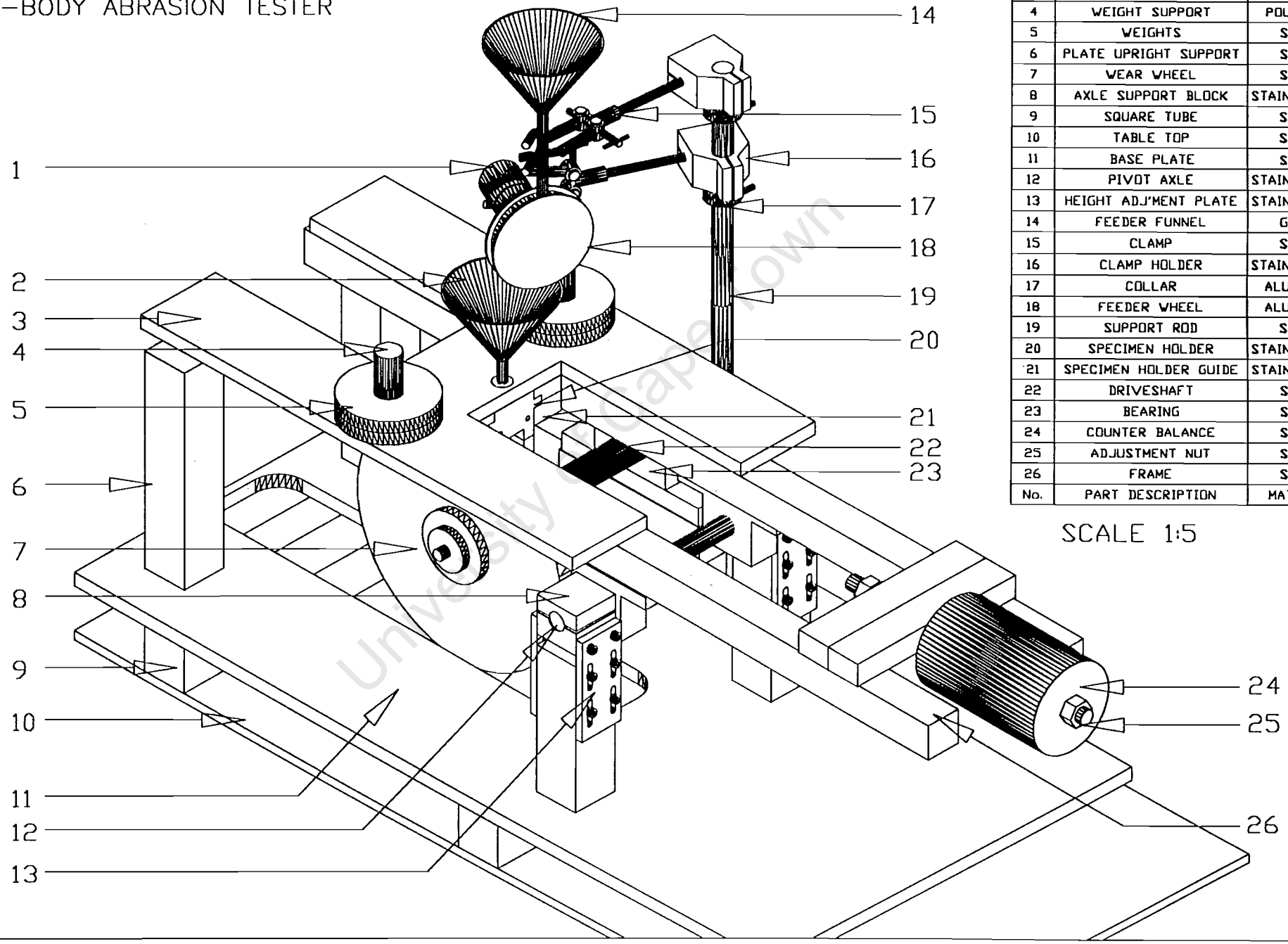

No.	PART DESCRIPTION	MATERIAL
1	MOTOR	N/A
2	BOTTOM FUNNEL	GLASS
3	LOAD PLATE	ALUMINIUM
4	WEIGHT SUPPORT	POLYPROP.
5	WEIGHTS	STEEL
6	PLATE UPRIGHT SUPPORT	STEEL
7	WEAR WHEEL	STEEL
8	AXLE SUPPORT BLOCK	STAINLESS ST
9	SQUARE TUBE	STEEL
10	TABLE TOP	STEEL
11	BASE PLATE	STEEL
12	PIVOT AXLE	STAINLESS ST
13	HEIGHT ADJ'MENT PLATE	STAINLESS ST
14	FEEDER FUNNEL	GLASS
15	CLAMP	STEEL
16	CLAMP HOLDER	STAINLESS ST
17	COLLAR	ALUMINIUM
18	FEEDER WHEEL	ALUMINIUM
19	SUPPORT ROD	STEEL
20	SPECIMEN HOLDER	STAINLESS ST
21	SPECIMEN HOLDER GUIDE	STAINLESS ST
22	DRIVESHAFT	STEEL
23	BEARING	STEEL
24	COUNTER BALANCE	STEEL
25	ADJUSTMENT NUT	STEEL
26	FRAME	STEEL

SCALE 1:5

1:4.5

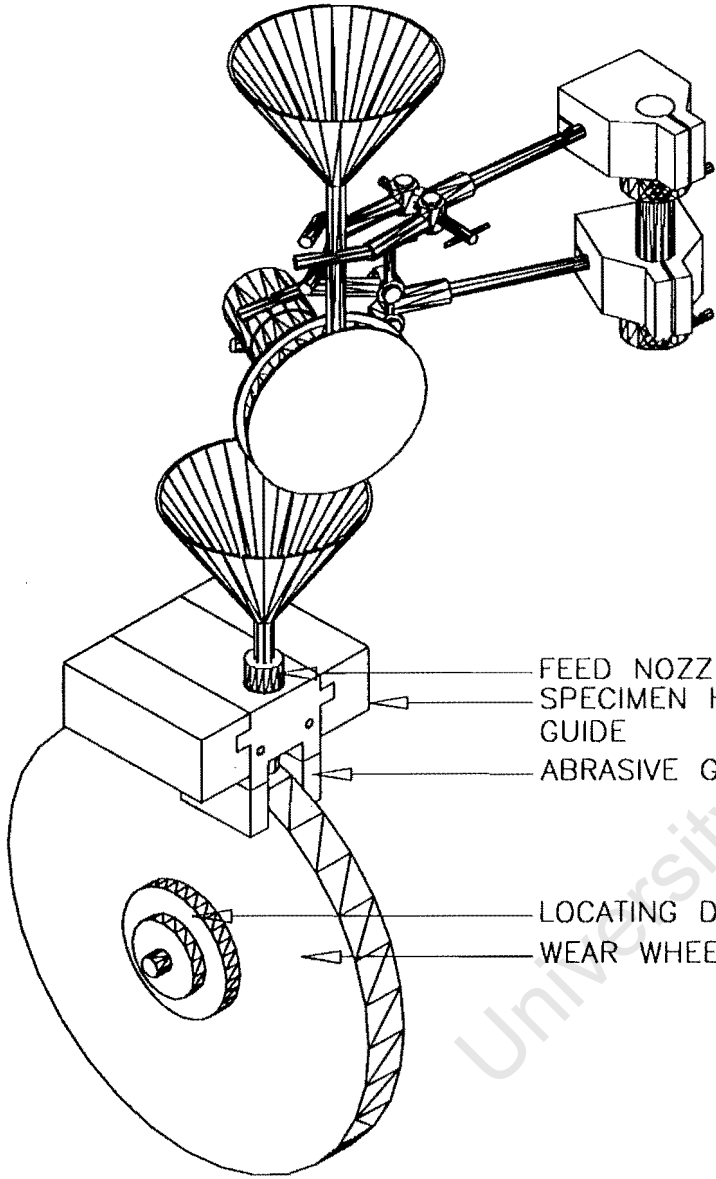

1:1.2

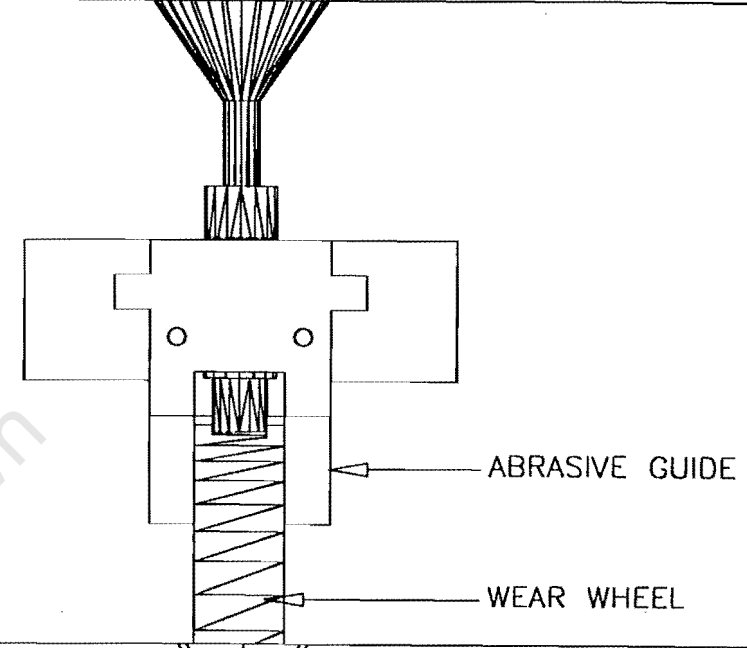

1:1.2

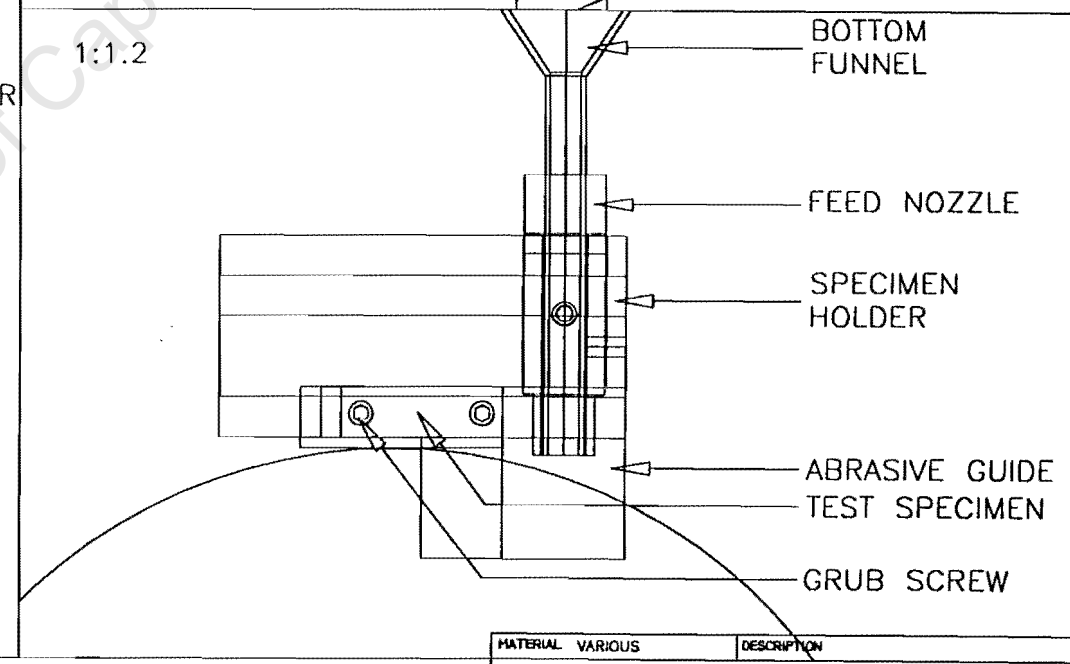

DIMENSIONS ARE IN MM AND SURFACE FINISHES IN IIC-3991. THE OVERALL TOLERANCE IS 0.1 MM IF NO OTHER IS STATED.

Department of Materials Eng.
University of Cape Town
Republic of South Africa

MATERIAL VARIOUS	DESCRIPTION
TITLE: DETAIL OF SPECIMEN LOCATION	
DRAWN BY G.J.JEWELL	APPROVED BY
DATE 20/4/00	DATE
SCALE mm / PLOT	
ACAD NAME SPECVIEW	DRAWING NO.
REV.	

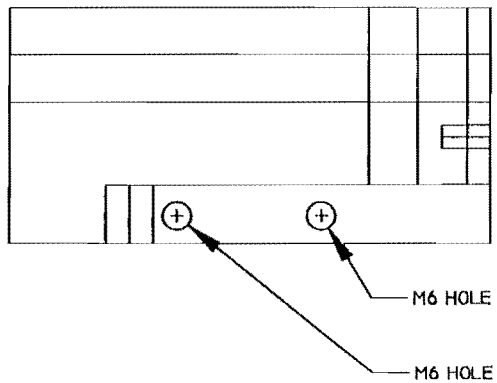

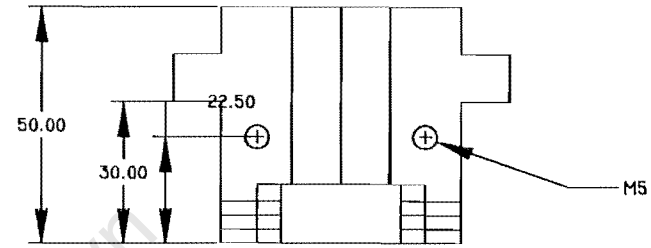

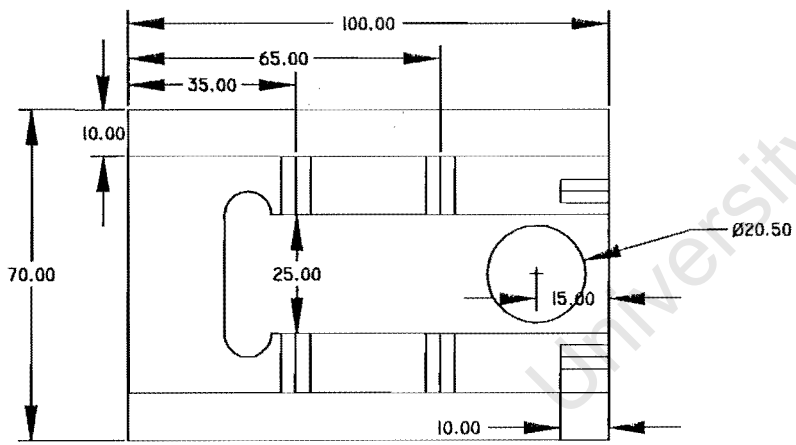

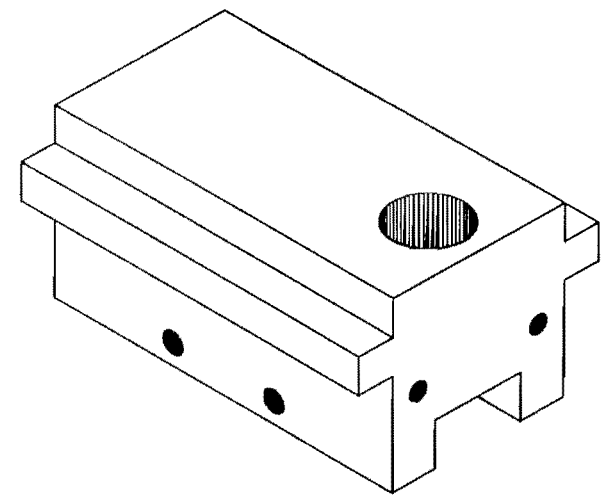

DIMENSIONS ARE IN MM AND SURFACE FINISHES IN RA 3µM. THE OVERALL TOLERANCE IS 0.1 MM IF NO OTHER IS STATED.

Department of Materials Eng.
University of Cape Town
Republic of South Africa

MATERIAL MARTENSITIC STAINL.STEEL	DESCRIPTION		
TITLE: SPECIMEN HOLDER			
DRAWN BY G.J.JEWELL	APPROVED BY	SCALE CRIS 1:1.62	PLOT 1:1.62
DATE 21/4/00	DATE		
ACAD NAME SPECHOLD	DRAWING NO.	REV.	

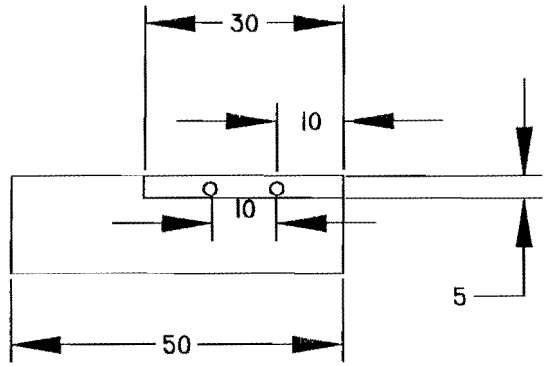

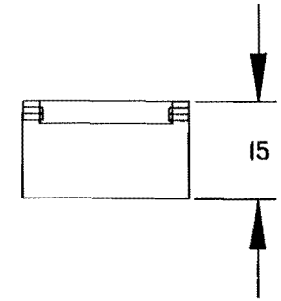

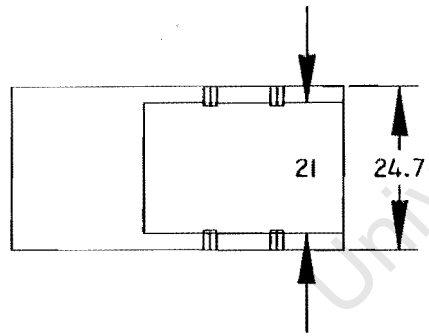

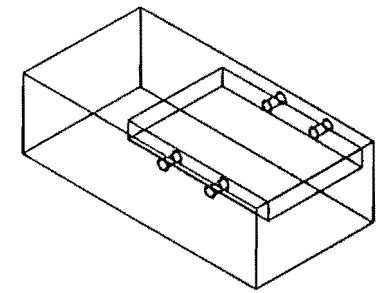

3mm grub screws
hold the smaller
specimens in place

DIMENSIONS ARE IN MM AND SURFACE FINISHES IN RA-3MM. THE OVERALL TOLERANCE IS 0.1 MM IF NO OTHER IS STATED.

Department of Materials Eng.
University of Cape Town
Republic of South Africa

MATERIAL 3CR12	DESCRIPTION
TITLE: DUMMY SPECIMEN	
DRAWN BY G.J.JEWELL	APPROVED BY
DATE 17/7/98	DATE
SCALE orig 1:1.36	plot 1:1.36
ACAD NAME	DRAWING NO.
REV.	

IV

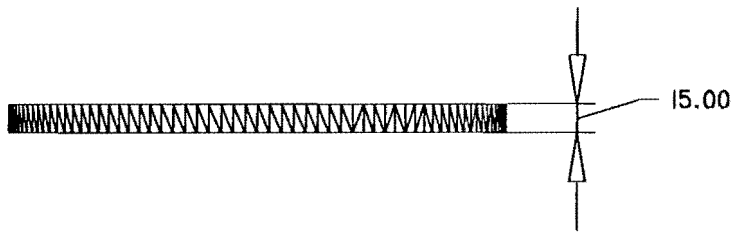

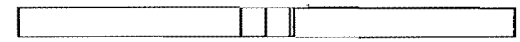

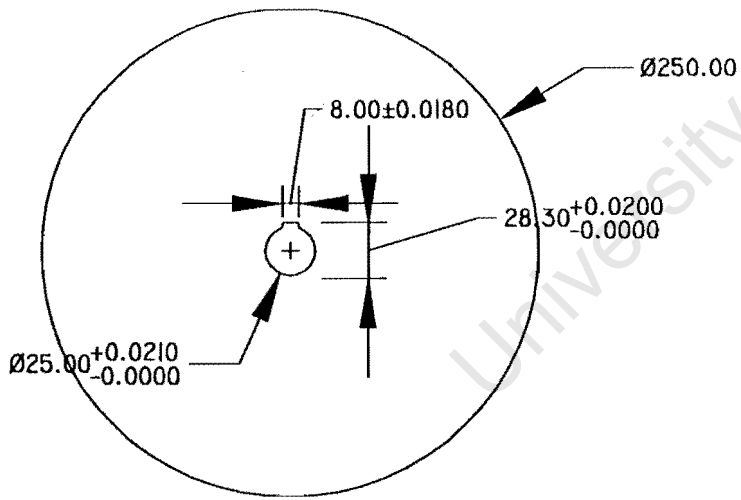

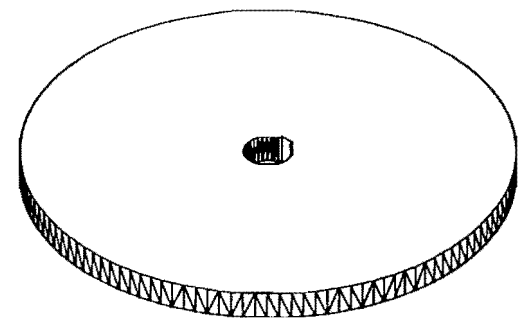

DIMENSIONS ARE IN MM AND SURFACE FINISHES IN RC-3MM. THE OVERALL TOLERANCE IS 0.1 MM IF NO OTHER IS STATED.

Department of Materials Eng.
University of Cape Town
Republic of South Africa

MATERIAL MILD STEEL		DESCRIPTION	
TITLE	WEAR WHEEL		
DRAWN BY G.J.JEWELL		APPROVED BY	SCALE DWG 1:3.85 PLOT 1:3.85
DATE 21/4/00		DATE	
ACAD NAME WHEELDIM	DRAWING NO.		REV.

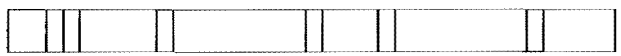

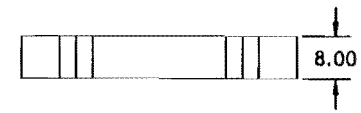

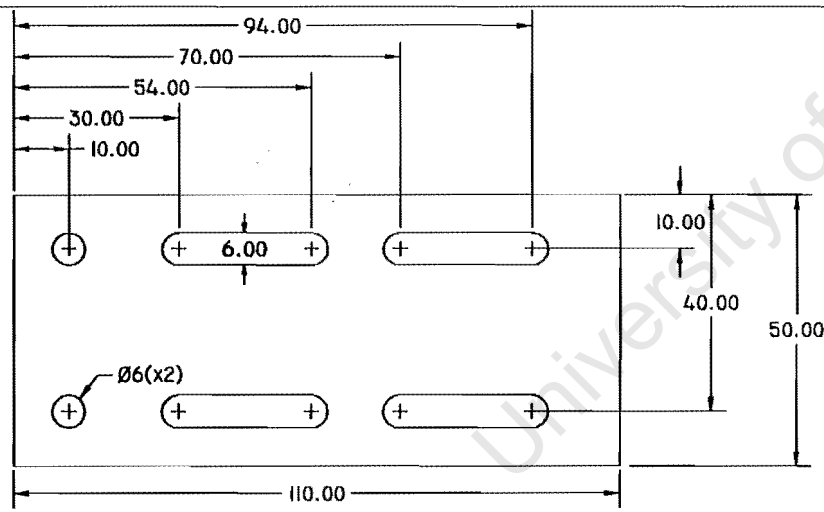

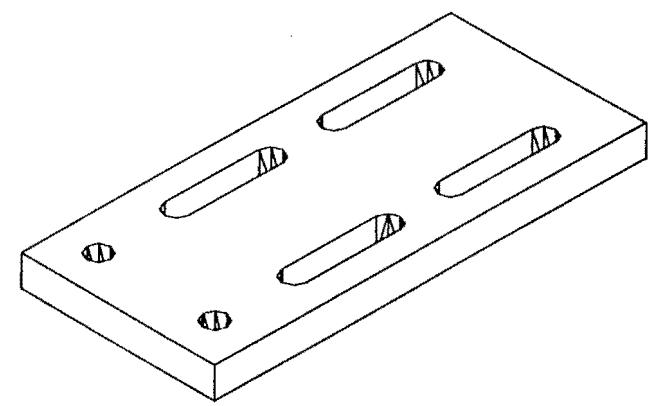

DIMENSIONS ARE IN MM AND SURFACE FINISHES IN Ie-3mm. THE OVERALL TOLERANCE IS 0.1 MM IF NO OTHER IS STATED.

Department of Materials Eng.
University of Cape Town
Republic of South Africa

MATERIAL	3CR12		
TITLE	HEIGHT ADJUSTMENT PLATE		
DRAWN BY	G.J.Jewell	APPROVED BY	SCALE DWG 1:1.375 PLOT 1:1.375
DATE	21/4/00	DATE	
ACAD NAME	slotplt1	DRAWING NO.	REV.

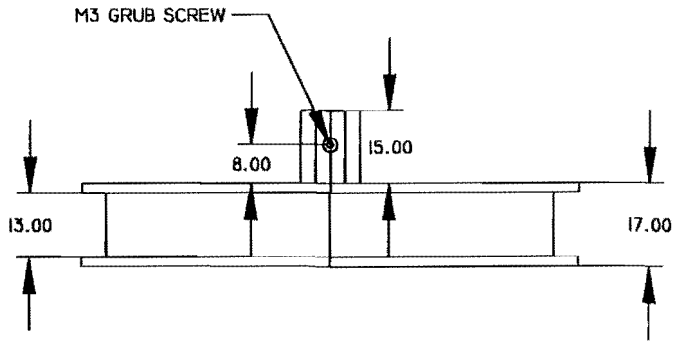

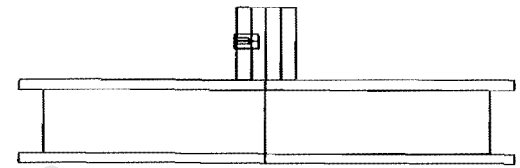

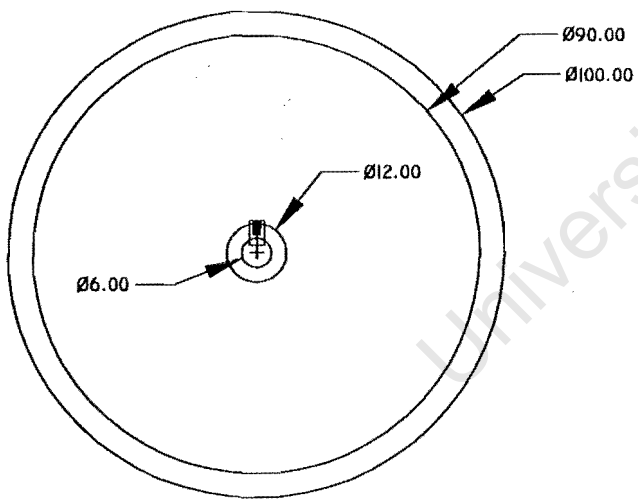

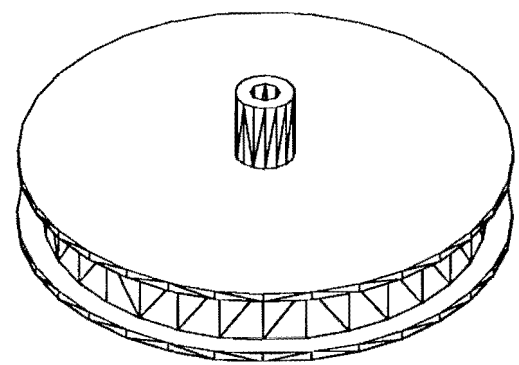

VII

DIMENSIONS ARE IN MM AND SURFACE FINISHES IN RA-3MM. THE OVERALL TOLERANCE IS 0.1 MM IF NO OTHER IS STATED.

Department of Materials Eng.
University of Cape Town
Republic of South Africa

MATERIAL ALUMINIUM		DESCRIPTION	
TITLE	FEEDER WHEEL FOR ABRASIVE		
DRAWN BY G.J.JEWELL		APPROVED BY	SCALE DWG 1:1.375 PLOT 1:1.375
DATE 21/4/00		DATE	
ACAD NAME FEEDWOIM	DRAWING NO.		REV.

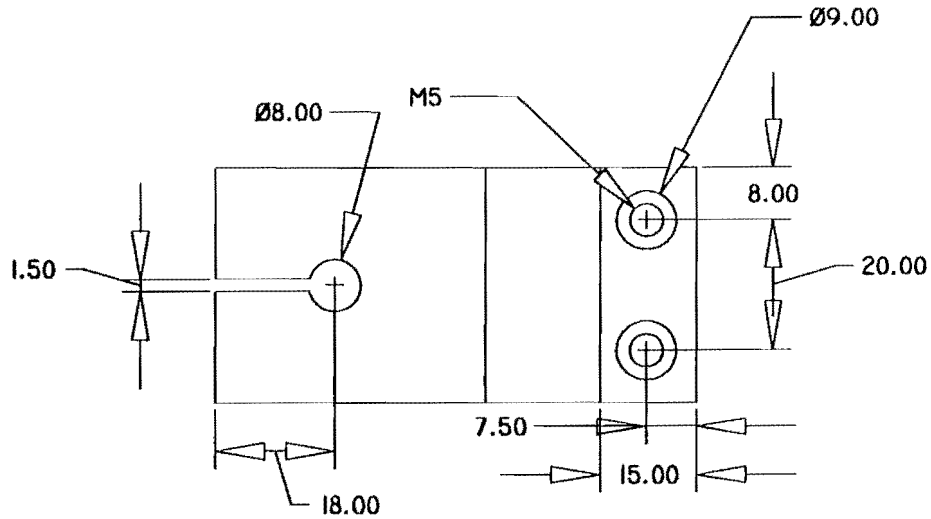

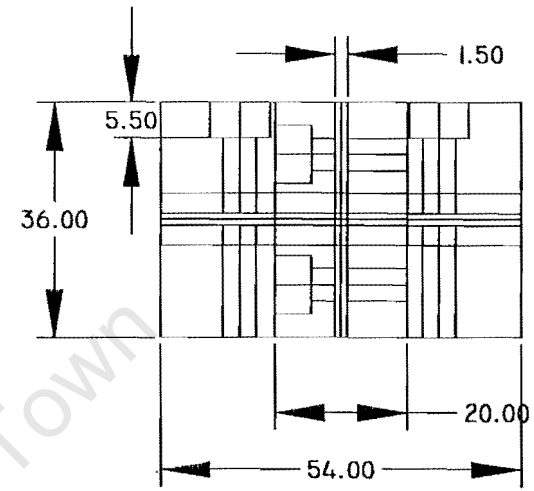

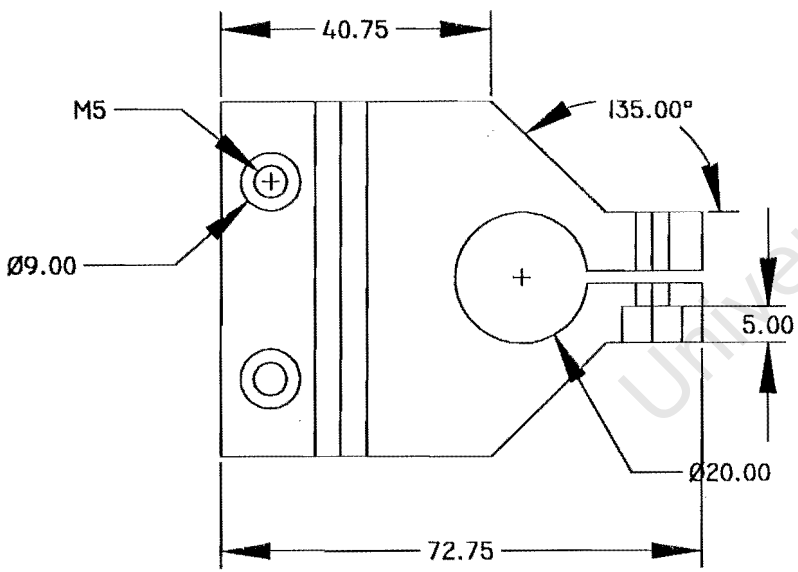

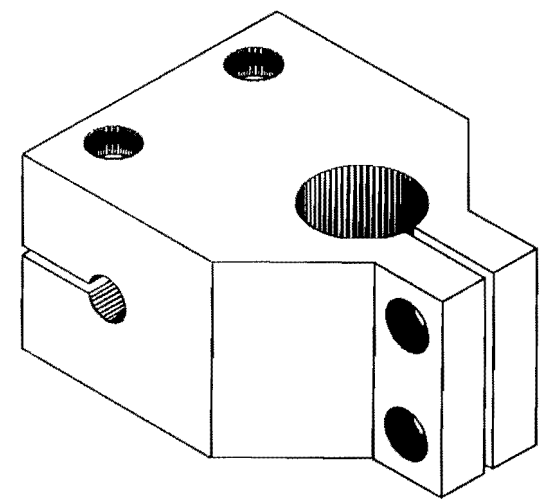

DIMENSIONS ARE IN MM AND SURFACE FINISHES IN RₐSPM. THE OVERALL TOLERANCE IS 0.1 MM IF NO OTHER IS STATED.

Department of Materials Eng.
University of Cape Town
Republic of South Africa

MATERIAL ALUMINIUM	DESCRIPTION
TITLE: CLAMP HOLDER	
DRAWN BY G.J.JEWELL	APPROVED BY
DATE 22/4/00	DATE
SCALE DWG 1:1.15 PLOT 1:1.15	
ACAD NAME CLAMBLCK	DRAWING NO.
REV.	

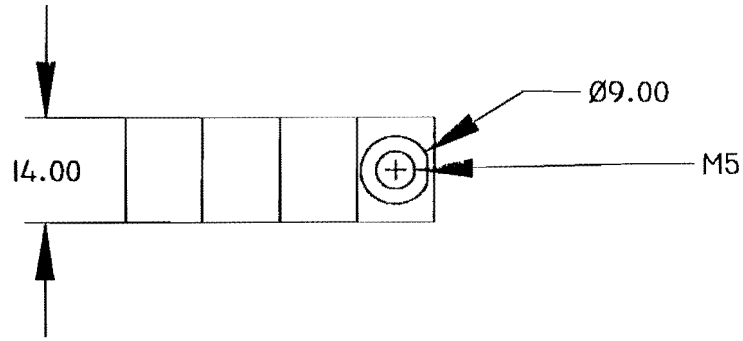

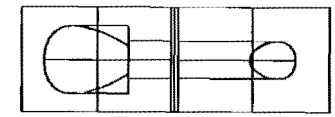

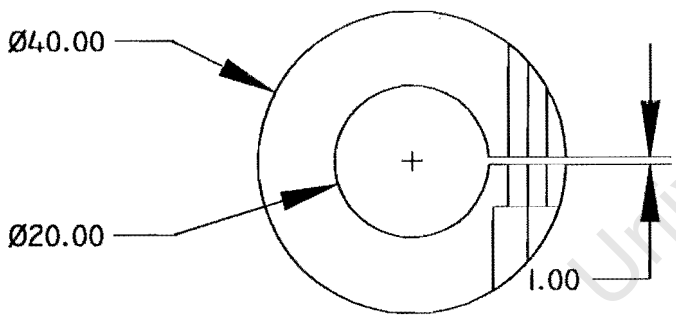

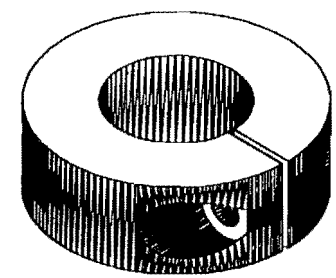

DIMENSIONS ARE IN MM AND SURFACE FINISHES IN RE-3μm. THE OVERALL TOLERANCE IS 0.1 MM IF NO OTHER IS STATED.

Department of Materials Eng.
University of Cape Town
Republic of South Africa

MATERIAL STAINLESS STEEL		DESCRIPTION	
TITLE	COLLAR		
DRAWN BY G.J.JEWELL		APPROVED BY	SCALE 1:1
DATE 21/4/00		DATE	PLOT 1:1
ACAD NAME COLLARDIM	DRAWING NO.		REV.

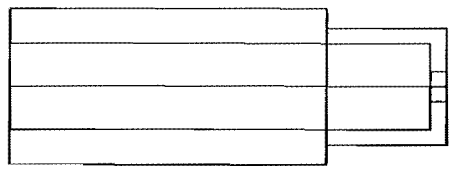

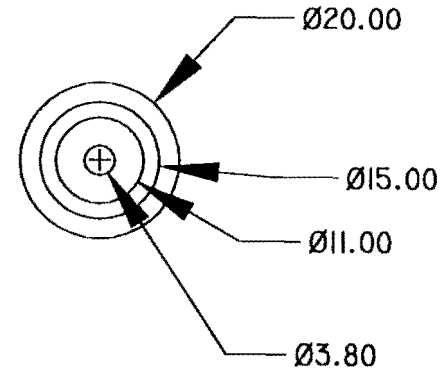

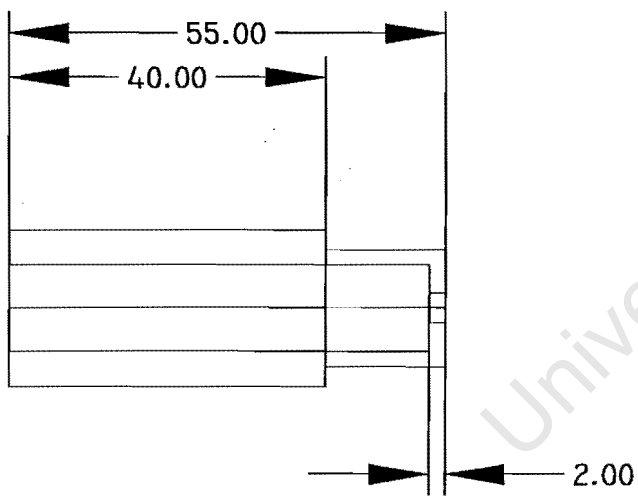

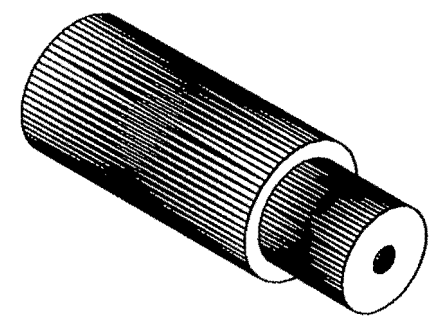

DIMENSIONS ARE IN MM AND SURFACE FINISHES IN RC-3/M1. THE OVERALL TOLERANCE IS 0.1 MM IF NO OTHER IS STATED.

Department of Materials Eng.
University of Cape Town
Republic of South Africa

MATERIAL TEFLON	DESCRIPTION
TITLE: FEED NOZZLE	
DRAWN BY G.J.JEWELL	APPROVED BY
DATE 21/4/00	DATE
SCALE: DWG 1:1 PLOT 1:1	
ACAD NAME NOZZDIM	DRAWING NO.
REV.	

APPENDIX B

COMPOSITIONS AND HARDNESSES OF TESTED MATERIALS

Table 1 Nominal compositions of the metals tested (weight%)

Material	hardness HV	Cr	Ni	C	Mo	Mn	Ti	Si	Fe	N	P	S	V	Cu
Mild Steel	138			0.2		0.06			rem.		0.06			
304 Stainless steel	231	18-20	8-12	0.08 max		2.0 max		1.00 max	rem.					
310 Stainless steel	203	24-26	16-22	0.25 max		2.0 max		1.00	rem.					
Cromanite	358	18-20	1.00			9.5-11		1.0 max	rem.	0.4-0.6	0.045 max	0.015 max		
3CR12	207	11-12	1.5 max	0.03 max		1.5 max	0.6 max	1.0 max	rem.	0.03 max		0.03 max		
VRN 600 overlay	792	24-30	0.20 max	3.5		3.0-4.0		1.0 max	rem.		0.04 max	0.04 max		0.1
VRN 500	432	0.4-1.2	1.00max	0.35max		1.60		0.55	rem.		0.03 max	0.03 max	0.1	
VRN Ti-Hard	509	0.94		0.29max	0.2 max	0.7	0.42	0.35 max	rem.		0.007max	0.002		
Abroclad	620	1.6	0.4	0.280	0.20 min	1.60			rem.		0.015	0.005		

Table 2 Nominal compositions of the matrices and hardnesses of tungsten carbide composite materials

Material	hardness of grit HV	hardness of matrix HV	Cr	Ni	C	Mo	Mn	Si	Fe	Cu	Zn
Tungrit	1925	68		6						rem.	47
Tungenia	1077	327	15	rem.				1	4		
Tungweld	1600	717	12		2.5	6	1.7		rem		

Table 3 Properties of the ceramic materials tested

Ceramic	Nominal composition	grain size (μm)	density (g/cm^3)	hardness HV 30kg load
Alumina MP92	92% pure alumina	3.24	3.62	1105
Alumina MP96	96% pure alumina	3.86	3.75	1277
Alumina MP99	99% pure alumina	2.51	3.85	1442
MZF	Alumina and stabilised zirconia	3.56	4.2	1792

APPENDIX C

PUBLISHED WORK

THREE -BODY ABRASION OF MATERIALS IN THE POWER GENERATION INDUSTRY

G.J. Jewell and C. Allen

Department of Materials Engineering, University of Cape Town

Three-body abrasion is a form of wear in which hard particles are free to move between two sliding surfaces, causing material to be removed from one, or both, of the surfaces. The resultant degradation of the component surfaces may adversely effect their performance.

One example of three-body abrasion occurs in coal-fired power stations. During the process of electricity generation, coal is milled into a fine powder and then burnt in a boiler. The residual products of the combustion are coarse ash and fly ash particles. The coarse ash, which falls out of the bottom of the boiler, needs to be removed with the aid of mechanical scrapers. The abrasive nature of the ash results in three body abrasive wear taking place, particularly of the scraper blades. These blades need to be replaced periodically, leading to operational downtime and financial losses.

Three-body abrasion conditions have been reproduced in a laboratory using a purpose designed and built three-body wear apparatus, which enables abrasive particles to be introduced between a moving surface and specimens made from candidate materials. The abrasive particles employed were ash and silica sand, which is a principal constituent of the ash and is widely used in laboratory abrasion tests. All the testing was carried out under high stress[1] conditions in which the abrasive particles are crushed. A wide range of materials has been tested for three-body abrasion resistance, including steels, hard metals, coatings and ceramics. Factors such as the abrasive particle size, sliding speed, abrasive feed rate, and load, have also been examined.

The use of scanning electron microscopy (SEM) has been shown to be extremely useful in elucidating the total process of wear and determining the mechanisms involved in the material removal process. For example, scanning electron microscopy was used to examine the abrasive particles, to characterise their shapes, and to see the extent of particle damage during abrasion testing. The non-conductive particles were mounted on aluminium stubs and sputter-coated with gold-palladium to ensure electrical conductivity. An acceleration voltage of 20kV was used to prevent the particles becoming charged. Fig. 1 shows unused silica particles, which, in general, have rounded edges.

SEM was also used to examine the various materials following abrasion. Fig. 2 shows the wear track on a mild steel specimen caused by the passage of a hard particle. Extensive ploughing and plastic deformation is apparent, which eventually leads to rupture and the loss of small particles of material. Fig. 3 shows the ruptured material inside the wear track at higher magnification.

The extent of material loss has, in general, been found to be dependent on the relative hardness of the abrasive and material. Materials whose hardnesses are in excess of 1200 Vickers are expected to perform satisfactorily as scraper blades in the power generation industry.

The support of Eskom TSI is gratefully acknowledged.

References

1. Hutchings, I.M. (1992) Tribology: Friction and Wear of Engineering Materials. London, Edward Arnold, 134.

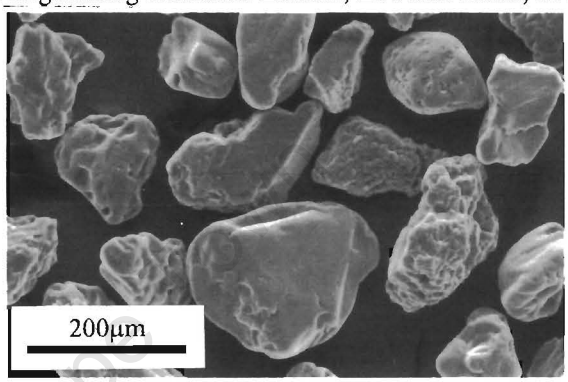

Fig. 1 Silica sand particles used for abrasive testing showing the rounded shape of the particles.

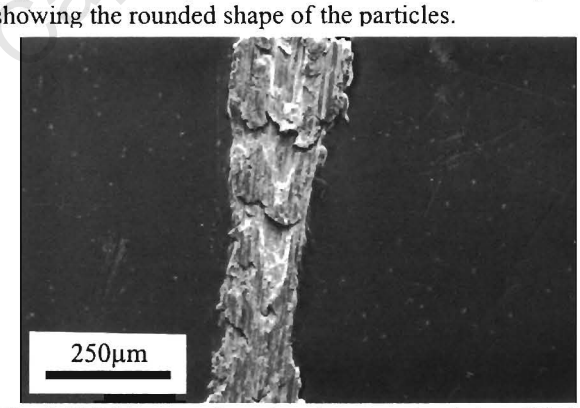

Fig. 2 SEM image of an abrasive wear track in mild steel caused by a particle of silica.

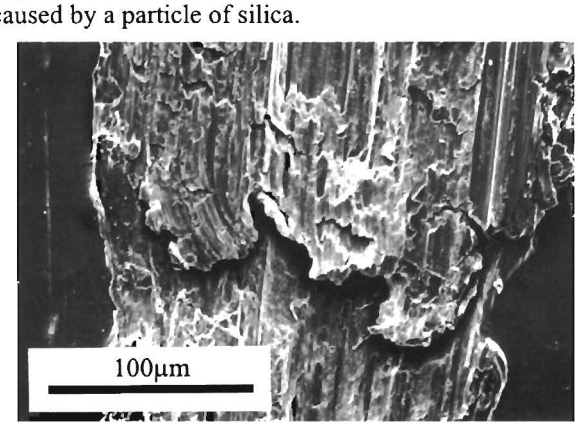

Fig. 3 SEM image showing plastic deformation of mild steel which will lead to subsequent material removal.